Science Achievements and Applications

The Science Derived from Lunar Laser Ranging

Peter J. Shelus
McDonald Observatory/Department of Astronomy/Center for Space Research
University of Texas at Austin
Austin, TX 78712-1083
USA

Abstract

This paper deals with lunar laser ranging and the science that is derived from it. The LLR data that have been gathered for more than a quarter of a century fill an important niche in Astronomy. They form a foundation for many fundamental astronomical disciplines and provide the grist for a multi-disciplinary analysis mill, the benefits of which are found in such areas as the solid Earth sciences, geodesy and geodynamics, Solar System ephemerides, terrestrial and celestial fundamental reference frames, lunar physics, general relativity, and gravitational theory. They contribute to our knowledge of the precession of the Earth's spin axis, the lunar induced nutation, polar motion and Earth rotation, the determination of the Earth's obliquity to the ecliptic, the intersection of the celestial equator and the ecliptic, lunar and solar solid body tides, lunar tidal deceleration, lunar physical and free librations, and energy dissipation in the lunar interior. They provide vital input into the lunar surface cartographic and surveying system. They determine Earth station and lunar surface retroreflector location and motion, mass of the Earth-Moon system, lunar and terrestrial gravity harmonics and Love numbers, relativistic geodesic precession, and the equivalence principle of general relativity.

1.0 Introduction

Positional astrometry has always played an important role in Astronomy. It contributes to our knowledge of reference frames, time keeping, position on the Earth, rotation of the Earth, positions and motions of the major and minor planets and natural satellites, proper motions and parallaxes of stars. Providing the base for the distance scale of the universe, it provides us with a better understanding of the Earth, the Solar System, the local solar neighborhood, the Milky Way Galaxy, the local group, the hierarchy of galactic clustering, the universe itself. Originating with naked-eye observations using the crudest of instruments and progressing to the filar micrometer and the photographic plate, there has been a steady evolution to more accurate and precise instrumentation, reduction, and analysis. Today we have CCD imaging, optical interferometry, very long baseline interferometry (VLBI), artificial satellite ranging (SLR), lunar laser ranging (LLR), the Global Positioning System (GPS) as well as radar and spacecraft Doppler. In addition, the availability of powerful and inexpensive desktop computers and workstations has provided a vast increase in our analytical capabilities. All of this gives us a better understanding of the universe around us. Each new step depends upon the successes of the past and leads to a better future. LLR is one of the most modern and exotic of the astrometric techniques that are used in basic scientific studies. The analysis of the constantly changing Earth-Moon distance, using different observatories on the Earth and different retroreflectors on the Moon, provides for a wide array of terrestrial, lunar, solar system, and relativistic science [Bender, et al 1973; Mulholland, 1980; Dickey, et al 1994; Nordtvedt, 1996].

2.0 Observation to science

Observations without science are meaningless. By applying a procedure that can be called "dynamic parameter improvement" [Mulholland, 1976], to a set of LLR measurements, one can obtain as much information about the dynamics of the site from which the observations are being

made as about the dynamics of the target itself and the universe around us. This procedure requires that not only the set of measurements be available for analysis but also, for each one of those measurements, a prediction of what that measurement would have been if the universe acted in conformity with some specific, well-defined model. Let us begin with a convenient definition of the topocentric distance, r, between an observing station and some target on the Moon. In vector form,

$$r = R(\text{geocenter-selenocenter}) - R(\text{geocenter-observatory}) + R(\text{selenocenter-reflector}).$$

This can be approximated in scalar form, by dotting the station vector into the remaining part, i.e.,

$$r = R_1 - \rho \cos(\delta) \cos(H) - z \sin(\delta),$$

where R_1 is the geocentric distance to the target, ρ is the perpendicular distance of the station from the Earth's spin axis; z is the perpendicular distance of the station from the Earth's equatorial plane; δ is the declination of the target; and H is the local hour angle of the target. Although this is a simple looking equation, it is a complicated function of the time. And, the LLR measurement is not simply one of distance, it is a measurement of an out-and-back time interval. Therefore, it is necessary to use this equation in an iterative scheme to obtain the prediction for a two-way transit time, τ, with the Earth and the Moon each being in motion; we cannot just use an instantaneous distance. In any event, the evaluation of a predicted transit time for any given laser firing, requires the knowledge and application of a gravitational and relativistic theory, all of the motions affecting the station and the target, precession and nutation, polar motion and Earth rotation, lunar libration, the elastic deformations of the Earth and the Moon, models of atmospheric refraction, as well as the nominal body-fixed coordinates of the telescope and the target, just to mention a few. The increase in our knowledge comes from comparing our predicted transit times with the ones that we have measured. Were prediction and observation to agree, our model would be accurately representing the universe. It is the residual between prediction and observation that allows us to study the workings of the universe. As already mentioned, to evaluate the above equation and then to use it to predict a transit time requires that we have estimated values for a large number of physical parameters, e.g., the masses, radii, internal make-up, and gravitational harmonics of the Earth and the Moon, the value of the Gravitational constant, the locations of the telescope on the Earth and the corner retroreflectors on the Moon, and many others. Further, for each of these parameters, κ_i, one must have a partial derivative $\delta\tau/\delta\kappa_i$, i.e., the manner in which the transit time, τ, would vary, were we to change the value of only that particular parameter in our model. Each observation then provides an equation of condition of the form

$$\Delta t = \Sigma (\delta t/\delta\kappa_i) \Delta\kappa_i$$

and this system of equations of condition can be reduced by a suitable regression algorithm to provide improvements to the estimated values of each of the various parameters, κ_i. Table 1 lists some of the more important parameters derived using LLR data. Following that table are short descriptions of some of scientific disciplines being addresses via LLR scientific analyses.

Table 1. Parameter values derived from LLR

Parameter	Value
Gravitational Physics and relativity parameters	
Principal of Equivalence parameter, E	$(3.2 \pm 4.6) \times 10^{-13}$
Parameterized Post-Newtonian (PPN) superposition parameter, β	1.003 ± 0.005
Parameterized Post-Newtonian (PPN) curvature parameter, γ	1.000 ± 0.005
Deviation from the expected geodetic precession, K_{GP}	-0.003 ± 0.007

Change in gravitational constant (G-dot)/G			$(1 \pm 8) \times 10^{-12}$/yr
Geophysical Parameters			
GM_{EARTH}			$398{,}600.443 \pm 0.004$ km^3/s^2
Luni-solar precession constant at year 2000			50.3845 ± 0.0004 arcsec/year
18.6-year nutation corrections			
In-phase terms			
$\Delta\varepsilon$	2.8 ± 1.1 marcsec	$\sin\varepsilon\,\Delta\psi$	-2.9 ± 1.4 marcsec
Out-of-phase terms			
$\Delta\varepsilon$	0.6 ± 1.3 marcsec	$\sin\varepsilon\,\Delta\psi$	0.5 ± 1.0 marcsec
n-dot secular acceleration of the moon			
Total			-25.88 ± 0.5 arcsec/century^2
Diurnal term			-4.04 ± 0.4 arcsec/century^2
Semidiurnal term			-22.24 ± 0.6 arcsec/century^2
Lunar contribution			+0.40 arcsec/century^2
Increase semimajor axis rate			3.82 ± 0.07 cm/year
Lunar parameters			
Love number, k_2			0.0302 ± 0.0012
Normalized moment of inertia, C/MR^2			0.3940 ± 0.0019
Dissipation parameters			
Q	26.5 ± 1.0	k_2/Q	0.001136 ± 0.000016
Second-degree moment differences			
$\beta_L = (C - A)/B$	$631.72 \pm 0.15 \times 10^{-6}$	$\gamma_L = (B - A)/C$	$227.88 \pm 0.02 \times 10^{-6}$
Low-degree gravitational harmonics			
J_2	$204.0 \pm 1.0 \times 10^{-6}$	J_3	$8.66 \pm 0.16 \times 10^{-6}$
C_{22}	$22.5 \pm 0.11 \times 10^{-6}$		
C_{31}	$32.4 \pm 2.4 \times 10^{-6}$	S_{31}	$4.67 \pm 0.73 \times 10^{-6}$
C_{32}	$4.869 \pm 0.025 \times 10^{-6}$	S_{32}	$1.696 \pm 0.009 \times 10^{-6}$
C_{33}	$1.73 \pm 0.05 \times 10^{-6}$	S_{33}	$-0.28 \pm 0.02 \times 10^{-6}$

3.0 Real-Time Earth Orientation Parameters

The attempt to model all of the Earth's motions affects many scientific disciplines. Although precession and nutation were well observed by the 19th century, it was not until the turn of this century that the irregularities in the Earth's rotation and the phenomenon of polar motion were clearly recognized. By the 1960's, largely from optical observations, augmented by artificial satellite Doppler measurements, 5-day mean values for each component of the polar motion were believed accurate to ± 40 cm and angular position of the Earth accurate to ± 0.03 arcseconds. From its inception in the late 1960's, LLR was a source for accurate Earth rotation and polar motion information. Project EROLD (Earth Rotation from Lunar Distances) was conceived in 1974 under the auspices of COSPAR. The first series of LLR results for Universal Time was published in the Annual Report of the Bureau Internationale de l'Heure (BIH) for 1978. Project MERIT (Monitor Earth Rotation and Intercompare Techniques) was held in the early 1980's and LLR played a fundamental role in that campaign to pave the way for the replacement of the BIH with the International Earth Rotation Service (IERS) in the 1990's. Now, co-mingled with results from SLR, VLBI, and GPS, LLR monitors the rotational characteristics of the Earth at the few millisecond of arc level. Although often not as dense as data from some of the other techniques, LLR data is often the most timely data type, enhancing the predicative capabilities of the USNO's NEOS Earth Orientation predictions.

3.1 Solar System Dynamics

The Moon's orbit around the Earth is strongly perturbed by the Sun. This perturbation gives rise to a rich spectrum of range signatures that, in turn, give sensitivity to a wide variety of Solar System parameters. The LLR data set provides a dramatic improvement compared to classical

optical data in the accuracy with which the lunar orbit can be known. For example, the lunar orbit orientation is determined at least two orders of magnitude more accurately and the radial component is determined at least four orders of magnitude more accurately than previously, through the use of the LLR data type. In fact, the radial distance variations are determined slightly better than the present 2-3 cm LLR range accuracy and the angular rate uncertainty is no more than 0.15 milliseconds of arc per year. The lunar orbital components that have the greatest uncertainties are the mean distance, presently 0.4 m (due to correlation with the retroreflector coordinates in the mean Earth direction) and the orientation of the lunar orbital plane with respect to the Earth's equator, 1.5 milliseconds of arc (3 m at the Earth-Moon separation)

The strong influence of the Sun on the Moon's orbit also permits LLR data to be used efficiently to determine the mass ratio $Mass_{Sun}/(Mass_{Earth} + Mass_{Moon})$ as well as the relative orientation of the Earth-Moon system orbit around the Sun. The actual size of the Earth-Moon orbit is determined by the gravitational constant multiplying the sum of the masses of the Earth and the Moon, with the Moon's orbit being perturbed from a simple Keplerian ellipse by the Sun. The two largest solar perturbations for the Moon, the monthly and semimonthly variations in distance, are determined from LLR data to a few cm. This corresponds to a 10^{-8} relative accuracy in the value of the mass ratio in question. Further, the analysis of LLR observations allows the relative geocentric positions of the Sun and the Moon to be determined to within 1 millisecond of arc. Since planetary positions are determined with respect to the Earth's orbit around the Sun, the geocentric position of the Moon and the heliocentric positions of the planets can be made internally consistent in their relevant orientation. Because LLR stations are located on a spinning Earth, the orientation of the Earth's equatorial plane is determined relative to both the lunar orbit plane and the ecliptic plane of the heliocentric Earth-Moon orbit. Thus, LLR data is sensitive to the mutual orientation of the planes of the Earth's equator, the lunar orbit, and the ecliptic. Hence, it locates the intersection of the ecliptic and equatorial planes (the dynamical equinox) and determines the angle between them (the obliquity of the ecliptic). This process allows the orienting of the planetary ephemerides onto the fundamental astronomical reference frame at the millisecond of arc level.

Of course, all of these accuracies are degraded when one extrapolates outside the span of observations. This means that a continual supply of high quality measurements and analysis are required to maintain and enhance these results. Using LLR data alone and in combination with the other modern observing techniques provides for the very best results available.

3.2 Relativity and Gravitational Physics

LLR has contributed greatly to Solar System tests of general relativity and gravitational theories. The Moon proves to be especially valuable for this because the ratio of non-gravitational to gravitational forces acting upon it is very small. LLR now establishes the definitive limit for both the strong and the weak equivalence principles[Williams, et al 1996], requiring that the ratio of gravitational mass to inertial mass be exactly unity. Therefore, all bodies must fall with the same acceleration in an external gravitational field, with the gravitational self-energy contributing equally to the gravitational and inertial masses. Although the Equivalence Principle was tested in the laboratory, until the coming of the LLR technique, it has not been tested for bodies large enough to have a significant fraction of their masses coming from gravitational self-energy. Roughly 4.6×10^{-10} of the Earth's mass derives from its gravitational self-energy; the corresponding fraction for the Moon is 1.9×10^{-11}. Considering the orbit of the Moon around the Earth, a violation of the Equivalence Principle would cause the orbit of the Moon about the Earth-Moon barycenter to be polarized in the direction of the Sun, the signature of which would have a synodic period of 29.53 days. This is the so-called Nordtvedt effect [Nordtvedt, 1988]. Today,

LLR analyses give $(M_G/M_I - 1) = (2 \pm 5) \times 10^{-13}$, the best current test of the Strong Equivalence Principle available. With feasible improvements in LLR data accuracy and with a longer span of data, further improvement is assured.

Another important test of gravitational physics is that coming from the measurement of the relativistic precession of the lunar orbit, i.e., geodetic precession. This was first predicted by deSitter in 1916. This effect should cause a precession of the entire lunar orbit with respect to the inertial frame of the Solar System by some 19 milliseconds of arc per year. The LLR data are sensitive to this effect mainly through the excess precession of the lunar perigee above and beyond that due to the Newtonian effects of the Sun, the Earth, and the other planets. Early LLR reductions agreed with the predictions of General Relativity to within 2%. More recent solutions give a difference of $-0.3 \pm 0.9\%$ from the expected value. At the present time the leading source of error in this result is an uncertainly in J_2, the primary lunar oblateness term. New, more, and better observations will be invaluable.

LLR data also provide information concerning the possible change of the gravitational constant, G, with time, because of the lunar orbit's sensitivity to the solar longitude. Adding cosmological interest to this situation is the suggestion that very large changes in G may have occurred during an inflationary phase in the early history of the universe. Estimates of limits on the rate of change of G currently range from $|(dG/dt)/G| \leq 1 \times 10^{-11}$ to 0.4×10^{-11} per year. The LLR value is presently $(0.1 \pm 0.8) \times 10^{-11}$ per year [Williams, et al 1996]. Other independent determinations can be made from Viking lander tracking data and binary pulsar data. The best results on G-dot will undoubtedly depend upon the analysis of a combination of all of these data types.

3.3 Lunar Science

The analysis of LLR data certainly provides an especially large amount of information about the dynamics and the internal structure of the Moon. Selenocentric reflector surface coordinates, moment of inertia ratios, as well as the second and third degree lunar gravity harmonics are determined with quite high accuracy using LLR data. The reflector coordinates, together with the ALSEP radio transmitter coordinates, serve as the fundamental control points for lunar surface cartography. The changing apparent distances, as monitored by LLR, between the several reflectors and the Earth provide information on the lunar physical librations and solid body tides. Values of the lunar gravity harmonics, the moments of inertia and their differences, the lunar Love number, k_2 (which measures the tidal change in the moments of inertia and gravity), and variations in the lunar physical librations are all related to the Moon's structure, mass distribution, and internal dynamics and, therefore, give us great insight into a much better understanding the lunar interior. Presently, the most accurate estimate of the lunar moment of inertia is obtained from a combination of moment of inertia differences determined by the LLR solutions and the lunar gravity field coefficients coming from lunar satellite Doppler observations and LLR.

The lunar mass distribution also perturbs the lunar orbit that, in turn, produces a secular precession in the lunar node and perigee directions. Lunar seismic data suggest a core and a mantle, with little definitive evidence of a core. The existence of a lunar core, as well as whether it is solid or liquid, are important questions for which the lunar polar moment, as derived from LLR results, can help set limits. Information concerning the apparent tidal distortion of the Moon and the mean direction of its spin axis can be inferred from the lunar librations, measured by LLR. However, because of insufficient LLR data accuracy and volume, complications exist in the interpretation of results. Better accuracy and greater amounts of multi-corner data are needed, since key answers depend on very small signatures. If the Moon were a perfectly rigid body, the mean direction of its spin axis would precess with the orbit plane. LLR data show that the true

spin axis is actually displaced from this expected direction. The two dissipative terms are due to solid and liquid dissipation. The presence of a fluid core with a turbulent boundary layer appears to be a plausible interpretation. However, the direct separation of the competing dissipative terms is difficult The differential signature arises in the lunar orbit acceleration, and separation requires an independent estimate of n-dot, due to the Earth's tidal friction. In principle, the difference in n-dot could be detected by comparing the total n-dot measured by LLR with n-dot predicted from artificial satellite measurements of ocean tides. Unfortunately, the present determinations are not yet precise enough to discriminate between alternatives.

The LLR data show an apparent rotational free libration in longitude for the Moon with a 2.9 year period and a 1.4 arcsecond amplitude. The free-plus-forced blend has a 1.8 arcsecond amplitude and is quite tricky to separate. Recently, also strongly seen in the LLR data, is a 74 year elliptical wobble of the lunar pole with semiaxes 3 by 8 arcseconds. Theoretically, separate from the lunar librations that are driven by the time-varying torques of the Earth, the Sun, and the other planets, i.e., the forced physical librations, three modes of free librations exist. One of these theoretical modes is a 2.9 year oscillation in lunar rotation speed. Without suitable recent exciting torques, and because of substantial dissipation, the amplitudes of all lunar free librations should be damped to zero. However, the observed 2.9 year free libration is complicated because two very small forcing terms in the lunar orbit, close to the resonance frequency for the free libration, are amplified to mimic the observed free libration. Numerically integrated lunar rotational motions have been compared to semi-analytic calculations of the forced angular motions in an attempt to separate out the free libration. Seismic events on the Moon would be insufficient to explain the observed amplitude. Other studies have been carried out to investigate whether the apparent free libration might have been excited by recent impacts on the Moon. Such excitation would have required an impact in very recent times by an object large enough to leave a crater with a 10 km diameter. A third free libration mode, much smaller than the others, i.e., only 0.02 arcseconds in magnitude, has only been recently detected; its small size nearly completely excludes impacts as being an important stimulating mechanism. As another possibility, Eckhardt has suggested that passes though weak resonances have occurred for the lunar rotation in the geologically recent past that can perhaps stimulate free librations in longitude. Another plausible explanation appears to be core-boundary effects, similar to those that are believed to account for the decade time-scale fluctuations in the Earth's rotation. This can oly be determined with more and better LLR data that can irrefutably define the third mode of libration and extend the span of measurement of the 74 year wobble.

3.4 Geodynamics

The classic geodynamical results from LLR derive from the long term study of the variation of the Earth's rotation, the determination of the constants of precession and nutation of the Earth, LLR observing station coordinates and motions, the Earth's gravitational coefficient, and solid-body and ocean tides that accelerate the motion of the Moon. LLR observations supplement and complement the results being obtained from other space-based observing techniques, but with an almost three decade long span of data, LLR data exceeds that available from any other space geodetic technique. The very accurate value of the LLR-derived Sun/(Earth + Moon) mass ratio can be combined with the solar GM and the lunar GM (from lunar-orbiting spacecraft) to give the Earth's GM in an geocentric reference frame with an accuracy of 1 part in 10^8. Within the uncertainties, this value is quite compatible with that derived from SLR.

Tidal dissipation of energy on the Earth causes a misalignment of the Earth's tidal bulge to the Earth-Moon line. This bulge exerts a secular torque that causes both the Moon to increase its distance from the Earth and the Earth's rotation rate to decrease. The resulting change has been

seen in the geological record. With respect to specific Earth tides, the span and accuracy of the LLR data is such that the diurnal and semi-diurnal tides can be resolved from the amplitude of the 18.6 year along-track tidal perturbation. Due to the gravitational attraction of the Sun, Moon, and other planets the Earth's spin axis precesses and nutates in space. These motions depend on the flattening of the Earth, its moment of inertia, the flattening of the core-mantle interface, the Earth's anelasticity, as well as ocean and solid body tides. Both LLR and VLBI analyses indicate that significant corrections are required to the standard precession and nutation models. The almost 30 year span of LLR data is a distinct advantage when attempting to separate precession and the 18.6 year nutation correction. Joint VLBI and LLR solutions [Charlot, et al 1995] combine the strength of the LLR data for long period terms and the high resolution of the VLBI data for shorter periods.

4.0 Summary

A great deal of science has been accomplished using LLR data over the past 30 or so years. We expect that a great deal more will be accomplished in the future. LLR analysis efforts in the fields of relativity and gravitational theory are continuing to reduce the uncertainty of the Principle of Equivalence parameter, the relativistic precession of the lunar orbit, as well as the rate of change of the gravitational constant; today, LLR provides the only high accuracy testing of a significant number of relativistic and gravitational theory parameters. Further, within the lunar sciences, significant LLR analytical effort is being applied to studies of the lunar interior, especially those that deal with the dissipation of rotational energy in the Moon, the shape of the lunar core-mantle boundary, the lunar Love number k_2, and the free librations of the Moon. Finally, in geodynamics, LLR analytical efforts will continue to contribute to studies that deal with fundamental coordinate frames, the variation of the Earth's rotation, precession, nutation, and the tides.

Because of the passive nature of the lunar reflectors and the steady improvement in observing equipment, the LLR data type will continue to provide for state-of-the-art results in many disciplines of Astronomy. Similar to other astrometric techniques, LLR is broad ranging in results and its gains are steady as its data base continues to be extended. As a basic astronomical data type, longevity and continuity must be assured. It is interesting to note that we are approaching the 30th anniversary of the first emplacement of a reflector package on the lunar surface. LLR remains the only active Apollo experiment and it is still marching at the forefront of science with its ever expanding results. During these times of austerity, it is important to cite examples of efficient and cost-effective progress of research. LLR, and the science it is able to produce, is a source of special pride within the scientific community.

5.0 Acknowledgments

I wish to acknowledge and thank Peter L. Bender, Jürgen Müller, and James G. Williams for helpful advice and counsel during the preparation of this paper. A part of this effort is currently being supported by NASA Grants and Contracts NAS5-32997, NAGW-2970, NAGW-4277, NAGW-4862.

6.0 References

Bender, P. L., Currie, D. G., Dicke, R. H., Eckhardt, D, H., Faller, J. E., Kaula, W. M., Mulholland, J. D., Plotkin, H. H., Poultney, S. K., Silverberg, E. C., Wilkinson, D. T., Williams, J. G., and Alley, C. O., 1973, Science, 182, 229.

Charlot, P., Sovers, O. J., Williams, J. G., and Newhall X X, 1995, Astronomical Journal, 109,

418.
Dickey, J. O., Bender, P. L., Faller, J. E., Newhall, X X, Ricklefs, R. L., Ries, J. G., Shelus, P. J., Veillet, C., Whipple, A. L., Wiant, J. R., Williams, J. G., and Yoder, C. F. 1994, Science, 265, 482.
Mulholland, J. D., 1976, Scientific Applications of LLR, J. D. Mulholland, Ed., Reidel, Dordrecht, Netherlands, 9.
Mulholland, J. D., 1980, Reviews of Geophysics and Space Physics, 18, 3.
Nordtvedt, K., 1996, Physics Today, 49, No. 5, 26.
Williams, J. D., Newhall, X X, and Dickey, J. O., 1996, Physical Review D, 53, 6370.

Applications of Accurate SLR Station Positioning

Peter Dunn for the GSFC SLR Analysis Group

Introduction

The technical applications of SLR data cover a variety of scientific areas. The satellite position defined by a network of SLR stations enables us to improve the gravity model of the Earth and to investigate other force model effects on the orbit. The network also defines high resolution Earth orientation parameters from observations of geodetic satellites in stable orbits, such as the LAGEOS and ETALON constellations, and the scale of the measurements allows very accurate definition of the center of mass of the Earth, as well as the dimensions of the planet and its gravitational constant. This paper will describe some accomplishments of SLR analysis in the field of station and network positioning, which includes the determination of the velocity of the most accurate SLR Observatories.

Geomagnetic Time Scale Revisions

The SLR-defined global and regional kinematic velocity models have suggested that the relative velocities of SLR stations on the stable interiors of tectonic plates were about five percent slower than those expected from the NUVEL-1 geophysical model (Smith et l.,1990). This observation supports the recent revision of the Potassium/Argon-defined paleomagnetic time scale based on astro-geochronology, which forms the basis of the NUVEL-1A model (Demets et al.,1994). The correlation with NUVEL-1A computed by by the GSFC SLR group for a recent global solution is shown in Figure 1 as the solid line: it has a slope of 0.970 =/- 0.034, whereas the comparison with NUVEL-1 has a slope of 0.928 +/- 0.032. The SLR velocities in this solution are thus still 3 percent slower than the prevailing geophysical model, but with an uncertainty which suggests marginal significance. The correlation measures are influenced by the choice of stations to represent stable plate interiors, and rely on the assumption of uniform motion over the differing observation spans for the chosen stations.

The motion of the Easter Island station on the Nazca plate with respect to neighbouring stations on the Pacific plate is the largest of all plate pairs, and the results in Figure 1 suggest that it's velocity is slower than the NUVEL-1A value. There is emerging evidence from GPS observations (Heflin et al., 1994) that supports the SLR velocity at Easter Island as slower than the geophysical prediction. This calls into question the validity of the choice of this station as representative of a stable plate interior, or could also suggest that the NUVEL-1A model for the behavior of the Nazca Plate should be re-addressed. SLR observations collected around the Gulf of California analysed by Dunn et al. (1995) have confirmed the early indications from GPS observations (Dixon et al, 1992.) that the Gulf is extending faster than predicted by the Gulf rise spreading rates. DeMets (1995) has conducted a reappraisal of these seafloor spreading lineations which contradicts the assumption that Baja California has been rigidly coupled to the Pacific plate since 3.6 Ma. DeMets concludes that PA-NA motion is now 4 mm/year faster than that predicted by the 3 Myear average of NUVEL-1A, and this faster rate is closer to the rate determined from the space geodetic measurements. We can thus see how the space measurements can check and even challenge the integrity of the latest geophysical models.

Evidence for Regional Deformation

The SLR velocity model has indicated that several other areas exhibit regional deformation which should not be considered as representative of stable plate interiors. The successful

deployment of transportable systems with the WEGENER campaign in the Mediterranean has confirmed the expected extension in the Aegean, and the SLR geodynamic observations can now be combined with earthquake moment tensors for regional seismic risk assessment (Jackson et al, 1994). The direction of the motion of SLR observatories located behind island arcs in Simosato, Japan and at Arequipa, Peru is aligned with that of the subducting plate; Robaudo and Harrison (1993) have concluded that strain expected to be relieved at the trench is carried over onto the over-riding plate, to be compensated by a mechanism for which a model has yet to be developed.

SLR Measurements of the Vertical

The definition of horizontal position and velocity is easier than that of the vertical component because tracking geometry is strong enough that the effects of orbital and instrumental errors on station latitude and longitude largely cancel over the time span of the orbital arc. A modern laser system can be calibrated to a ranging accuracy of a few millimeters (Degnan, 1993) and atmospheric refraction errors for the optical measurements are unaffected by the variable water vapor component. The positioning accuracy of the SLR systems has progressively improved as the instruments were up-graded and the network expanded. This progress will continue with the deployment of advanced stations: MLRO (Varghese et al., 1992), TIGO (Sperber et al., 1994), SALRO (Wetzel et al. 1994), SLR2000 (McGarry, et al.1996) and positioning capability can be further enhanced by measurements to new, stable satellite targets. The contribution of LAGEOS II has been particularly helpful in the definition of the vertical component of station position, by reducing the influence of orbit force model errors on a station's height estimate, as the second satellite improves the tracking geometry.

Station Height Resolution

The best current SLR systems provide range measurements with an accuracy at their noise level of one to three millimeters. The LAGEOS position determined from these observations is limited by force and Earth model errors to a few centimeters, and the position determined at a station is dependent on the quality of the instrumentation. Since daily monitoring of the vertical is limited by visibility constraints, the best use of the currently available laser data is in defining longer period motion on the scale of months and years and in detecting coherent signals with known spectral characteristics, such as the tidal response of the Earth.

The vertical resolution of a modern SLR station can be seen in the plots of height values shown in Figure 2, which were determined in monthly arcs of LAGEOS I and II data as part of a global solution conducted by the GSFC SLR analysis group. The scatter in height estimates for independent solutions for the Yarragadee laser is listed in the Figure as 7 mm, although formal errors for a simultaneous solution from both satellites' data are as low as one or two millimeters for strong cases. The total spread of heights determined in the two-satellite solution is about twenty millimeters, but the systematic nature of the height variation suggests
that this spread is not a good three sigma error estimate. The scatter can be reduced to 6 mm if the effect of atmospheric pressure loading is modelled (VanDam and Wahr, 1987), as this can amount to several millimeters amplitude with an annual period at Yarragadee. The relatively abrupt change in height seen at GGAO in January 1994 is also observed in the TOPEX/Poseidon orbit analysis, and is thus unlikely to be caused by satellite mis-modeling. It could be due to thermal loading in the region, caused by the formation of a permafrost layer during a particularly heavy winter. Unfortunately, the GPS receiver at the GGAO site was affected by the severity of the weather and there are no GPS results available to compare during this period. The variation in the monthly height of RGO shows strong systematic trends, and suggests that the random fluctuations occur at the millimeter level during some periods.

GeoCenter Determination

Mass redistribution in the atmosphere, hydrosphere, cryosphere, and atmosphere causes the center of mass of the Earth to move relative to the geocenter defined by the observing network. Earth orientation and geocenter are both influenced by tidal and wind-driven ocean mass change, variations in atmospheric pressure, and large earthquakes. Watkins et al. (1995) have shown that geocenter motions determined with LAGEOS observations exhibit annual and semi-annual signals of two to four millimeter amplitude, and Pavlis (1995) and Anderson (1995) have also demonstrated that variations of the geocenter due to ocean tides can be resolved with sub-millimeter accuracy at some tidal frequencies.

The geocenter resolution which can be reached with the data from the best SLR observatories with regular tracking data from LAGEOS I and II is shown in Figure 5. The estimates were made as part of the global solution for station motion, Earth orientation and orbit parameters conducted by the GSFC Laser Ranging Group (Kolenkiewicz et al, 1996). The equatorial components of geocenter motion can be resolved with an rms variation of 5 mm in the x direction, in the Greenwich meridian, and with 3 mm scatter in the y direction. The motion is restricted to an area of 2.4 cm by 2.2 cm, and most of this variation occurs within a block which is only one centimeter square. The polar component is not as well resolved as the equatorial component from satellite observations, and the scatter of the z-component about a mean position is 11 millimeters. The structure in the geocenter motion is caused by Earth mass redistribution, but measured with a network which is not geographically balanced. Improved resolution of these global parameters will become possible as the SLR network expands and is supplemented by automatic, low maintenance continuously tracking systems like SLR2000.

Tidally driven geocenter motion

Variations in the geocenter caused by the lack of symmetry of the ocean tides have been described by Schwiderski (1980), Brosche and Wuensch(1993) and Ray et al. (1994). Watkins and Eanes (1993) have extended the approach they originally adopted to determine coherent nearly diurnal and semi-diurnal variations in the Earth's orientation to include geocenter variations affecting the SLR network. The three year data span of LAGEOS II observations has enabled us to combine this information with that of LAGEOS I to make an accurate assessment of the tidal spectrum, which can be compared with the theoretical models, as well as that developed by Watkins and Eanes. The comparison of tidal coefficients in Figure 6 shows the values in each model for the Z-component in M2, which is the strongest
signal in the spectrum, and the extent to which the difference between the results from LAGEOS I and LAGEOS II can be used to qualify those from the combined solution.

SLR Positioning in the Future

The unique capabilities of SLR systems can be exploited to make important contributions to geodetic science and geodynamics, and we anticipate advances in positioning techniques to produce a variety of valuable products. These will include time series of height estimates at each SLR station which are free of the influence of instrument error, and which can be used for monitoring regional characteristics of the Earth in the vicinity of the station, calibrating the atmospheric pressure loading response of a spherically stratified Earth, or an Earth with assumed lateral crustal inhomogeneities. Furthermore, events and trends in these vertical measurements which indicate stress in the crust can be used to anticipate Earth movement and other natural hazards. An SLR-determined geocenter time series will accurately reflect the common signal in the position variation of the best SLR stations in the network and will define a reference system for monitoring Earth/ocean/atmosphere interactions. In order to reach this goal, coefficients of the

ocean tidal geocenter variation must be determined, taking advantage of the atmospheric loading and Earth tidal modelling results, and with error characteristics calibrated using independent estimates from LAGEOS I and II data.

The combination of space technologies of SLR, VLBI, GPS, DORIS and PRARE systems will enable us to compute a reference system which will provide the accurate long-term stability necessary for rigorous monitoring of important Earth processes in four dimensions. Improved knowledge of the motion in space of geodetic tracking sites is integral to our understanding of global and regional dynamic processes at work within the Earth, including the contemporary behavior of the Earth's major plates, deformation along plate boundaries, and deformation within plate interiors. Combining data from various space geodetic networks to form solutions for site motions will provide the detailed description of global and regional tectonics required to derive more detailed models of the kinematics of the lithosphere and to better understand the mechanisms which drive the plates, produce deformation, and trigger earthquakes. The resulting inertially oriented, accurately scaled reference frame will enhance our ability to accurately model and monitor processes which link the Earth, the oceans and the atmosphere.

REFERENCES

Anderson, P. H., Measuring rapid variations in Earth orientation, geocenter and crust with satellite laser ranging, Bulletin Geodesique, 69, 233-243, 1995.

Brosche, P, and J. Wunsch, Variations of the solid Earth's center of mass due to oceanic tides, Astron. Nachr., 314, 87-90, 1993.

Degnan, J. J., Millimeter accuracy Satellite LASER ranging: a review AGU Geodynamics Series, V.23, pp. 133-162, 1993.

DeMets, C., A reappraisal of seafloor spreading in the Gulf of California: Implication for the transfer of Baja California to the Pacific plate and estimates of Pacific-North America motion, Geophys. Rsch. Lett., 22, 1995.

DeMets, C., R. G. Gordon, D. F. Argus, and S. Stein, Effect of recent revision to the geomagnetic reversal time scale: on estimates of current plate motions, Geophys. Rsch. Lett., 21, 20, pp, 2191 2194, 1994.

Dixon, T. H., G. Gonzalez, S. M. Lichten, D. M. Tralli, G.E. Ness and J. P. Dauphin, Preliminary determination of Pacific-North America relative motion in the sourther Gulf of California using the Global Positiong System,Geophys. Rsch. Lett., 18, 20, pp, 861-864, 1991.

Dunn, P. J., J. W. Robbins, J. M. Bosworth, and R. Kolenkiewicz, Crustal deformation around the gulf of California, Geophys. Rsch. Lett., 23, 2, pp, 193 196, 1996.

Heflin, M., D. Jefferson, Y. Vigue, M. Watkins, F. Webb, J. Zumberge, and G. Blewitt, GPS Times Series: January 22, 1991 - April1, 1994, JPL Interoffice Memo, November 23, 1994.

Jackson, Haines and Holt, A comparison of satellite laser ranging and seismicity data in the Aegean region, Geophys. Res. Lett., 21, pp. 2849-2852,1994.

Kolenkiewicz, R., D. E. Smith, P. J. Dunn, M. H. Torrence and E. C. Pavlis, Geodynamics from LAGEOS I and II, Eos Trans., 77, 17, 1996.

McGarry, J. F. , J. J. Degnan, B. Conklin, P. J. Titteton, Sr., and P. J. Dunn, Automated tracking for advanced satellite LASER ranging systems, SPIE Proc. 2739, April, 1996.

Pavlis, E. C., TRF Determined From Multiple Space Techniques, Eos Trans., 76, 17, 1995.

Ray, R. D., B. F. Chao, B. V. Sanchez and R. S. Nerem, Some geodetic alications of the new Topex/Poseidon oceanic tide models, Eos Trans., 75. 44. 1994.

Robaudo, S, and C. G. A. Harrison, Plate tectonics from SLR and VLBI global data, Combinations of Space Geodesy in Geodynamics; Crustal Dynamics, AGU Geodynamics Series, V.23, pp. 51 72, 1993.

Schwiderski, E. W., Ocean tides, Part I: Global ocean tidal equations, Marine Geod., 3, 161-216, 1980.
Smith, D,E,, R. Kolenkiewicz, P.J. Dunn, J.W. Robbins, M.H. Torrence, S.M. Klosko, R.G. Williamson, E.C. Pavlis, N.B. Douglas, and S.K. Fricke, Tectonic motion and deformation from satellite laser ranging to LAGEOS, J. Geophys. Res., 95, 22013-22041, 1990.
Sperber, P., The Transportable Integrated Geodetic Observatory (TIGO), Ninth International Workshop on Laser Ranging Instrumentation, Canberra, Australia, November, 1994.
vanDam, T. M. and J. A. Wahr, Displacements of the Earth's surface due to atmospheric loading: effects on gravity and baseline measurements, J. Geophy. R., 92, 1281-1286, 1987.
Varghese, T., W. Decker, H. Crooks and G. Bianco, Matera laser ranging observatory (MLRO): an overview, Proc. Eighth International Workshop on Laser Ranging Instrumentation, Annapolis, Maryland, May, 1992.
Watkins, M. M., D. N. Dong, J. O. Dickey, M. B. Heflin, R. J. Eanes and S. Kar, Observations of Seasonal Translations Between the Earth's Mass Center and Lithosphere, Eos Trans., 76, 17, 1995.
Watkins, M. M. and R. J. Eanes, Long Term Changes in the Earth's Shape, Rotation, and Geocenter, Adv. Space Res., 13, 11, 11251-11255, 1993.
Wetzel, S., J. Horvath, V. Husson, G.Su, B. Greene and J. Guilfoyle, The ALRO/MOBLAS-7 Collocation Results, Ninth International Workshop on Laser Ranging Instrumentation, Canberra, Australia, November, 1994.

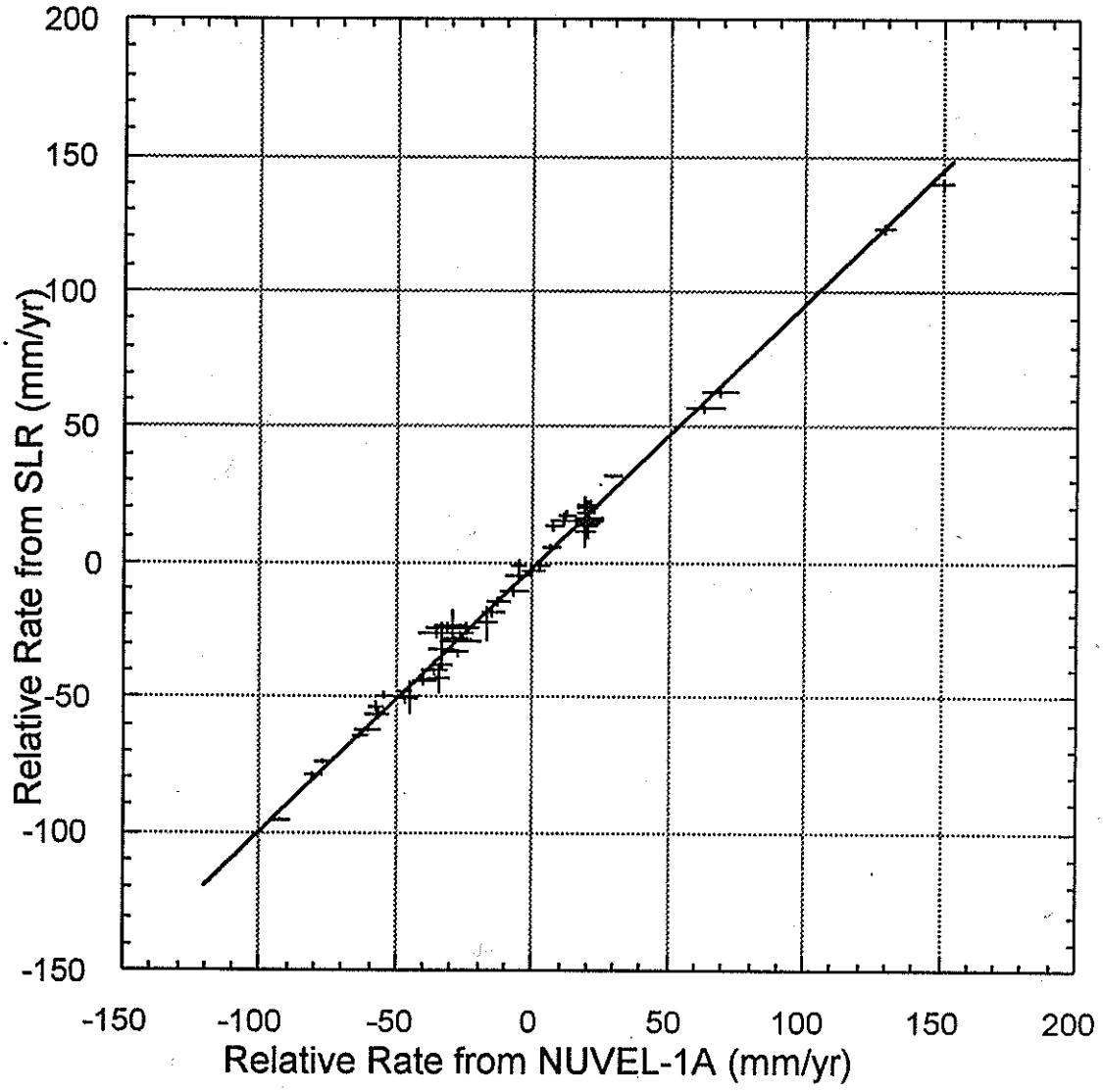

Figure 1: The correlation between the geophysical model NUVEL-1A and an SLR global solution has a slope of 0.970 +/- 0.034. The correlation with NUVEL-1 gave a slope of 0.928 +/- 0.032.

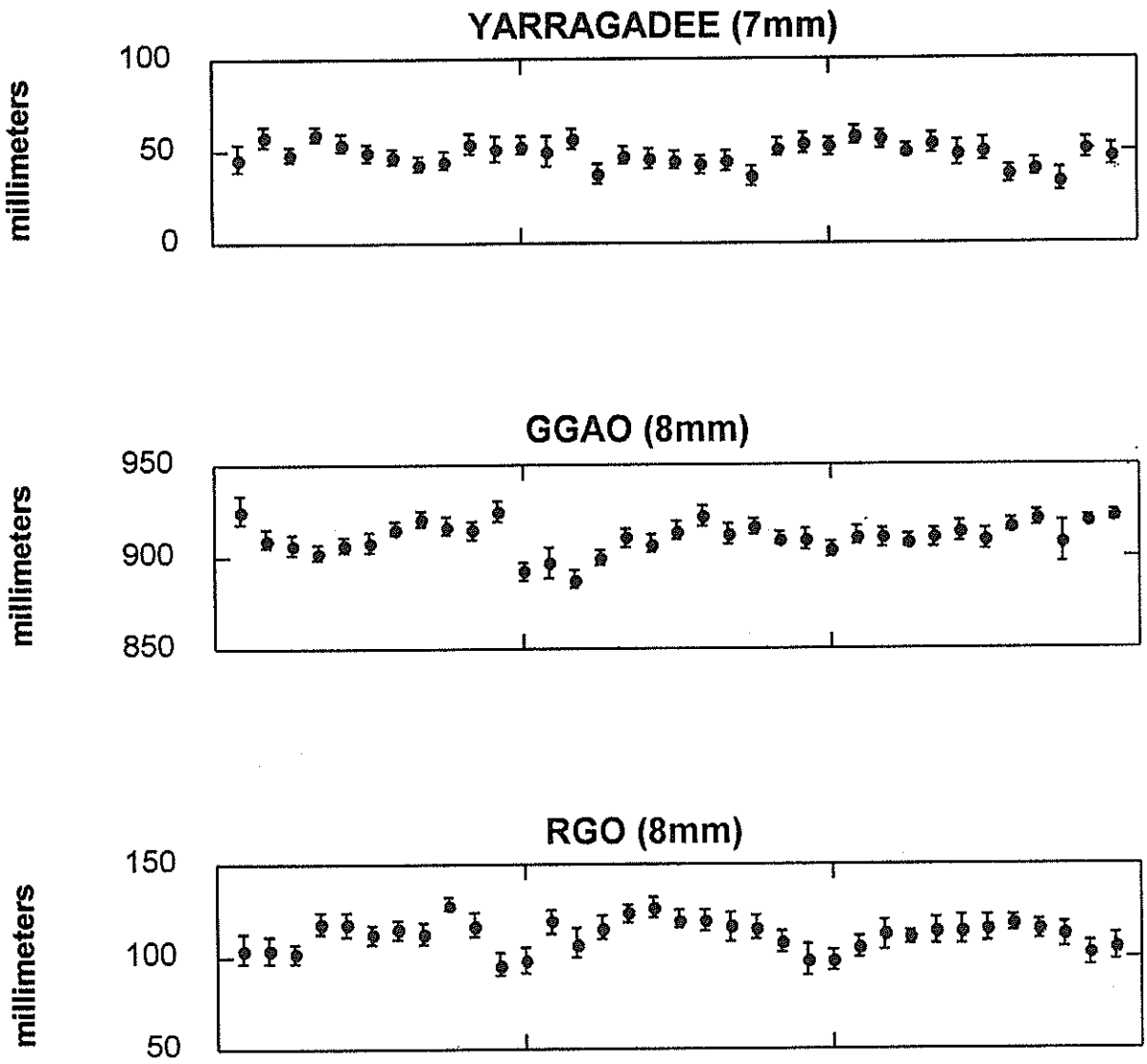

Figure 2: Monthly height values for the stations in Western Australia, at Greenbelt, Maryland, and on the south coast of England exhibit systematic signals, with a local scatter of 2 or 3 mm. The frame titles give the scatter to a mean height estimate.

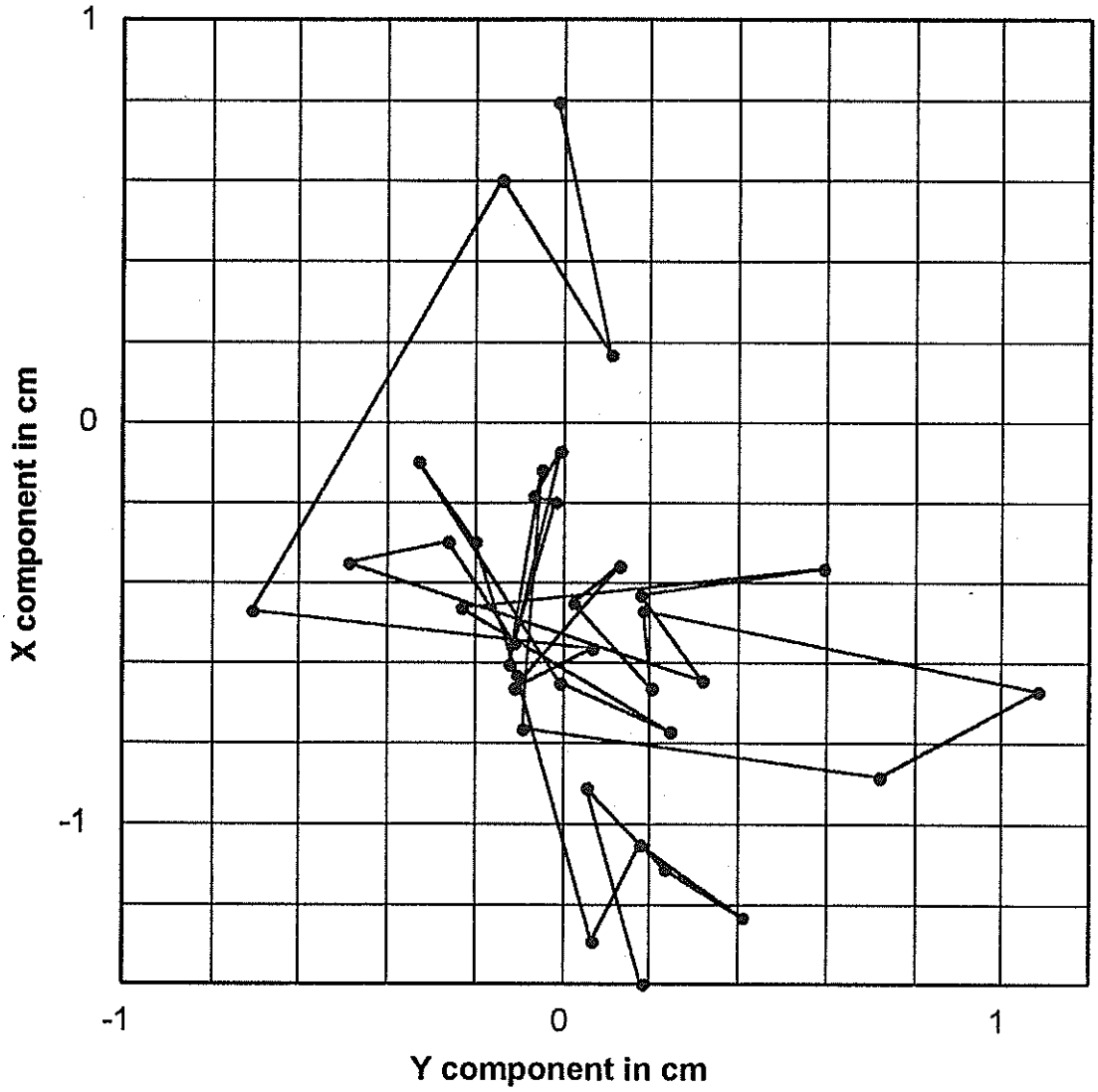

Figure 3: Geocenter estimates from a global solution using SLR observations from LAGEOS 1 and II show a 5 mm RMS scatter in x and 3 mm scatter in y. The motion is restricted to an area of 2.4 cm by 2.2 cm, which is the size of a domestic postage stamp (U.S. or Chinese): most of the variation occurs within a block which is only one centimeter square.

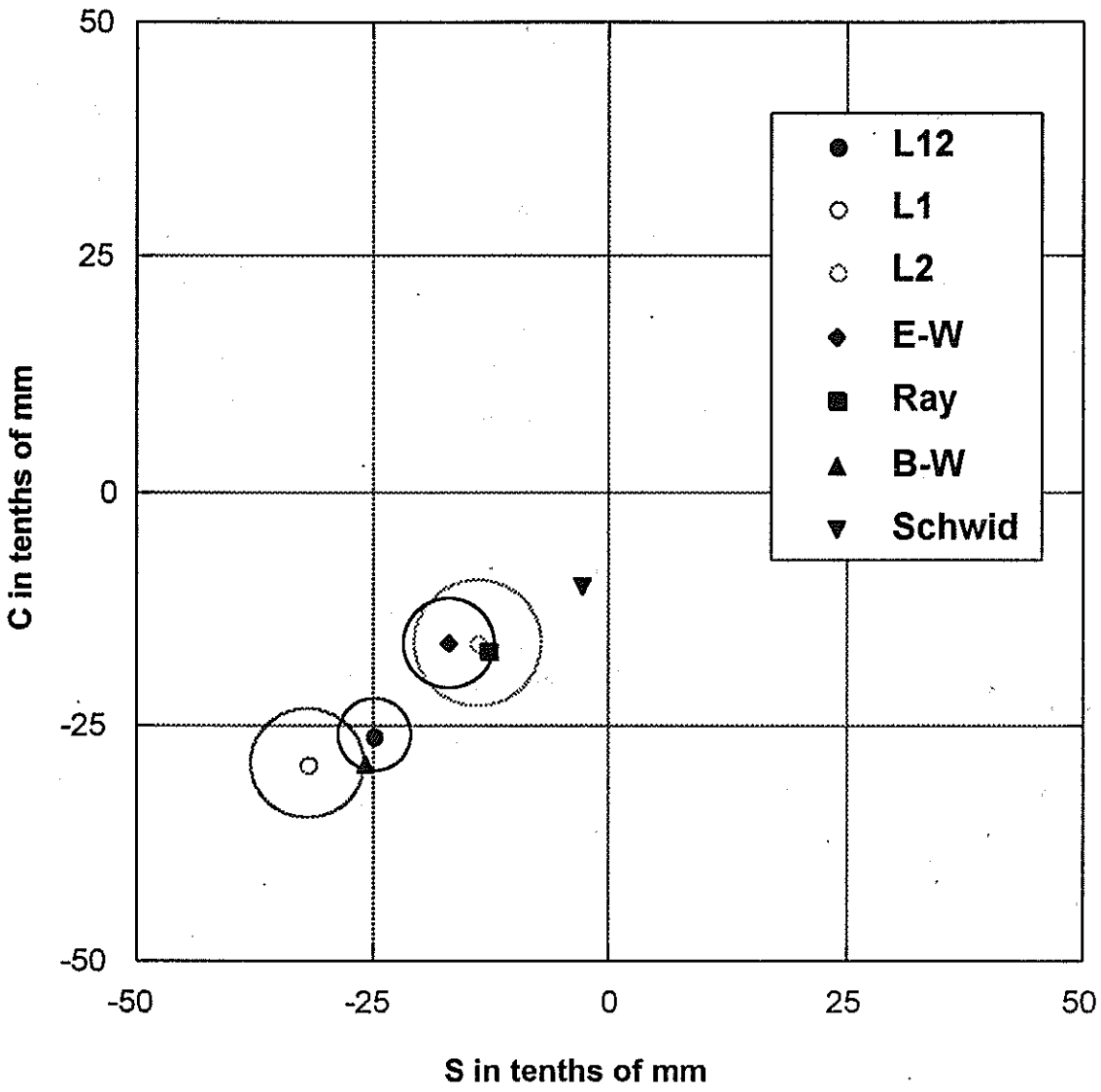

Figure 4: Tidal coefficients for geocenter variations of the Z-component predicted by three theoretical models at the M2 frequency are compared with measured values from CSR (diamond) and with GSFC solutions using LAGEOS I, LAGEOS II (open circles), and a LAGEOS I/II combination (closed circle)

Quality Checks within the EUROLAS Cluster

G.M. Appleby
Royal Greenwich Observatory,
Madingley Road,
Cambridge CB3 0EZ,
England

1 Introduction

The cluster of European satellite laser ranging stations (EUROLAS) provides a unique opportunity to monitor the precision and accuracy of the observations routinely carried out by a group of high-precision systems. Analysis of simultaneously tracked passes has the potential to identify at the centimeter level subtle biases in the measurements of one station with respect to others, and provide early warning of possible system degradation. On behalf of the EUROLAS stations, the Royal Greenwich Observatory (RGO) has begun a feasibility study to determine whether such a technique can add significant new information on potential observational bias to that already available on a routine weekly basis from the Center for Space Research, University of Texas. The strategy that we adopted is to compute month-long orbits and fit them to sets of on-site Lageos and Lageos-2 normal points, using the RGO SLR analysis package SATAN. Passes within the data sets that were tracked simultaneously by two or more Eurolas stations are then used to form short-arc corrections to the orbit, and residuals from the corrected orbit used to monitor observational bias. The results in numerical and graphical form from the monthly long-arc and from the Eurolas short-arc solutions are made available to the tracking and analysis community via the World Wide Web, ideally within a few days of the end of each month. The results are accessible via the Web pages of the RGO (http://www.ast.cam.ac.uk/RGO)
This paper describes the methods used and results to date, and points to potential further development.

2 Monthly Solutions

30-day orbits of Lageos-1 and Lageos-2 are fitted to the normal point data available through the CDDIS, using tracking station coordinates and velocities taken from the ITRF94 solution. We adjust the initial state vectors of the satellites, a solar radiation coefficient and empirical along-track acceleration, and also solve for corrections to the initial set of Earth rotation parameters, which are taken from the IERS Bulletin A results. We finally achieve a post-fit residual rms of about 6 cm for both satellites, where rejection of outliers is carried out at about a 3-sigma (20 cm) level. The series of post-solution range
residuals for each station provides a graphic indication of the general health of the system; any systematic trends or out-lying points indicate some bias in the range or epoch measurement, or transient fault in the on-site noise filtering process. Shown in Figure 1 are four typical sets of range residuals from a fitted orbit of Lageos-2 for 1997 February. The residual scale is +/- 1m, and deliberately no data editing has been carried out when generating the plots. Any residuals that were greater in size than one meter have been set equal to 1m for the plots. Included in the plots are the means and standard deviations of the residuals that were accepted for the orbital fitting process.

2.1 Discussion

From several months of such analyses, we find that some stations performed significantly better than others. The best stations produce almost no outliers, have residual mean values close to zero and residual standard deviations of around 30-40mm, which principally reflects the precision of the 30-day orbital model. However some stations do show clear bias and often produce significant numbers of out-lying points. There is also evidence that such bias values are sometimes different for each pass. Of course it is inevitable that the data produced by a large number of disparate systems will be variable in precision; some stations do not have access to the highest precision interval counters, or the shortest laser pulses or the fastest detectors. However, it is considered vital that all stations make every effort to eliminate systematic bias from their data, since it cannot be right that the analyst should have to estimate in some cases large pass-by-pass bias as well as the geodetic or geophysical parameters which he seeks. It is also very important that the numbers of outlying points are reduced considerably, since such data lead to great difficulty for orbit determination, particularly if the tracking data is sparse, or the initial orbit poorly known. We feel that the availability of these simple residual plots may act as a stimulus for improvement.

We could use these residuals to solve for station range and time bias values. However, measurement bias determined in this way may be corrupted by imperfections in the force model used, thus limiting the effectiveness of the long-arc solution for precise determination of system bias.

3 Short-Arc Solutions

We can remove much of the effect of force model error by using a short arc technique to solve both for corrections to the long-arc orbit and for station range and time bias. The method used here is that developed at RGO (Sinclair, 1989) and requires that at least two stations quasi-simultaneously track a given satellite pass. For each of the short-arcs that pass this criterion, we use a constrained six-parameter model to correct the orbit in the along-track, cross-track and radial directions, and also to solve if required for station range and time bias. We now use this method to analyse Lageos-1 and Lageos-2 observations made by the EUROLAS Cluster of stations. We take a core set of the best Eurolas stations, find the passes of Lageos-1 and Lageos-2 that were tracked by two or more of these stations, and use their observations in an iterative solution to correct the original long arc orbit, for the duration of each of the passes. Typical values of the post-fit residual rms are at the 1 or 2 cm level. We then compute residuals from these improved orbits for all the Eurolas stations that were tracking the passes, and finally carry out a simultaneous solution for orbit corrections and time and range bias for selected stations. To complement these numerical results, we plot for each pass the range residuals for all the tracking stations prior to the final solution for range and time bias. In this way, we can visualize those stations whose observations stand off from the corrected orbit. We consider that biases at the level of one or two cm can be routinely determined by this method. However, we do emphasize that all such residuals are with respect to the coordinates of the stations given in the ITRF94 solutions; deliberately no adjustments to those coordinates have been carried out. Such a re-adjustment will be the aim of further work on this topic. Shown in Figure 2 are four sets of residuals derived from this short-arc technique. All residuals that are greater than the range of the plot axes (± 10cm) are set equal to ± 10cm, and thus appear at the limits of the plot. The versions of the plots presented on the WWW are colour-coded with a key to identify residuals with station numbers; as a guide to station identification for the results shown in monochrome in Figure 2, we change with tracking station the symbols used to plot the points, from a

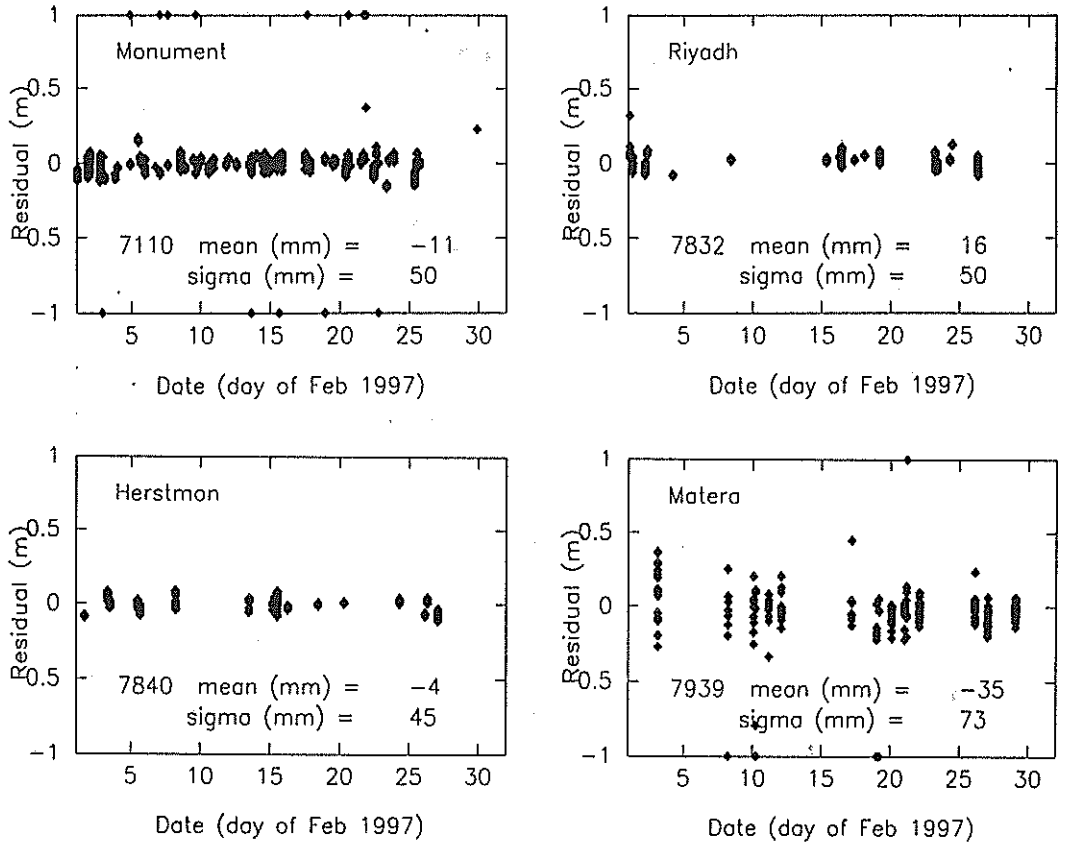

Figure 1: Range residuals from month-long Lageos-2 orbit.

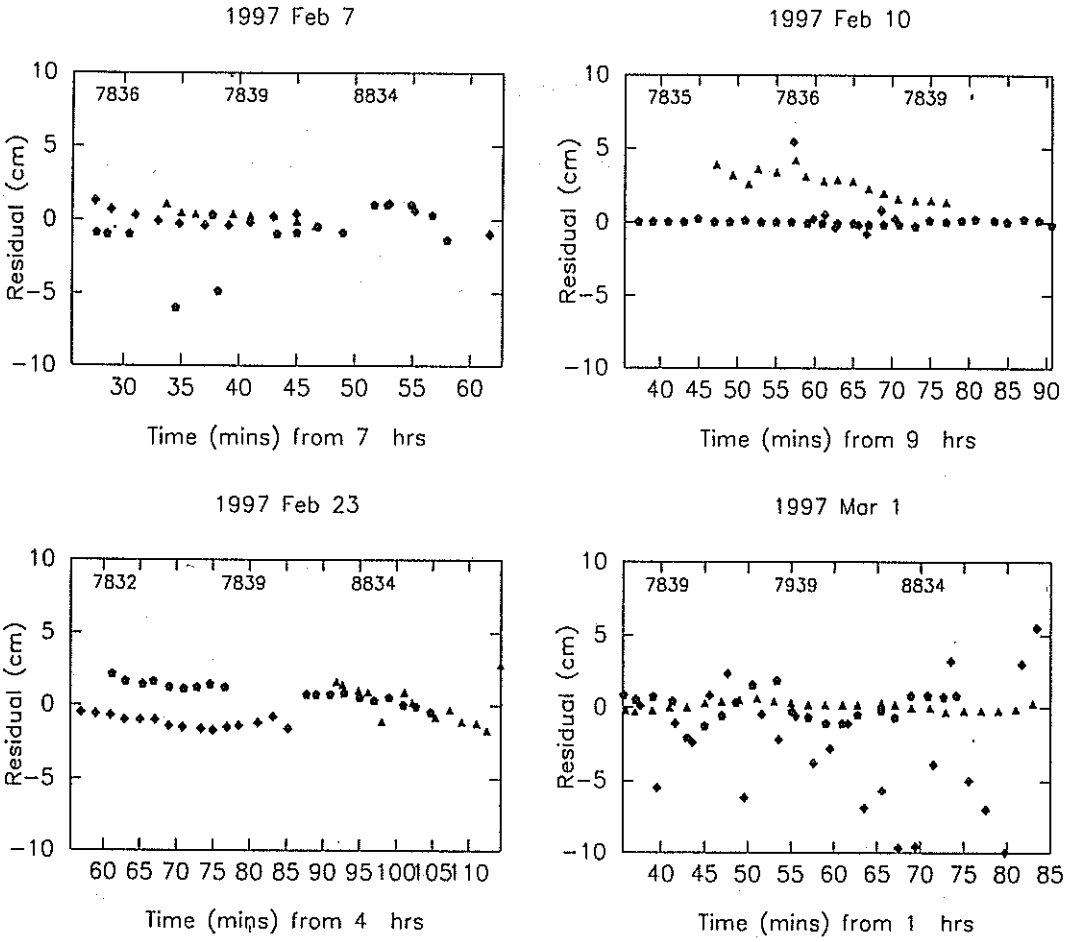

Figure 2: Range residuals from short-arc solutions.

triangle for the first station in the key, to a square for the next, to a pentagon for the next and so on.

3.1 Discussion

The plots show that most of the residuals are small, with occasional out-lying points, and occasional clear bias in the measurements from one or more stations. Also clear is the different precision achieved amongst the cluster of stations. We consider that at the very least the method clearly identifies individual out-lying points at the level of a few cm, and should thus be useful for stations wishing to trace the cause of such problems.

The power of the method is illustrated by the pass observed by the three stations 7835 Grasse, 7836 Potsdam and 7839 Graz on 1997 February 10, where post-solution residuals are shown in the second plot of Figure 2. Observations from Potsdam and Graz were used initially to correct the long-arc orbit for the duration of the 50-minute pass, and then observations from all three stations were used to solve additionally for time and range bias for those stations. A single out-lying point was identified for Potsdam, and for Grasse we determined a significant range-bias (28 ± 1mm) and time-bias ($-7 \pm 1\mu$s). We note that the weekly analyses carried out at the University of Texas assume for Grasse a constant range bias of 30mm, in good agreement with our result for this single pass. As a further check on our procedure, we took the observations from all three stations and used them to solve for corrections to the orbit. The resulting residuals showed significant trends, confirming that the method is sensitive to bias in one or more of the sets of observations, and cannot absorb such bias into meaningful corrections to the orbit.

We have also carried out a similar short-arc analysis for four NASA stations working in the USA. The stations involved are 7080 MLRS at McDonald, 7105 Moblas 7 at GGAO, 7110 Moblas 4 at Monument Peak and 7210 at Mt Haleakala, Hawaii. At present, we have used only Lageos-1 for this analysis. The arcs tend to be shorter than those tracked by the European stations because of the greater inter-site distances between the NASA stations, but in general the agreement between the systems is very good. Results from these solutions are also available on the WWW.

4 Further Development

To be of maximum use to the tracking community, and to complement the work carried out by the University of Texas, we consider that these results should be available very soon after the observations have been made. Ultimately we plan to generate automatically short-arc solutions as soon as suitable observations from the EUROLAS cluster are available. In this way system problems can be rapidly identified, ideally before the data are made available to the analysis community. We will also consider analysing data from other lower or higher satellites, in order to distinguish constant range bias from scale error, such as might arise from a frequency error in the time-of-flight measurement device. A preliminary analysis using residuals from Lageos-1, Lageos-2, Etalon-1 and Etalon-2 to solve simultaneously for orbital corrections and station bias has suggested for example that station 7236 Wuhan has a scale measurement error of some 75mm per Mm. Such a method using Stella, Ajisai, Topex/Poseidon and Lageos has been successfully applied by

Eanes, Bettadpur and Reis (1996), and we feel that the short arc technique described here could also make a contribution to this particular investigation.

5 References

Eanes, R.J., S.V. Bettadpur, J.C. Reis. 1996. Multi-Satellite Laser Range Residual Analysis for Quality Control of the SLR Network. In Proc. Ninth International Workshop on Laser Ranging Instrumentation, Vol 1, pp 131-146, Canberra.

Sinclair, A.T. 1989. The determination of station coordinates and baselines from the 1986 and 1987 WEGENER/MEDLAS data by global and short-arc solutions. Fourth international conference on the WEGENER/MEDLAS project, Schevenin

COMPACT LASER TRANSPONDERS FOR INTERPLANETARY RANGING AND TIME TRANSFER

John J. Degnan
NASA Goddard Space Flight Center
Greenbelt, MD 20771 USA

ABSTRACT

A conceptual design for a laser transponder, capable of precision ranging and time transfer to spacecraft orbiting about or on the surface of the inner planets of the solar system , is described. The proposed transponder, designed to operate in conjunction with the SLR2000 satellite laser ranging system, makes use of two key SLR2000 subsystems - a high repetition rate Q-switched microlaser transmitter and a correlation range receiver (CRR) which simultaneously provides centimeter precision ranging and subarcsecond level pointing corrections, even in a high background noise environment. A third important element is an ultraminiature laser-diode pumped cesium atomic clock developed by Westinghouse Corporation for the Advanced Research Projects Agency (ARPA).

The proposed transponder optical head contains a small (15 cm diameter) telescope and a low power (300 mW) microlaser transmitter and is designed to mount on the microwave communications antenna of a planetary lander or orbiter. It is assumed that the microwave communications link provides the initial crude pointing (to $\pm$ 0.3° or about 10% of the microwave beamwidth); this allows the transponder optical head to be mounted on either a two-axis tilt table or gimbal mount of limited angular range. The onboard CRR, combined with a quadrant detector, provides subarcsecond pointing angle corrections during two-way transponder operations. We demonstrate through analysis that a 2 Khz Asynchronous Transponder/ SLR2000 system, operating between Mars and Earth, is capable of recording up to several thousand two way measurements per minute and several tens of thousands of one way measuements per minute. Two way measurements allow determination of the range and the time offset between the ground and spaceborne clocks whereas one way ranges help to maintain a common boresight between the Mars and Earth-based systems and enable temporal locking as well. Decimeter accuracy interplanetary range measurements and subnanosecond clock offset determinations can easily be achieved. Improved accuracies may be possible if a ground-based maser is used to drive the SLR2000 system and "discipline" the spacecraft clock. Based on past experience with the Viking lander on Mars, current microwave system precisions appear to be limited at the few meter level. Furthermore, unlike microwaves, the absolute accuracy of an optical link is not affected by uncertainties in propagation delays induced by the interplanetary solar plasma.

1. INTRODUCTION

Lunar laser ranging (LLR) has been routinely achieved by only three stations over the past 28 years since Apollo 11 carried the first passive retroreflector array to the Moon in July, 1969 [1]. For good reasons, all LLR stations (McDonald Observatory in Texas, Grasse in France, and HOLLAS on Mt. Haleakala in Hawaii) were located at astronomical sites with above average atmospheric "seeing", and they typically employed the largest telescopes and most powerful lasers in the SLR network . In spite of these advantages, the mean signal strength is still well below a single photoelectron because of the familiar R^4 dependence of signal strength on range. The signal return rates from the Moon are sufficiently low that lunar operations are only carried out at night using special post-detection Poisson filtering techniques which extract the range signal from background noise [2] although it should be mentioned that the McDonald Laser Ranging System (MLRS) has recently demonstrated a strong lunar capability with a relatively modest telescope aperture (76 cm) and laser energy (on the order of 100 mJ) [3]. The scientific information extracted from centimeter accuracy LLR data has been enormous and includes ultraprecise measurements of the lunar ephemeris and librations, insights into the internal makeup of the Moon, as well as important tests of General Relativity and its associated metrics [1]. The

ability to extend these precise range measurements to the inner planets, or to spacecraft in orbit about the Sun, would certainly result in a similar array of important scientific results.

The most precise ranging to another planet was achieved when the radio telescopes of the NASA Deep Space Network (DSN) were in communication with the Viking Lander on Mars. This two-way microwave link resulted in measurements at the subdecameter level with 3 meters precision being the best internal consistency ever reported [4]. However, absolute range accuracies over interplanetary distances are limited by the presence of the interplanetary solar plasma which, like the similarly charged ionosphere, can have a significant impact on the propagation delay at microwave frequencies. Light frequencies, on the other hand, are much too high to be affected by the charged solar plasma, and therefore transmission media-dependent range errors are largely limited to propagation delays in the Earth and ,in the case of a Lander, planetary atmospheres which are on the order of a centimeter or less. Furthermore, the shorter optical wavelengths allow the transmitted energy to be propagated in tight, few arcsecond divergence beams resulting in larger photon fluxes and smaller collecting and transmitting apertures at both ends of the link. On the down side, much improved pointing is required to take advantage of the reduced divergence.

Although modern SLR systems, using picosecond pulse lasers and high bandwidth receivers, are capable of few mm ranging precisions and 50 picosecond time transfer between remote clocks over typical near-Earth satellite distances, extending these unique capabilities to the inner planets and beyond requires that we solve a number of important new technical issues. First of all, to overcome a prohibitively large R^4 loss, we must abandon our usual single-ended SLR station and utilize two-way laser links which we will refer to generically as "transponders". The use of microwave or laser transponders had previously been proposed for lunar ranging [5].

2. LASER TRANSPONDERS

In the simplest and most familiar transponder scheme, the ground station sends out a pulse which is detected at the spacecraft and triggers a response pulse which is in turn received by the ground station. We will refer to this as an "echo transponder". With this type of transponder, one can subtract the delay between the received and transmitted pulses at the spacecraft from the overall roundtrip time-of-flight (TOF), as measured by the ground station, to compute a range to the spacecraft. The transponder delay is either known a priori from careful preflight calibration or measured onboard the spacecraft and transmitted via microwave communication link to the ground station. The signal return rate at the ground station is then equal to the fire rate of the laser multiplied by the probability that pulses are detected at both ends of the link. This simple approach works very well when there is in a high probability of detection on both ends of the link, i.e. when both the uplink and downlink are strong and pointing uncertainties are small compared to the transmitted beamwidths. For example, an echo transponder would work quite well in conjunction with the SLR2000 ground station over lunar distances since the photon fluxes are high and well above the threshold for detection due to the smaller R^2 losses (see Figure 3). A one inch telescope aperture on the Moon would collect hundreds of SLR2000 photons per pulse in spite of its low output energy on the order of 150 μJ. However, over interplanetary distances, it is worthwhile considering an alternative approach, the "asynchronous laser transponder", which can operate effectively even when mean signal strength and detection probabilities are relatively small.

In the asynchronous laser transponder, shown in Figure 1, the ground and spacecraft lasers both fire independently at a common predetermined rate, R. The times of departure and arrival of the outgoing and incoming pulses are recorded at each end of the link and timetagged with respect to their respective system clocks. There are four possible outcomes within a given "transponder cycle" of period $\tau_c = 1/R$.

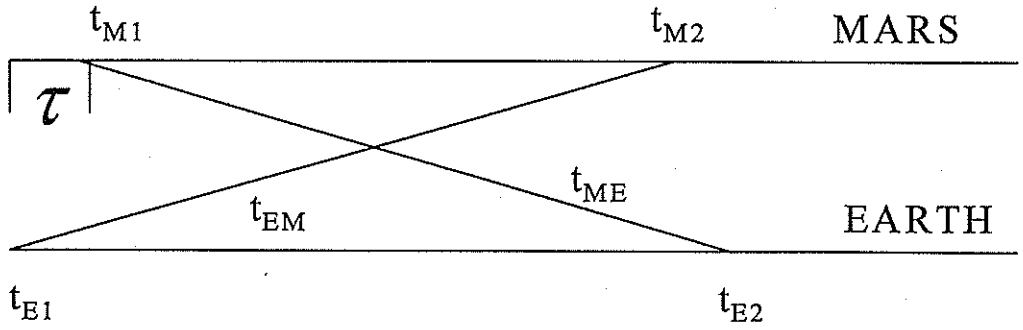

Figure 1: Timing diagram for an asynchronous laser transponder on Mars exchanging pulses with an Earth station. A pulse leaves the Earth station at time t_{E1}, travels to Mars in a time t_{EM}, and arrives at Mars at time t_{M2}. During the same transponder cycle, a pulse is transmitted from Mars at time t_{M1}, travels to Earth in a time t_{ME}, and arrives on Earth at time t_{E2}. Times of departure and arrival are referenced to that terminal's clock, and the Mars values are transmitted to Earth over the microwave communications link. The quantity τ is the time interval between the departure of pulses from the Earth and Mars stations within the same transponder cycle (500 μsec time bin for a 2 KHz system) and, combined with the outgoing pulse times, provides the offset between the ground and spacecraft clocks.

(1) No incoming pulses are detected at either terminal = $(1-P_s)(1-P_g)$
(2) An incoming pulse is detected only at the ground station = $P_g(1-P_s)$
(3) An incoming pulse is detected only at the spacecraft = $P_s(1-P_g)$
(4) Incoming pulses are detected at both ends of the link = P_gP_s

We will refer to outcome (1) as a "null event", to (2) and (3) as "one-way events", and (4) as a "two way event". Two way events allow the post facto calculation of an instantaneous spacecraft range and spacecraft clock offset via the equations:

$$R=\frac{c}{2}\left(t_{ME}+t_{EM}\right)=\frac{c}{2}\left[\left(t_{E2}-t_{E1}\right)+\left(t_{M2}-t_{M1}\right)\right] \qquad (1)$$

$$\tau=\frac{\left[\left(t_{E2}-t_{E1}\right)-\left(t_{M2}-t_{M1}\right)\right]}{2\left(1+\frac{\dot{R}}{c}\right)} \qquad (2)$$

where the intervals $\left(t_{E2}-t_{E1}\right)$ and $\left(t_{M2}-t_{M1}\right)$ are measured by the Earth and spacecraft rang receivers respectively. In (1) and (2) , R and τ are the instantaneous range and clock offset at the point in time when the "photon world lines" marked t_{EM} and t_{ME} in Figure 1 cross each other.

In (2), the small correction term, $\dot{R}/c$, corresponding to the instantaneous range rate between the Earth station and the spacecraft divided by the speed of light, can be estimated from planetary ephemerides or the microwave communications link or iteratively solved for from the laser range data.

Null events provide no useful information and can be ignored. At a minimum, one way events provide a means of acquiring and tracking (in both angle and time) the opposite terminal togreatly improve the probability of a two way event. Combined with one-way events observed in the opposite terminal during other transponder cycles, they may permit accurate interpolation of range and clock offsets between two way events.

3. MEASUREMENT ACCURACY

Unlike artificial satellite ranging, clock effects can dominate interplanetary ranging errors with interplanetary pulse transit times on the order of several minutes. From Equations (1) and (2), the errors in the measured range and clock offsets due to a constant frequency offset error in the Earth and spacecraft clocks are

$$\Delta R = \frac{c}{2}\left[\Delta\left(t_{E2}-t_{E1}\right)+\Delta\left(t_{M2}-t_{M1}\right)\right] \approx \frac{R}{2}\left[\frac{\Delta f_E}{f_E}+\frac{\Delta f_M}{f_M}\right] \qquad (3)$$

and

$$\Delta\tau = \frac{\left[\Delta\left(t_{E2}-t_{E1}\right)-\Delta\left(t_{M2}-t_{M1}\right)\right]}{2\left(1+\frac{\dot{R}}{c}\right)} \approx \frac{R}{2c\left(1+\frac{\dot{R}}{c}\right)}\left[\frac{\Delta f_E}{f_E}-\frac{\Delta f_M}{f_M}\right] \qquad (4)$$

We see from the latter equations that the fractional error in range is equal to the average of the fractional errors in the two clocks whereas the fractional error in the spacecraft clock offset is proportional to the difference between the fractional errors in the two clocks. The variance in the range and offset measurements is in turn given by

$$\left\langle \Delta R^2 \right\rangle \approx R^2\left[\frac{\left\langle \Delta f_E{}^2 \right\rangle}{f_E{}^2}+\frac{\left\langle \Delta f_M{}^2 \right\rangle}{f_M{}^2}\right] \qquad (5)$$

and

$$\left\langle \Delta\tau^2 \right\rangle \approx \left(\frac{R}{2c\left(1+\frac{\dot{R}}{c}\right)}\right)^2\left[\frac{\left\langle \Delta f_M{}^2 \right\rangle}{f_M{}^2}+\frac{\left\langle \Delta f_E{}^2 \right\rangle}{f_E{}^2}\right] \qquad (6)$$

for two independent free-running clocks.

Thus, the single shot ranging precision and time transfer will be limited by the less accurate of the ground and spaceborne clocks. If both clocks were of maser quality (1×10^{-15} over time intervals of several minutes), clock instabilities would introduce submillimeter errors over distances of 1 AU and range accuracy would be limited at the cm level by uncertainties in the atmospheric propagation path as in SLR. If the spaceborne clock had the stability of a good rubidium (1×10^{-12}), as discussed in the next section, decimeter single shot range accuracies would result. With respect to single shot time transfer, the latter clock would introduce errors on the order of 250 picoseconds.

4. A TRANSPONDER CONCEPTUAL DESIGN BASED ON SLR2000

Laser and receiver technology being developed for SLR2000 lends itself extremely well to the interplanetary transponder problem because the system is designed to operate in daylight at mean signal levels as small as .0001 photoelectrons [6,7].As a result, few demands are placed on either the ground or space segments with regard to size, weight, or prime power in order to accomodate high power lasers or large optical telescopes and their equally large pointing gimbals.

A conceptual design for an asynchronous laser transponder, capable of decimeter precision ranging and subnanosecond time transfer to spacecraft orbiting about, or on the surface of, the inner planets of the solar system , is described in Figure 2. The transponder, which is designed to operate in conjunction with the SLR2000 satellite laser ranging system, makes use of two key SLR2000 subsystems - a high repetition rate Q-switched microlaser transmitter [8] and a correlation range receiver (CRR) which simultaneously provides centimeter precision ranging and subarcsecond level pointing corrections, even in a low signal-to-noise environment [6]. A third important element is an ultraminiature laser-diode pumped cesium atomic clock [9] developed by Westinghouse Corporation for the Advanced Research Projects Agency (ARPA) which weighs only 60 grams and has a spatial volume of 25 cm^3, a power consumption of only 300 mW, and the performance of a good rubidium time reference (i.e. 1 part in 10^{12} over several minute intervals typical of interplanetary light transit times).

The microlaser is anticipated to be very lightweight and could be designed to operate at about 15% optical efficiency with only a few watts of prime power to the pump diodes. A flight-qualified event timer, the major component of the CRR, has been developed by the Smithsonian Astrophysical Observatory (SAO). It has a 10 picosecond resolution, weighs less than 1 Kg, and consumes about 9.25 Watts of prime power [10]. With the exception of the flight computer, which is expected to consume on the order of 7 Watts, the other transponder components in Figure 3 consume little or no power, and it is therefore not unreasonable to propose an interplanetary laser transponder weighing a few Kg and consuming less than 20 Watts of power.

The transponder optical head contains a small (15 cm diameter) telescope and a low power microlaser transmitter and is designed to mount on the microwave communications antenna of a planetary lander or orbiter. It is assumed that the microwave communications link provides the initial crude pointing to about $\pm$ 0.3° or roughly 10% of the microwave beamwidth for a nominal one meter antenna operating in X-band (7.9 GHz). This allows the transponder optical head to be mounted on either a two-axis tilt table or gimbal mount of limited angular range. These can be driven by simple stepper motors.

The distance between Earth and Mars is routinely known to about 100 meters using ephemerides provided by the Jet Propulsion Laboratory [4], and, as mentioned previously, microwave communications to the lander reduces this uncertainty below 10 meters. Thus, if we knew when the pulse left the opposite terminal, the pulse arrival time uncertainties would be between 100 nsec and 1 μsec , similar to the range gates used by SLR2000 in acquiring artificial satellites in daylight. However, due to the asynchronous nature of the link, the pulse departure time from the opposite terminal is generally not known a priori (although prior successful transponder experiments can greatly narrow the range of search if the laser fire times are tied to their respective clocks). At night, the relatively narrow transponder field of view defined by the microwave antenna pointing uncertainty can be monitored for incoming pulses by an integrating CCD array in the telescope focal plane which views the Earth through a narrowband 532 nm filter. A rapid buildup of photoelectron counts within one or more localized pixels in the approximate 200 by 200 pixel array indicates the presence of a beam from Earth and provides an intermediate

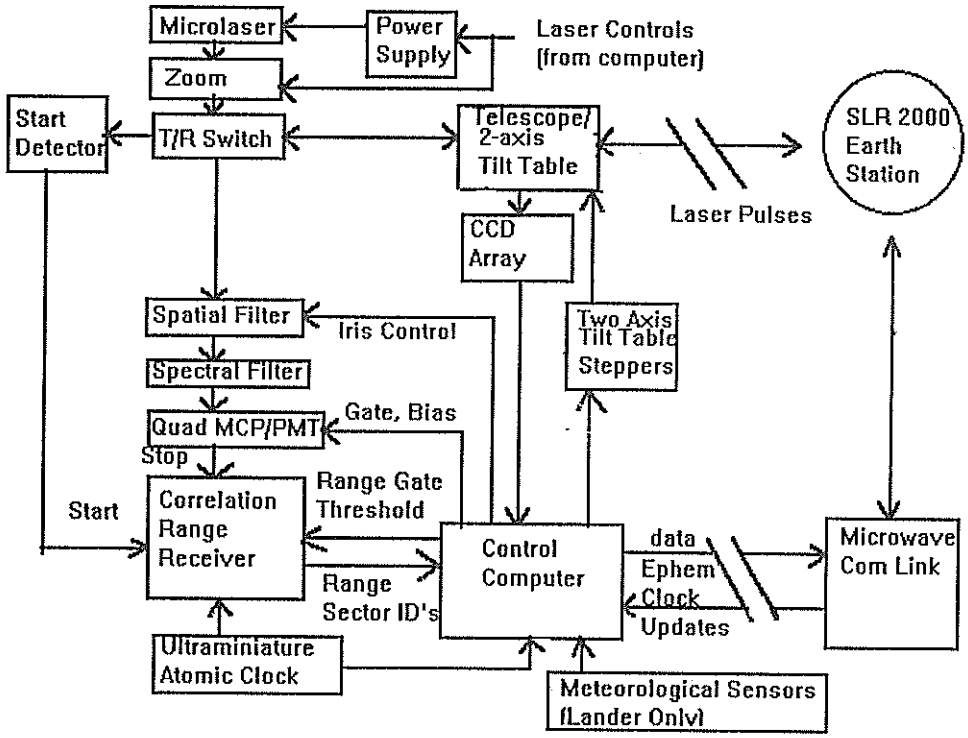

Figure 2: Block diagram of an Asynchronous Laser Transponder working in tandem with an SLR2000 Earth Station.

level of pointing correction at the few arcsecond level which places the Earth station within the transponder beam. In daylight, one can add an optical gating mechanism, if necessary, to reduce background noise . In the worst case,a terminal in daylight conditions must conduct a temporal scan of the range gate over the 500 μsec cycle time (in few microsecond increments) in order to acquire and lock onto the opposite terminal. Fortunately, the Earth station pointing can be quite accurate due to a combination of precise ephemerides, routine star calibrations, and accurate mount modelling.

The Q-switched microlaser emits 150μJ, 140 psec pulses at a repetition rate of 2 KHz through the 15 cm telescope which reduces the transponder beam divergence to about 40 μrad (2X diffraction limit). During transponder operations, the onboard CRR, with input from the quadrant timing detector, provides fine pointing angle corrections at the subarcsecond level [6] and keeps the small transponder telescope pointed at the Earth source while the ground-based SLR2000 receiver performs a parallel function using the incoming transponder pulses as a guide.

5. EXAMPLE: EARTH-MARS LINK USING SLR2000 AS A BASE STATION

We now consider the example of SLR2000 ranging to a transponder on the surface of Mars. Among the inner planets, this represents a worst case scenario since the distance between Earth and Mars varies between 0.52 and 2.52 astronomical units (between 80 and 380 Million Km). The output energies of both Nd:YAG microlasers are set at 150 μJ per pulse, the maximum eyesafe energy allowed for an Earth-based telescope aperture of 40 cm. With a repetition rate of 2 KHz, this corresponds to an average output power at the green 532 nm wavelength of 300 mW. On the transponder end, where there are (presumably) no eye safety issues , the radiation exits through a relatively small 15 cm transmit/receive aperture. The full angle beam divergence at both ends of

the link is assumed to be the SLR2000 value of 40 microradians. We have also assumed a rather conservative value for the detector quantum efficiency (20%) and realistic values for the throughput of the transmit (80%) and receive (54%) optics and the atmospheric channel (70%) on each end of the link. We further assume that the threshold is set at one photoelectron at both ends of the link resulting in a probability of detection given by Poisson statistics

$$P_D = 1 - e^{-n_s} \approx n_s \tag{7}$$

where n_s is the mean signal level (different at the two terminals due to the different collecting aperures)and the approximation holds for $n_s << 1$. Over the range of Earth-Mars distances, mean signal n_s varies from about 0.1 to about .005 pe/pulse for the Mars terminal and about a factor of seven higher at the Earth terminal due to its larger telescope. Thus, the Earth terminal records about seven times more one way eventsthan the Mars terminal.

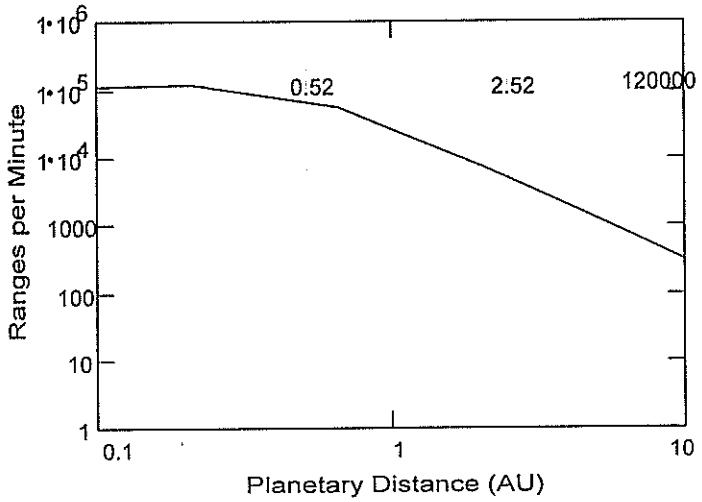

Figure 3: The number of "two-way" events (dashed line) and the number of non-null events (solid line) per minute as a function of range in AU. The Mars-Earth distance varies between 0.52 and 2.52 AU and represents a worst case for the inner solar system. The SLR2000 laser fire rate is 120,000 pulses per minute (2 KHz).

In Figure 3, the number of "two way" events per minute is represented by the curved dashed line whereas the curved solid line represents the summed rate of "two-way" and "one-way" ("non-null") events. The SLR2000 laser fire rate of 120,000 pulses per minute is indicated by the horizontal dashed line near the top of the graph and is included for reference. The two verical dashed lines represent the extremes of the Earth-Mars distance. We note from the figure that the number of "two-way" events varies from several thousand per minute at its nearest approach to Earth (0.52 AU) to about 20 per minute as Mars moves to the opposite side of the Sun from Earth (2.52 AU). Similarly, the number of "non -null" events (sum of one-way and two-way events) falls from several tens of thousands per minute to several thousand per minute. This high "non-null" rate should allow both the ground and space-based systems to effectively lock onto each other with respect to both pointing angle and range gate. Note that, with the simple "echo transponder" discussed previously, the ground station would only record events at the "two-way" rate since the "echo transponder" only fires a pulse upon detecting a pulse from Earth. Thus, an "echo transponder" makes it much more difficult for the Earth station to actively lock onto the spacecraft laser relative to the asynchronous case, although, as mentioned previously, open loop pointing to the spacecraft should be relatively accurate.

6. SUMMARY

We have demonstrated through analysis that a compact, low power Asynchronous Laser Transponder working with the SLR2000 system, each operating at 2 KHz rates between Mars and Earth, is capable of recording up to several thousand two way measurements per minute and several tens of thousands of one way measurements per minute. Two way measurements allow precise determination of the range and the time offset between the ground and spaceborne clocks whereas one way ranges help to maintain a common boresight between the Mars and Earth-based systems and can potentially provide other useful information. Due to interplanetary light travel times which are several orders of magnitude longer than is typical for artificial satellites, the absolute accuracy of the range and clock offset measurements is determined more by the frequency accuracy and stability of the ground and spaceborne clocks than by errors in the range vernier or propagation delays in the transmission channel, which are typically at the subcentimeter level. Decimeter accuracy interplanetary range measurements and subnanosecond time transfer would appear to be easily achievable with the conceptual system described here. If a ground-based maser were used to govern the SLR2000 timing and to "discipline" the onboard ultraminiature atomic clock, significantly greater accuracies might be achieved. Based on past experience with the Viking lander on Mars, current microwave system precisions appear to be limited at the few meter level. Furthermore, unlike microwaves, the absolute accuracy of an optical link is not affected by uncertainties in propagation delays induced by the interplanetary solar plasma.

REFERENCES

1. Dickey, J. O. , P. L. Bender, J. E. Faller, X. X. Newhall,R. L. Ricklefs, J. G. Ries, P. J. Shelus, C. Veillet, A. L. Whipple, J. R. Wiant, J. G. Williams, and C. F. Yoder, "Lunar laser ranging: a continuing legacy of the Apollo Program", Science, 265, pp. 482-490, 1994

2. Abbott, R. I., P. J. Shelus, R. Mulholland, and E. Silverberg, "Laser Observations of the Moon: Identification and Construction of Normal Points for 1969-1971", The Astronomical Journal, 78, pp. 784-793 , 1973.

3. Shelus, P. J., J. R. Wiant, R. L. Ricklefs, A. L. Whipple, and J. G. Rie, "The impact of technology on LLR at MLRS", these Proceedings

4. Lemoine, F. J., NASA Goddard Space Flight Center, private communication.

5. Bender, P. L., J. E. Faller, J. L. Hall, J. J. Degnan, J. O. Dickey, X.X. Newhall, J. G. Williams, R. W. King, L. O. Machnik, D. O'Gara, R. L. Ricklefs, P. J. Shelus, A. L. Whipple, J. R. Wiant, and C. Veillet, "Microwave and Optical Lunar Transponders", in Astrophysics from the Moon, AIP Conf. Proc. Series, (American Institute of Physics New York) April, 1990.

6. Degnan, J. J. , J. McGarry, T. Zagwodzki, P. Titterton, H. Sweeney, H. Donovan, M. Perry, B. Conklin, W. Decker, J. Cheek, A. Mallama, and P. Dunn, "SLR2000: An inexpensive, fully automated, eyesafe satellite laser ranging system", these proceedings.

7. McGarry, J., "SLR2000 Performance Simulations", these proceedings

8. Degnan, J. J., "Optimal Design of Q-switched Microlaser Transmitters for SLR", these proceedings.

9. Lieberman , I. and H. Nathanson, Westinghouse Corporation, Pittsburgh, PA, USA, private communication.

10. Mattison, E., Smithsonian Astrophysical Observatory, Cambridge, Massachusetts, USA, private communication.

A Wide Angle Airborne or Spaceborne Laser Ranging Instrumentation for Millimeter Accuracy Subsidence Measurements

O. BOCK and M. KASSER
Ecole Supérieure des Géomètres & Topographes, 18 allée Jean Rostand, 91025 EVRY Cedex, France

Ch. THOM
Institut Géographique National, Laboratoire d'Optoélectronique et de Microinformatique, 2 avenue Pasteur, BP 68, 94160 Saint Mandé, France.

I. INTRODUCTION

A wide-angle airborne laser ranging system is under investigation at IGN [i, ii]. This system is intended to achieve a new geodesy technique, based on aerial multilateration. Extension to a spaceborne system is also considered. The technique should have the capability of detecting height displacements of ground-based benchmarks with sub-millimeter accuracy in a very short time (a few hours). It would be particularly adapted to the daily monitoring of a network of typically 100 benchmarks, extending over an area of 10 by 10 km. For instance, it would be adequate for estimating surface effects induced from fluid withdrawal or solid extraction [iii]. But it can be extended to periodic monitoring of more general geophysical processes where a millimeter accuracy of the vertical component is required, e.g., tectonics, volcanology, and geology. Assuming that some benchmarks are fixed, i.e., that they are far away from the deformation area, only relative locations are to be considered since one is interested in displacements not locations.

Airborne or spaceborne laser ranging systems, with the ranging system onboard, appear as attractive solutions for monitoring large networks of ground-based retroreflectors. Several such systems have been studied during the last fifteen years [iv, v, vi]. But the use of multi-beam, servo-controlled, pointing systems made them rather complicated and they were, in a first time, transformed into single narrow beam systems and, finally, abandoned. Using a wide-angle beam simplifies considerably the instrumentation while needing a proper signal processing, in order to identify which reflectors are measured. In order to assess the accuracy of such a system, we have developed a first instrument made several terrestrial experiments.

In section 2 of this paper, we describe the principle of wide-angle aerial and spatial multilateration. Such techniques are based on simultaneous distance measurements, achieved, in our case by the use of a wide angle laser beam. The instrumentation and its associated signal processing is presented in section 3. In section 4 we analyze the main error sources : atmospheric effects, laser effects, and effects from the detection electronics (signal-strength related biases, electrical noise, and temporal jitters). In section 5 we present experimental results, obtained from three different terrestrial experiments. Finally, in section 6 we propose an optimization of the current instrumentation, to fulfill the requirements for airborne and also spaceborne configurations.

II. PRINCIPLE OF WIDE-ANGLE AERIAL AND SPATIAL MULTILATERATION

The aerial or spatial multilateration technique is based on range measurements, to a network of ground based benchmatrks, performed from an airborne or spaceborne platform

(Figure 1). By using an inverse method, benchmarks can then be positioned, with an accuracy depending only on the accuracy and number of measurements and the geometrical configuration. Typically, the single-shot ranging accuracy is a few centimeters, and requires negligible biases.

We investigated this technique a few years ago, by a numerical simulation approach, based on the assumption that an ad hoc instrument could be developed to fulfill these requirements. We found that the objective of a vertical precision of 1 mm could be achieved, using a least-squares adjustment method, with some requirements on measurements. A priori locations of the aircraft and the benchmarks have to be known within a few decimeters. This requirement is not critical because it is used only as a first trial of a few iterations. On the other hand, the accuracy of relative distances and the number of measurements are critical. They must respectively be, for example, a few centimeters and a few thousands per retroreflector. The a priori locations are easily achievable by GPS techniques, e.g., Differential-Trajectography for the aircraft, and Rapid-Static for the ground based benchmarks. Note that the complete network survey for a priori locations has only to be performed once, before the first aerial survey. Posterior surveys can simply use the previous results.

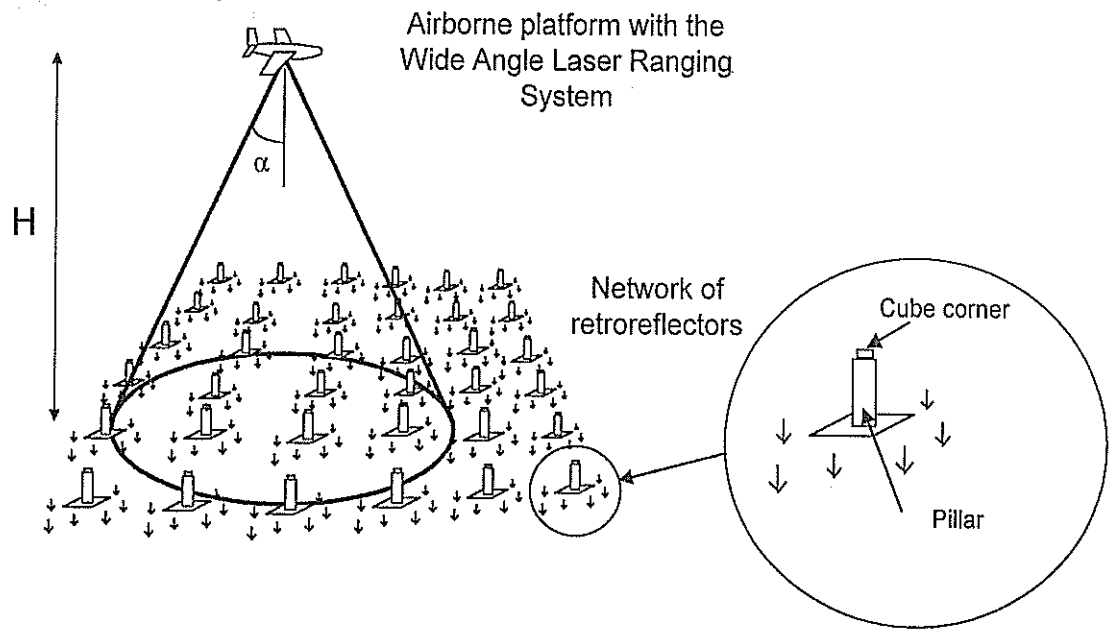

Figure 1: View of a typical airborne configuration, over a ground-based retroreflector network.

The use of a widely diverging laser beam (± 15 ° around nadir), illuminating the network of ground-based optical cube corners, seems a good solution to this problem. For one pulse transmitted by the laser, several echoes (typically ten) are retroreflected. By estimating precisely their times-of-flight and correcting for the mean refraction effect we achieve simultaneous range measurements and create strong constraints on both the coordinates of the laser source with respect to the network of reflectors, and between the coordinates of the reflectors. Note also that, the more the laser beam is divergent, the best is the horizontal accuracy of the positioned benchmarks. But since we are mostly interested in the vertical component, the range measurements are preferably done in a moderate field with around nadir. Atmospheric refraction effects are thus not critical to correct. By a proper modeling of both direct and inverse problems, one can also add other unknowns to the fundamental model, like a range bias fluctuating from shot to shot. By taking into account such a range bias, one has only to estimate arrival times of the laser echoes. The associated ranges are then called pseudo-distances, as in GPS where the transmitter

and receiver clocks are not synchronized. Relative pseudo-distances become then fundamental observations. Modeling the range bias has two interesting consequences. Firstly, it relaxes the constraints on refraction index correction as only differential variations need to be corrected. Secondly, it allows to record the detected signal only during the time window where echoes are expected. The amount of static memory of the recorder (digital oscilloscope, cf. next section) can thus be reduced.

III. INSTRUMENTATION AND SIGNAL PROCESSING

A. Instrumentation

A block diagram of the wide angle laser ranging system is illustrated in Figure 2. The mode-locked Nd:YAG laser transmitter (modified Quantel, from the Mobile Satellite Laser Station, Observatoire de la Côte d'Azur, Grasse, France) is based on a stable cavity with uniform reflectivity mirrors, aperture for TEM_{00} mode selection, passive Q-switch (saturable absorber) and active mode-locking (acousto-optic modulation). Mode-locking produces a train of 100 psec pulses in an average waveform of 70 nsec (FWHM), of which one pulse is extracted and amplified up to 100 mJ by a double-pass Nd:YAG amplifier. The pulse repetition frequency is 10 Hz.

The wide-angle beam is produced by whether a diverging lens or a ground glass plate, and is typically 15° at half-angle. But, in order to reduce irradiance fluctuations produced by speckle patterns, a diverging lens is preferred [vii]. For each laser shot, multiple echoes, arising from the network of retroreflectors, are detected and their waveforms are recorded. The photodetector is composed of a large area (1 cm^2) PIN photodiode (EG&G, YAG 444). The long transit-time of the photodiode (about 6 nsec), combined with a high transimpedance amplifier (3000 V/A gain, 50 MHz bandwidth), produces electrical response pulses of typically 13 nsec (FWHM), with a 4 nsec leading edge. The electrical signal is sampled by a digital oscilloscope (Lecroy 7200), with a 1 nsec period, and stored, whether in central memory of the oscilloscope or on the hard-drive of a host computer (Fieldworks 7500, PC) in real-time by GPIB. Note that the hardware of our system is much simpler than earlier proposed airborne and spaceborne systems [iv, v, vi], and also than current SLR systems [viii]. In return, the digitized signal has to be processed properly to retrieve the times-of-flight of laser pulses.

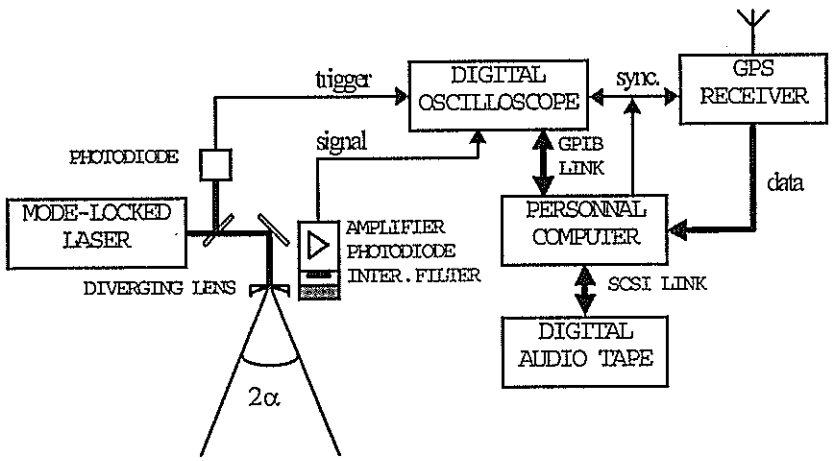

Figure 2 : Block diagram of the wide-angle airborne laser ranging instrument. A fixed GPS receiver (not shown) is also required at a ground station for differential trajectography.

B. Signal processing

The signal processing is composed of two steps. Firstly, measured echoes have to be properly identified, i.e., detected pulses have to be assigned reflector numbers. Therefore, the range bias is roughly estimated by correlating the measured signal with a Dirac comb composed of delta-functions at the approximate arrival times, calculated from a priori locations. The resulting range bias is accurate within one sampling interval, i.e., 1 nsec (15 cm), which is far enough for detecting 13 nsec FWHM pulses. Remember that the residual range bias is accurately estimated during the global inversion. Secondly, times of arrival of the detected pulses are estimated with an accuracy of, say, 100 psec (15 mm). To achieve this, one can implement either sub-optimum methods, or optimum methods, e.g., minimum mean-square error and maximum likelihood methods. We analyzed several ones, such as leading-edge threshold detection, center-of-gravity, cross-correlation and deconvolution. The first two belong to the sub-optimum estimator class, while the last two are two implementations of the same optimum method. Table 1 compares the theoretical precision of these methods.

Estimation method	Leading edge	Center-of-gravity	Cross-correlation
Single-shot accuracy	42 psec (6.3 mm)	29 psec (4.3 mm)	23 psec (3.4 mm)

Table 1 : Theoretical single-shot precision, i.e., standard deviation or estimation error in presence of additive noise, of several time-of-arrival estimators. Signal and noise characteristics are representative of the current instrumentation, assuming an electrical SNR of 100.

When combining the approximate range bias, i.e., the time of departure of the laser pulse, and the estimated times of arrival of the reflected pulses, one has a set of simultaneous "pseudo" times-of-flight. Here again, "pseudo" refers to the fact that only relative times-of-flight are known with the proper accuracy. When converting these times to distances, with the help of an atmospheric refraction model, e.g. [ix], one gets a set of simultaneous pseudo-distances. Therefore, we consider only relative distances.

Cross-correlation is an efficient pseudo-range estimator for individual pulses. But in operational configurations several pulses are reflected simultaneously. Pulse-superimposition, when reflectors are close in distance, produce then biases because pulse shapes are altered. In order to take into account the mutual effect of pulses, it is necessary to estimate simultaneously all the echoes in the oscilloscope trace. Therefore, we implemented a deconvolution method, fitting pulses of a synthetic trace on every measured trace by a least-squares adjustment. The reference pulses of the synthetic trace must be close, in their waveforms, to the real pulses. Therefore, we use an average measured pulse. Note that this method is, on a mathematical point of view, equivalent to the cross-correlation, with a reference function equal to the average measured pulse. In a second step we perform a sorting of the ranges estimated, rejecting all ranges closer than 4 m to another range. In this way we avoid to use estimations from pulses which may be affected by superimposition effects or even which may be wrongly affected a reflector number.

IV. Error sources in wide angle laser ranging

A. Atmospheric effects

The first error source stems from atmospheric refraction.Since we are interested in relative distances, only differential refraction effects have to be corrected, i.e., stemming from the part of atmosphere between the reflectors. When using local meteorological measurements, one is able to correct for this effect with an accuracy of a few mm with a spherical shell model [ix]. In a typical application, these parameters are necessary in order to correct for tropospheric effects of

GPS measurements, at the reference, ground based, station and in the aircraft. It is thus necessary to relate the atmospheric parameters at the reflectors of the network to these meteorological measurements. This can be done with the help of basic thermodynamics. Deviations of local parameters from this model, especially in the boundary layer, should lead to biases lower than 1 mm. On the other hand, turbulence produces also path length fluctuations. The strength of this effect can be evaluated by the path length structure function [x]. It should remain below the millimeter level both in the case of the terrestrial experiments presented in section 5 and in the case of a typical airborne experiment. In the general case, refraction effects can thus be neglected.

A second effect, induced by atmospheric turbulence, is irradiance fluctuations, or scintillation. Phase perturbations of the propagating optical wave induce interference effects and, therefore, intensity, phase and angle-of-arrival fluctuations at a point receiver. In weak turbulence regime, intensity statistics are governed by a log-normal probability density function (pdf) [xi], whereas in strong regime, the pdf become rather exponential [xii]. We can therefore expect, in aerial, and even more in spatial, configurations near unity scintillation contrasts. The main effect of these fluctuations is a reduction of the number of simultaneous measurements above a fixed SNR threshold. The impact of the remaining atmospheric induced scintillation, on the constraints created by the measured pseudo-distances on the multilateration problem, is one of the next effects to be analyzed. A statistical analysis of this phenomenon would be useful to optimize instrumental parameters, such as beam divergence, pulse repetition frequency, and aerial survey duration or number of satellite passes.

B. Laser beam effects

Wavefront distortions in laser beams have been well known to the SLR community, because they are among the most limiting phenomena at the instrumentation [xiii]. Biases up to a few nanoseconds have been reported in Q-switched lasers [xiii]. We have also investigated two different laser transmitters and measured biases reaching half the pulsewidth at the edge of the beam [ii]. The first laser was an unstable cavity resonator, with super-gaussian mirrors (Quantel, Brillant), transmitting a 4 nsec, 350 mJ pulse. The second laser was the mode-locked laser, described in section 3. We showed that our mode-locked laser produces biases, in the near-field, of about 100 psec (15 mm) at the edge of the beam ($1/e^2$ intensity), or 50 psec (7.5 mm) at FWHM, while for the unstable cavity laser, biases reach 2 nsec at the edge [ii]. Mode-locked lasers have the advantage of producing a smooth temporal waveform pulse and low far-field angular biases thanks to the transverse mode stability achieved by the long build-up of the beam. Nevertheless, there exist some other means of achieving picosecond laser pulses, with consequently low wavefront distortion, such as pulse compression techniques, e.g., backward Stimulated Brillouin Scattering [xiv]. But such devices have not yet been evaluated.

C. Signal strength related biases in the detection stage

The second, deterministic, error source is a temporal bias depending on the signal magnitude, stemming from both the photodiode and the amplifier. As the signal magnitude fluctuates, this effect increases the bias and the standard deviation of range measurements. A characterization of the detection stage revealed this effect was present predominantly in the amplifier but was not significant in the photodiode. A linear relationship, with a slope of 0.5 m/V, has been reported [vii]. It can thus be corrected on individual range measurements, knowing their amplitude. Without correction, biases of almost 20 cm may arise, whereas corrected data exhibit a gaussian scatter of a few cm standard deviation [vii].

D. Electrical noise in the detection stage

Electrical noise in the detection stage is mainly composed of additive Gaussian noise from the photodetector, amplifier and oscilloscope. The predominant noise in the photodiode is shot-

noise stemming from the received laser pulses, solar background illumination, and dark current. The solar irradiance is reduced by an interference filter of large bandwidth (20 nm at 1.064 μm), allowing transmission of the wide angle beams. This current is, with the dark current, generally negligible with respect to the signal photocurrent. Thus, only shot-noise produced by the laser pulses has to be considered. The total shot-noise is about 70 μV for a 100 mV signal magnitude at the output of the amplifier. Electrical noise in the amplifier is mainly produced by active components, such as bipolar transistors. It reaches 260 μV rms for a 95 MHz bandwidth. The oscilloscope produces electrical noise and quantization effects, though the second effect is negligible. We measured typical values of 230 μV, rms, at 5 mV/div.

We compared photodiode shot-noise, amplifier noise and oscilloscope noise, for caliber ranging from 5 mV/div. to 500 mV/div., and assuming the detected signal is of 5 divisions magnitude (in order to compute the photodiode shot-noise) [vii]. Since the electrical noise in the oscilloscope is roughly proportional to the caliber, it is always superior to the photodiode shot-noise. The amplifier noise becomes predominant only for weak signals. The noise spectral density has to be considered, since in bipolar transistor devices, such as amplifiers and oscilloscopes, it is generally not constant. On the other hand, since non-stationary noise, e.g., shot-noise, can be neglected with respect to the other noise sources, the overall noise can be assumed stationary.

We analyzed the variance, σ^2, of the cross-correlation time-of-arrival estimator in presence of additive gaussian noise [vii]. The ranging precision, i.e., standard deviation, can be put into form

$$\sigma \approx \frac{K}{SNR}$$

where $SNR = \frac{a}{\sigma_n}$ is the signal-to-noise ratio, σ_n^2 the noise variance, a the magnitude of the measured pulses, and K a waveform dependent parameter [vii]. Parameter K can be related to the rise time and fall time of the impulse-response of the detection stage. Thus, for a typical value of K=0.3 m, an SNR of 100 yields a ranging accuracy of 3 mm, independently of other error sources.

E. Temporal jitters

Time-of-arrival uncertainty of single photons is a fundamental temporal limitation. But, in our system, the detected laser pulse contains typically 10^4 photons, this effect can thus be neglected. On the other hand, the digital signal is affected by a temporal uncertainty with respect to the sampling grid of the oscilloscope. We evaluated this uncertainty, which is also an estimate of the sampling clock stability, to be at a few picoseconds level, over a typical 10 μsec interval. It can, therefore, be neglected. In order to analyze the effect of the signal sampling, we performed numerical simulations. A careful modeling of the instrumentation yielded a dispersion of 20 psec (3 mm).

F. Budget of error sources

Error source	Type	Order of magnitude	Conditioning parameters
1. ATMOSPHERE			
Mean refraction correction	systematic	< 1 mm, 1 °C deviation	Micro-meteorological effects
Pathlength fluctuations	random	0.8 mm, $C_n^2 = 10^{-14}$ $m^{-2/3}$	Turbulence structure constant, C_n^2
Scintillation	random	shot-to-shot SNR fluctuations	C_n^2 and SNR
2. LASER			
Wavefront distortion	systematic	< 1 cm, 100 psec FWHM laser	Cavity mode build-up

3. RECEIVER			
Electronic noise	random	3 mm, SNR=100	K, SNR
Magnitude related biases in the amplifier	systematic	negligible, after numerical correction	Correction model
Sampled signal aliasing	random	< 3 mm, 1 nsec sampling	sampling period, detection response-time
4. WIDE-ANGLE RANGING			
Pulse superimposition	systematic	negligible, when using deconvolution estimator and proper data sorting	Reference-pulse waveform, instrumental pulse discrimination

Table 2 : Summary of error sources limiting the ranging accuracy

Table 2 summarizes the accuracy limitation from the error sources described in the previous sub sections. We can assume from this analysis that cm accuracy is achievable with the current system. In the next section we present an experimental verification of this assumption.

V. RANGING PERFORMANCE EVALUATION FROM TERRESTRIAL EXPERIMENTS

In order to assess for the ranging accuracy of the developed instrument we performed three terrestrial experiments, differing by pathlength, instrumental configurations and turbulence regimes. For each experiment, we evaluated the standard deviation for relative range estimations and compared it to the theoretical precision, predicted by the above equation of σ. The theoretical precision gives an estimate of the single-shot accuracy of a sequence of measurements, characterized by its accuracy-constant K, and its SNR. Since standard deviations do not reveal biases in relative-distances, we also performed repeatability tests. Therefore, we computed mean relative distances and error bars for several samples of 100 measurements. Discrepancies between mean relative distances and error bars, with respect to the overall mean value, were used as an indicator of biases. The results and main characteristics of these experiments have been presented in [vii]. We summarize then in Table 3.

The first experiment validated the proposed instrument, composed of a mode-locked laser with a low impulse-response photodetector, and cross-correlation as time-of-arrival estimator. The standard deviation of relative distances, defined as single-shot accuracy, was better than 8 mm (SNR around 30). Biases, estimated by means of the above-mentioned repeatability test, were about 4 mm (SNR around 30). The second experiment showed that, when employing a transimpedance amplifier, the instrument still achieves centimeter precision, even for very low SNRs (e.g., 5.4 cm for SNR=5). The third experiment confirmed these performances at even longer distances, up to 1 km. Note that in the last experiment a diverging lens was used to achieve the beam divergence.

Exp.	Number of meas./seq.	SNR	K (m)	standard deviation σ_ρ (mm)	repeatability $\Delta\rho$ (mm)
1	43 - 100	33 - 91	0.16 - 0.29	3.6 - 7.8	< +/- 4.0
2	23 - 70	5 - 62	0.24	4.6 - 54	
3	6 - 25	15 - 36	0.72	22 - 60	< +/- 20

Table 3 : Summary of the main characteristics of three terrestrial experiments and the achieved accuracy (standard deviation and repeatability).

Figure 3 illustrates the relationship between single-shot accuracy and SNR, from data of the three terrestrial experiments. One can note that good agreement is found between measured and predicted values, even for high SNRs. This is due to the fact that amplifier biases are properly corrected. This is a fundamental assumption. Moreover, in these experiments the pulse shape

control and noise spectral distribution were identified as critical to keep low values of K and thus high ranging precision.

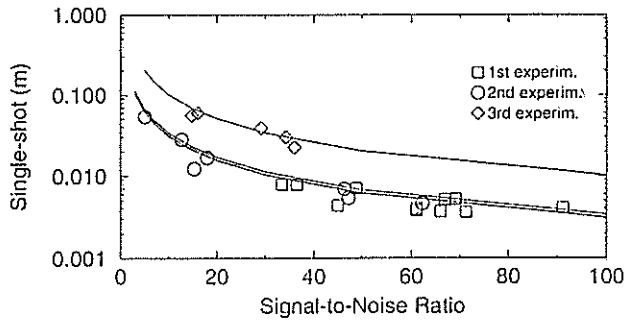

Figure 3 : Comparison of measured and predicted single-shot precision, versus SNR, for three terrestrial experiments. Note that, for K = *0.22 m, SNRs above 5 produce a 7 cm single-shot precision.*

In fact, the second experiment of Figure 3 was intended to test the performance of the inverse method of our multilateration technique from real data. It was implemented as a reduction of a typical aerial configuration to a two-dimensional terrestrial configuration. This experiment was conducted near Paris, in December 1995. After computation of the experimental range data, we found a relative positioning accuracy between 1 and 4.4 mm, rms, on the radial component, and between 1.8 cm and 7.8 cm on the transverse component [xv].These results are compatible with theoretical predictions from the covariance matrix and with numerical simulations, validating thus both the instrumentation and the simulation models. On the basis of these results, an aerial experiment simulation showed that the vertical component of retroreflectors could be estimated with a sub-mm accuracy, providing the instrumentation was adapted to the longer range constraint. An optimization of the present system is therefore proposed below.

VI. SYSTEM OPTIMIZATION

A. Aerial configuration

In a typical aerial configuration, i.e. 10 km altitude, the current instrumentation yields a SNR of 1.3 and a single-shot ranging accuracy of 21 cm. In order to satisfy the requirement of at least 3 cm ranging accuracy, we have to optimize the current instrumentation. This can be achieved by means of minimizing σ^2. As a first approach three different, though related, parameters can be considered. The first is the signal strength. Optimization could thus be achieved by maximizing the link budget (through the receiver surface or responsitivity), or the amplifier gain, or by reducing the response-time of the detection stage. The second is the overall electronic noise. Since it stems mostly from amplifier, this element should be optimized, e.g., by reducing the bandwidth. The third parameter is K. It can be lowered by reducing the response-time of the photodetector. When expressing σ^2 as a function of instrumental parameters, we identified the fundamental and independent parameters conditioning the ranging accuracy as being : amplifier gain, photodetector surface, and photodetector transit time. A further parameter can be investigated : the detector technology (APD vs. PIN photodiode).

1. Amplifier gain

Assuming the predominant noise source is the transimpedance amplifier, the SNR varies as the square-root of the gain, i.e., feed-back resistance. By taking into account the convolution effect of the impulse-response, for high gain, i.e., low bandwidth, the response is inversely

proportional to the gain, the accuracy is thus reduced. Identically, for low gain, i.e. high bandwidth, the fall-time of the impulse-response becomes independent of gain. The accuracy is therefore also reduced. An optimum gain near 1400 ohms can be found (see Figure 4), but the accuracy improvement is small. On must thus conclude that the amplifier gain can hardly be optimized.

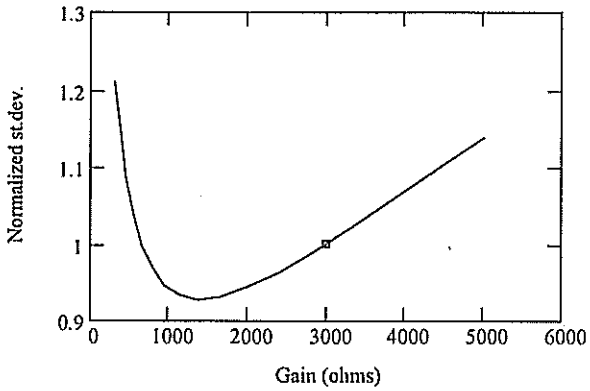

Figure 4 : Normalized accuracy (with respect to the current instrumentation, shown by the small box) vs. gain of the transimpedance amplifier

2. Photodetector surface

The photodetector surface must be high so as to keep an acceptable figure for the link budget with large field optics. But an increase of this surface produces an increase of the junction capacitance and, consequently, a reduction of the bandwidth. Finally, the accuracy becomes independent of the photodetector surface, for high values. Conversely, for low values the junction capacitance is no more a limiting parameter. Decreasing the surface just decreases the link budget and, therefore, the ranging accuracy. Hence, this parameter does not exhibit an optimum like the previous one (see Figure 5). A nearly asymptotic accuracy optimum could be achieved with a 10 cm^2 photosensitive surface detector. But this requirement seems rather unrealistic. Photodetector surface can, therefore, hardly be optimized.

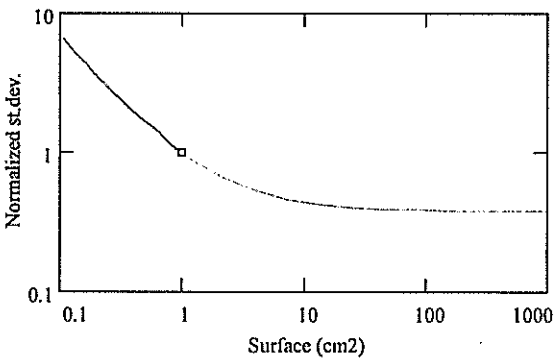

Figure 5 : Normalized accuracy vs. photodetector surface.

3. Photodetector transit time

Reduction of the photodetector transit time can be achieved, on a technological point of view, by reducing the width of the intrinseque zone (for a PIN structure). But the quantum efficiency is then consequently reduced. Again, this parameter does not exhibit any optimum and can hardly be improved (see Figure 6). But, once again, the current system is already near the optimum.

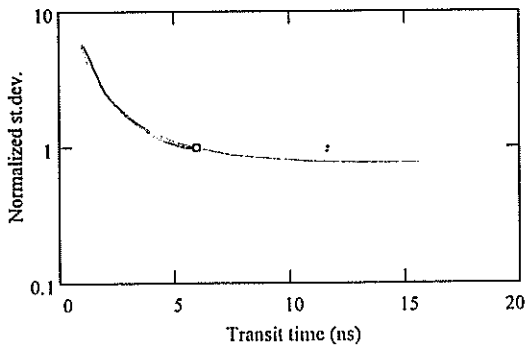

Figure 6 : Normalized accuracy vs. photodetector transit time.

4. Photodetector technology

Finally, there is an other fundamental parameter that we did not consider in the above optimization : the photodetector technology. The absorption coefficient of Si (of which the current PIN photodiode is made) is of 21 cm^{-1} at 1.064 µm whereas for Ge, it is about 10^4 cm^{-1} . But this latter technology is known as producing stronger electronic noise [xvi]. For InGaAs, sensitivities of 0.7 A/W are possible at 1.064 µm, but it seems that available detectors are limited to nearly 3 mm diameters. Actually, the best way to improve the current instrumentation seems to be the use of large photosensitive surface APDs. Such devices, with diameters up to 16 mm, are proposed by Advanced Photonix, for example. With a moderate avalanche gain of 100, a single-shot ranging accuracy of 1 cm should be achievable for an aerial configuration at 10 km altitude.

B. Spatial configuration

On the other hand, a spaceborne system would need a more fundamental revision of the instrumentation. To meet higher altitude requirements, the use of a telescope seems necessary and possible since, for the same network areas, the field of view is now much narrower, e.g., 0.01 rad. Velocity aberration correction can be achieved by the use of spoiled cube corners, but with a loss in the link budget amounting to a factor of 36. In order to achieve centimeter ranging accuracy, the instrumentation should be based on a 30 cm telescope, 1 J laser, 10 cm retroreflectors, 5 mm diameter APD of 10 A/W responsitivity, and 10,000 gain transimpedance amplifier. Actually, the single-shot ranging accuracy would then be between 2.3 cm and 5.3 cm from center to the half-width of the laser beam. A rough pointing system would also be necessary, in order to acquire data from an extended part of the orbit.

In this configuration, atmospheric effects are slightly different. On the transmission point of view, cirrus clouds have to be taken into account. Like for all spaceborne optical applications, cloud cover is a main limitation to the feasibility of surveys. Operational parameters, such as laser repetition frequency and spatial reflector density, have therefore to be carefully chosen in order to achieve the desired positioning accuracy from a single satellite passage. Concerning turbulence aspects, the dynamic layer is now located far away from the laser source. The main consequence on the link budget is that beam spreading and scintillation are stronger. For the same reasons, the pdf of scintillation becomes exponential, i.e., with unity intensity contrast. The effects of these error sources are still under investigation. But since the instrumental models have now been validated experimentally, they can be applied in numerical simulations of aerial and spatial configurations of the proposed positioning technique.

VII. Conclusion

A wide-angle laser ranging system, intended to achieve a new geodesy technique based on aerial or spatial multilateration, has been presented. A first instrumentation has been fully

validated on several terrestrial experiments. Results are compatible with theoretical predictions, related to the electrical SNR. An optimization for airborne experiments of the current instrument has been proposed. It consists mainly on replacing the PIN photodiode by a large aperture APD. This solution is now under investigation, with the aim of conducting an airborne experiment during 1997. From link budget considerations, an extension to a future spaceborne configuration seems also possible. But therefore, a more classical instrumentation, using a telescope, would be necessary.

ACKNOWLEDGMENTS

The authors would like to thank F. Pierron and his team of the Mobile Satellite Laser Station, Côte d'Azur Observatory, Grasse, France, for having made possible the experimentation with their mode-locked laser. They would also like to acknowledge Dr. J. Pelon, as well as D. Bruneau, of the Service d'Aéronomie, CNRS, Paris, France, for their contributions in meteorological aspects and advises in laser instrumentation, respectively.

REFERENCES

[i] M. Kasser and IGN, "Method for determining the spatial coordinates of points, applications of said method to high prescision topography, system and optical device for carrying out said method", US Patent 774,038, 1991

[ii] O. Bock, C. Thom, M. Kasser and D. Fourmaintraux : Development of a new airborne laser subsidence measurement system, aiming at mm-accuracy, Proceedings of the Fifth International Symposium on Land Subsidence (FISOLS-95), The Hague 16-20 October 1995, Balkema Publisher

[iii] D. Fourmaintraux, M. Flouzat, M.J. Bouteca, M. Kasser, (1994) Improved subsidence monitoring methods. SPE, paper 28095, Int. Symp. SPE-ISRM Eurock'94, Balkema Publisher

[iv] W. D. Kahn, J. J. Degnan and T. S. Englar, Jr : The airborne Laser Ranging System, Its Capabilities and Applications, Nasa Tech. Memo. 83984, Sept. 1982, Goddard Space Flight Center, Greenbelt, Maryland

[v] H. Lutz, W. Krause and G. Barthel : High-Precision Two-Colour Spaceborne Laser Ranging System for Monitoring Geodynamic Processes, 33rd Congress of the International Astronautical Federation, Paris, France, September 1982

[vi] S. C. Cohen, J. J. Degnan, J. L. Bufton, J. B. Garvin, J. B. Abshire : The Geoscience Laser Altimetry/Ranging System, IEEE Tr. on Geoscience and Remote Sensing, Vol. GE 25, No. 5, Sept. 1987

[vii] O. Bock, Ch. Thom, M. Kasser & J. Pelon, Ranging Performance Evaluation of the Wide-Angle Laser Ranging System, IEEE Tr. on Geoscience and Remote Sensing, to be published

[viii] J. J. Degnan : Millimeter Accuracy Laser Ranging : A Review, Geodynamics Serie volume 25, Contributions of Space Geodesy to Geodynamics: Technology, American Geophysical Union, 1993

[ix] J. W. Marini and C. W. Murray : Correction of laser range tracking data for atmospheric refraction at elevation angles above 10 degrees, GSFC, Nasa Technical Memo, Nov. 1973

[x] V. I. Tatarskii : Wave propagation in a turbulent medium, (translated by R.A. Silverman) McGraw-Hill, New-York 1961

[xi] M. E. Gracheva, A. S. Gurvich, S. S. Kashkarov and VI. V. Pokasov : Similarity Relations and Their Experimental Verification for Strong Intensity Fluctuations of Laser Radiation, Topics in Applied Physics, Vol. 25 : Laser Beam Propagation in the Atmosphere, Ed. J. W. Strohbehn, Springer-Verlag, 1978

[xii] J. W. Strohbehn : Modern Theories in the Propagation of Optical Waves in a Turbulent Medium, Topics in Applied Physics, Vol. 25, Laser Beam Propagation in the Atmosphere, Ed. J.W. Strohbehn, Springer-Verlag, 1978

[xiii] J. J. Degnan : Satellite Laser Ranging : Current Status and Future Prospects, IEEE Tr. on Geoscience and Remote Sensing, Vol. GE-23, No. 4, July 1985

[xiv] V. Kubecek, K. Hamal, I. Prochazka, R. Buzelis, A. Dement'ev, Optics Commun., Vol. 73, No. 3, 1989

[xv] O. Bock, M. Kasser Ch. Thom, & J. Pelon, "Precise Relative Positioning by Wide - Angle Laser Ranging", submitted to IEEE Tr. on Geoscience and Remote Sensing

[xvi] H. Melchior : Demodulation and photodetection techniques, Laser Handbook, Ed. F.T. Arecchi & E.O. Schultz-Dubois, North-Jolland Publishing Company, Amsterdam, 1972.

PROPOSITION FOR A NEW SLR METHODOLOGY USING CW OR LONG PULSE LASERS

M. Kasser, ESGT / CNAM, 18 Allée Jean Rostand, 91 025 EVRY Cedex, France
Fax : +331 69 36 74 21
C. Thom, LOEMI / IGN, BP 68, 94 160 Saint- Mandé, France

INTRODUCTION

The main goals of SLR, as an operational orbitographic tool or as a scientific one, derive from its capability to determine artificial satellite orbits with a centimetric accuracy. From the orbit one may deduce information of very high importance concerning earth rotation parameters, earth gravity field and its temporal variations, and a very high quality absolute positioning. In this area, SLR could be a very good candidate, if not the best on a long term basis, to provide millimetric absolute altimetry for studies concerning minute altitude variations (mountains formation, tectonic subsidences and surrexions, post-glacial rebound, oceanic loading over continental margins, etc...).

The main limitations of SLR in terms of accuracy, by descending order of importance, are probably : (i) the quite inhomogeneous repartition of SLR stations in the world, (ii) the technology of SLR that lets some important biases uncorrected, (iii) target temporal signatures, and (iv) tropospheric delay uncertainties.

Concerning (i), we observe regular improvements, but there will always be some basic limitations (due to semi-permanent cloud coverage in some parts of the world, for example). Concerning (iii), the models have considerably improved and some technological possibilities not yet used exist (Kasser & Lund 1994). And concerning (iv), the correction to look for is quite low if the pressure is correctly measured at the station (Kasser 1992), and in any case it is expected soon that two-colour ranging (Prilepin 1957) will achieve automatic corrections at the millimetre level. Thus we have worked on the point (ii), i. e. how to remove any sort of instrumental bias.

To achieve this goal we have looked for the solutions used by early geodesists with electronic distance measurements (EDM). These type of instruments have been explored through a wide range of different technologies, with only a small number of scientific publications as most of the knowledge in this domain is industrial and thus not disclosed. Nevertheless we know, from the publication of patents, what technologies are used :

- Use of pulsed diode lasers (long pulses, typically 200 ns), with the same detection for the start and return pulses, and a statistical reduction of the decimetric single shot r.m.s. up to one millimetre,

- Continuous modulation of light beams (often not coherent ones), with an efficient phase measurement over periods up to a few seconds, and a systematic internal calibration removing the biasses due to ageing of components and thermal effects,

- For the highest precision EDM (Mekometer, Geomensor, Terrameter), an electro-optical device is used to modulate twice the laser beam, one before and the other after the free space propagation, and then the accuracy may be below one tenth of millimetre, due to a totally bias-free operation.

This last solution has been explored in order to check its transposability to SLR. In some way it is complicated, but it has been found that it could be used with only minor modifications of existing stations.

PRINCIPLE OF THE METHODOLOGY PROPOSED

Today the highest precision EDM is a laser one, named Mekometer after its invention by MM. Froome and Bradsell (NPL, Teddington, UK) and now produced by LEICA (Switzerland) as Mekometer ME 5000 and by COM-RAD as the Geomensor. This type of instrument uses an extremely interesting laser modulation method, invented by Dr. Froome in the sixties, which allows to avoid completely any systematic errors. It relies upon the use of a Potassium Di Hydrogen Phosphate crystal, called KDP for ease. The KDP is optically an anisotropic crystal.

From one point, let us draw for each direction of the space a vector whose length is equal to the refraction index experienced by the electric field of the electromagnetic wave (called *polarisation* vector). If the medium is isotropic, the end of this vector is on a sphere. For the KDP, without any electric field applied, it is on a revolution ellipsoid. This sort of crystal is said *uniaxe*, the large axis is called **z**, and **x** and **y** are chosen parallel to the crystallographic axes. The electro-optic effect in such a crystal is the following : if we apply an electric field along **z** axis, the indexes along **x** and **y** are modified with the law :

$$n_y = n_0 - n_0^3 \, r_{63} \, E$$
$$n_x = n_0 + n_0^3 \, r_{63} \, E$$

where $\mathbf{r_{63}}$ means an electro-optical constant of the crystal and $\mathbf{n_z}$, that represents the index of refraction along **z** axis, is different from $\mathbf{n_x}$ and $\mathbf{n_y}$, and is independent from **E**. The modulator of the Mekometer uses such a "longitudinal" modulation, **E** being parallel to **z** axis.

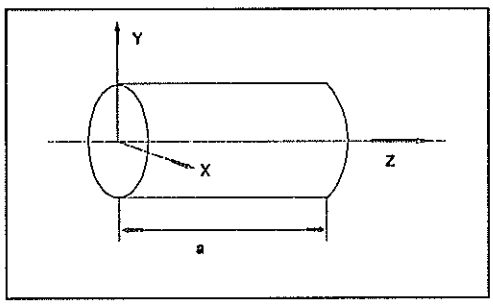

The section of the ellipsoid of refraction index in the **xOy** plane, that is a circle for $\mathbf{E} = 0$, becomes :

With $\mathbf{E} \neq 0$, if we enter the crystal along **z** axis, with the polarisation **P** at 45° of **Ox** and **Oy** directions (directions called neutral axes of the crystal because an incoming polarisation along one of these planes is not modified during the propagation), we decompose **P** into $\mathbf{P_x}$ and $\mathbf{P_y}$ that do not travel at the same speed (refraction indexes along **x** and **y** are different as soon as **E** is different from zero). The difference of phase R between the components of the electromagnetic wave $\mathbf{P_x}$ and $\mathbf{P_y}$ is at the exit of the crystal expressed by : $\mathbf{R = 4\pi n_0^3 r_{63} E.a/\lambda}$, λ being the wavelength of **P**.

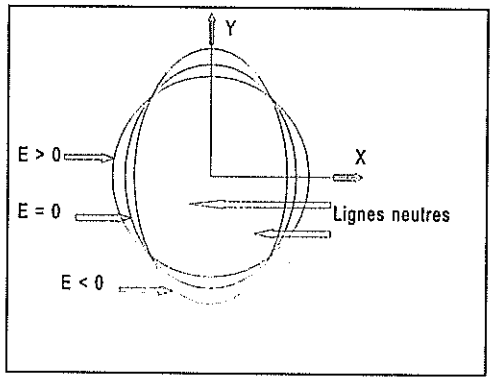

That way, with $\mathbf{R} = \pi/2$, the resulting polarisation from $\mathbf{P_x}$ and $\mathbf{P_y}$ at the end of the crystal is perpendicular to the initial orientation of **P** (for $\mathbf{R} = \pi/4$, **P** describes a circle at an angular speed of $2\pi c/\lambda$ rd/s). Thus generally, we note that the emitted light has an elliptic polarisation changing at the frequency **f** of modulation of the electric field **E**.

When the modulated laser light comes back from the reflector located at the far end of the line, it is sent back through the same crystal, experiencing the same alternative high frequency electric field **E**. Let us suppose that the total optical path **L** between the output of the crystal and its second input (close to half the distance to be measured) is equal to an integer number of modulation wavelengths plus half a wavelength. The laser light will see at the first passage in the crystal indexes $\mathbf{n_1}$ and $\mathbf{n_2}$ along the **x** and **y** projections of **P**. But when it will cross the crystal for the second time, the value of **E** will be the opposite of that during the first passage, so that the crystal indexes will now be $\mathbf{n_2}$ and $\mathbf{n_1}$ along **x** and **y** axes. And if we compute the total optical paths for polarisation along **x** and **y** axes, we find that they are exactly equal. It means that the outcoming polarisation is perfectly parallel to the initial incoming one : If at the output we observe the polarisation orthogonal to the input direction, in this very precise situation where $\mathbf{L = (K + 1/2).\ c/f}$ (K integer), the output signal intensity is null. And it is easy to see that for any other value of **L**, this intensity has a value following a cycle, whose shape is close to a sinusoid when **E** does not reach too high figures, and still cyclic but more complicated beyond e. g. one kilovolt.

General description of the "Mekometer" Geodetic EDM

The ME 5000 is working so as to detect the values of **f** for which the null return intensity occurs, then with such a set of measured values, it computes the integer **K** and then **L**. And if the value of **K** is provided to the instrument before the measure, the sequence is much faster. The light source employed is a He-Ne laser ; It allows to reach ranges up to 10 km if necessary, although for such distances, the excellent precision of the instrument is limited by the atmospheric index uncertainty.

The input end of the crystal is mechanically disposed at the exact intersection of the two axes of the instrument : that way, the zero error, to be added to the measurement to get the distance, is constant and depends only of the geometrical centring device employed for the reflector.

The accuracy is excellent (the instrumental standard deviation is close to 0.1 mm + 0.1 mm/km), due to the fact that this is a null measurement, for which no electronic drift of any type will influence the result. The 0.1 mm/km is only due to the frequency standard, and may be considerably improved if necessary, but this would be useless for terrestrial measurements where

the refraction index is hardly known to the 1 mm/km level.

HOW COULD SUCH A TECHNOLOGY BE USED FOR SLR ?

The main differences between SLR and an EDM are :

- A link budget that is fairly low (10^{-15} for example), which requires the use of powerful lasers (which in turn implies pulsed lasers, like YAG),

- A distances that varies all the time long during the flight of the satellite over the station.. If **Z** is the zenith angle of the satellite, the apparent speed from the station is **k.sin Z**, and the value for **k** is for example 2.6 km/s for Lageos, and 6.7 km/s for Starlette.

- Very long distances, which requires a very high quality oscillator (typically 10^{-11}), but that is now quite easy to obtain.

- A return signal that is frequency shifted due to the Doppler effect, because of the radial component of the relative speed of the satellite.

- The polarisation signature of the cube-corner retroreflectors which is quite complicated, and generally close to a quarter-wave plate (Kasser & Goupil 1996).

We have evaluated two different solutions in terms of modulation :

1/ A variable frequency, synthesised accurately from the ephemeris of the satellite and allowing a "fringe" movement (i.e. the passage to 0 of the intensity detected after the second passage in the crystal) quite steady, allowing for a very comfortable detection (e. g. at 100 Hz).

2/ On another hand, a fixed frequency and a measurement of the "fringe" movement in a much larger range. The elements we have used to perform simulations have been the following :

- Use of a YAG laser at 1.06 :m, 5 ns pulses at 10 Hz

- Atmospheric scintillation giving a random modulation of the return signal from 0 to 100 %.

- Intensity varying in $\mathbf{D^{-4}}$.

- A satellite like Lageos, with a tracking since $\mathbf{Z < 45°}$

- An overall modulation efficiency of 90 %

- A mean value of measurements for normal points each 15 s

The measuring equipment is composed of the following instruments :

- The YAG laser that receives the polarisation modulation at a fixed frequency. The KDP is in a tuned cavity, modulated with a peak voltage close to $V_{8/2}$, with its entrance as close as possible to the intersection of the axes of the telescope.

- The return signal is driven through the modulator once again and a polarizer to an avalanche photodiode optimal for YAG. The signal observed is a series of pulses, slightly

widened by the detection (e. g. 10 ns), and is amplified up to 0.5 V peak.

- The signal is then sampled by a 1 Gech/s oscilloscope, and the data and the related timing are transferred to a computer.

- The processing consists, for each period of integration used for one "normal point", in a correlation between received signals and theoretical curves corresponding to the a priori orbits provided by ephemeris.

The simulations performed show that the measurement noise is below the millimetre level, and on another hand no measuring bias is possible. Since the two-pass modulation process provides a curve that, although periodical is not purely sinusoidal and thus has a significant amount of 3rd harmonic, it is necessary to perform a correlation on the mean frequency and another on the third harmonic. In parallel an absolute chronometry is performed on the sampled pulses (with a modest precision, close to 0.1 m) in order to measure the integer number of half-wavelength of the frequency of modulation at a given moment.

If we compare with a classical SLR station, this new technology requires only a few modifications :

- On the laser, neutralisation of the mode-locking to go back to nanosecond pulses as energetic as possible.

- Installation of a modulator, fed by a synthesiser driven by an atomic oscillator, with a power amplification allowing to reach in a cavity a voltage close to $V_{\lambda/2}$. This crystal must be located as close as possible to the intersection of the mechanical axes of the telescope. The same crystal will be used to modulate the return signal.

- After the detection and the amplification, use of a fast sampling digital oscilloscope, linked to the computer.

The optimal frequency to be used in an exploratory configuration could be 500 MHz, frequency where power amplification is not too difficult, and where $\lambda/2 = 30$ cm allowing for an easy determination of the ambiguity figure in the measured distance. The following drawing provides a general scheme of a SLR station using this technology.

Interesting alternatives would be to use either a powerful CW laser (e. g. an Argon one), or a very different type of pulsed laser, optimised for very energetic but long pulses (relaxed injected YAG for example), or on another hand with short pulses at a high pulse rate (e. g. Cu vapour). The main technological problem to solve will be the modulator. KDP is not suitable for high peak optical power, and it is not able to bear an important HF power during a semi-CW duty cycle. Thus some possibilities must be explored :

- Lithium tantalate or lithium niobate instead of KDP, for their behaviour at high energy levels and their mechanical strength. But in large size such crystals are quite expensive. This type of crystal would have to be used in a cavity tuned on the central frequency of the synthesiser, used as an impedance transformer.

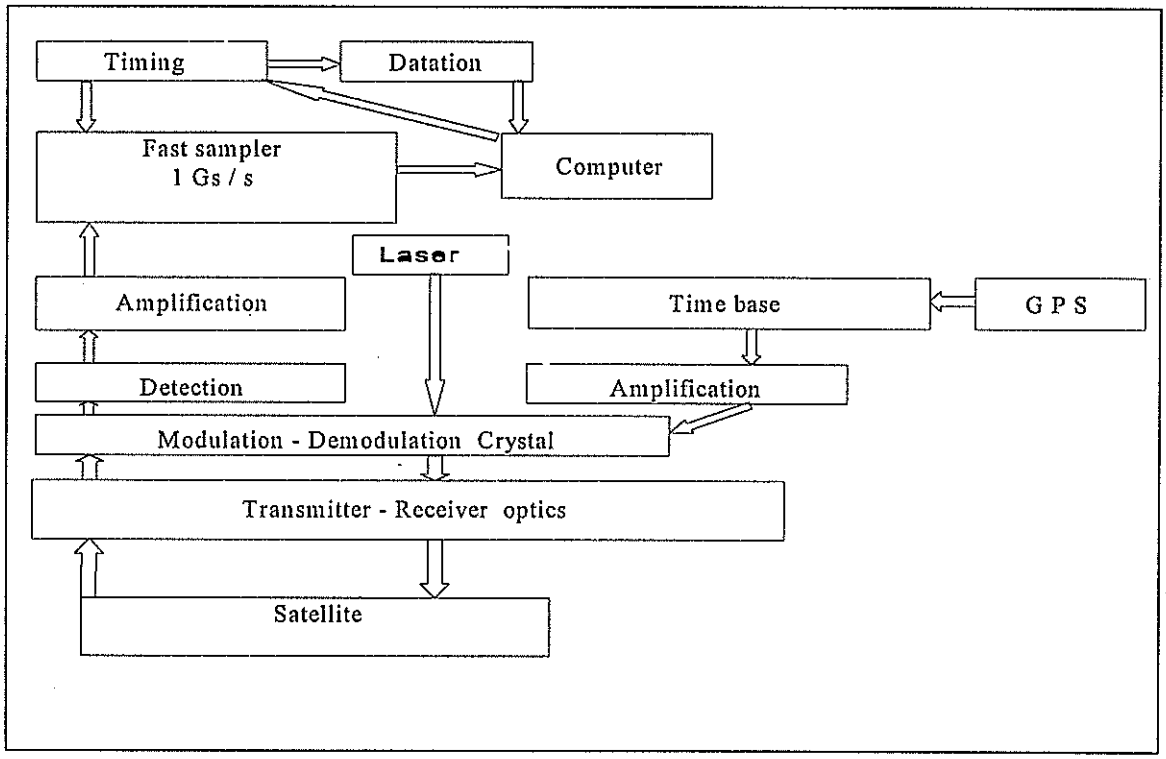

- Considering the uncertainties about the depolarisation due to the cube corner retroreflectors used on satellites, another situation must be explored, using two successive intensity modulations of the beam, as if in the previous situation presented here we would have used an intermediate polarising plate just after the first modulation and thus before the second one. The signal-to-noise ratio will be lower, but the first modulation could be obtained directly in the YAG laser, between the pilot and the amplifiers, at a low energy level. The only other drawback of such a configuration seems to be the geometric separation between the first and the second modulators, probably not very difficult to keep stable at the 0.1 mm level.

CONCLUSION

The methodology we present here is not new at all, and its main advantage relies on the fact that the detection has no requirement at all in terms of temporal jitters, it works at a very low speed so as to perform - more or less - just photometry measurements, and not timing measurements. Its use in geodesy since late sixties has been constant for very high precision distances, and excepted for the high power HF aspects, it is very simple to get operational.

We expect to have the possibility to test as soon as possible the instrumentation described here as a temporary modification of an existing SLR station (it would be advisable to start with a station benefiting of a large collecting area in order to work with a strong link budget). The problem of the elimination of the calibration and of any measuring bias seems possible, using a technical solution that has been proved as very efficient for EDMs for more than 20 years. Nevertheless, the question of the modulator has to be solved, and our first tests have shown that it was not a minor point. We hope that this new possibility will be evaluated by other teams and at least that a good solution (this one or any other one) will be found to remove any biases in SLR. Major scientific

goals will then be accessible, and especially we expect a significant improvement on the vertical component precision of the SLR stations co-ordinates.

BIBLIOGRAPHY

Prilepin, 1957. Aerial surveying and cartography, Trans. Inst. of Geodesy, URSS (114), pp. 127-130

Kasser, 1992. Improvement of SLR accuracy, a possible new step. *Proceedings of the 8th International Workshop on SLR Instrumentation, Annapolis, Nasa publication 3214, pp 8-23 to 8-29*

Kasser, Lund, 1994. A new concept of spatial retroreflectors for high precision satellite laser ranging. *Ninth International Workshop On Laser Ranging Instrumentation, 7-11 November 1994, Camberra, Australia*

Kasser, Goupil, 1996. The polarisation behaviour of cube corner retroreflectors used in slr satellites. *Tenth International Workshop On Laser Ranging Instrumentation, 11-15 November 1996, ShangaV, China*

Laser Ranging Performance Evaluation

Global SLR Performance Evaluation

Van S. Husson
AlliedSignal Technical Services Corporation
NASA SLR Program
7515 Mission Dr.
Lanham, Md 20706

1.1.1 Introduction

Global SLR system performance is currently measured in several different areas. The major areas of performance evaluation are data products, data quality, and data quantity. The goal of performance assessment is to identify any data problem in the global network as soon as possible in order that the cause of the problem can be corrected.

Currently, SLR data centers, analyst centers, and the stations assess system performance. Both data and analyst centers perform some redundant and unique evaluation functions. For example, data format adherence is usually verified by both data centers and analyst centers. But data accuracy can only be determined by analyst centers or data centers with orbit determination capabilities.

Historically, LAGEOS data have been the primary dataset that has been used for measuring system performance. This is because LAGEOS is in a very stable orbit and has a robust historical global dataset. Due to the dramatic increase in satellite missions the past six years and recent improvements in precision orbit determination of other satellites, like TOPEX/Poseidon, performance assessment can no longer be limited to just LAGEOS.

The globally recommended approach to performance assessment presented at the Shanghai SLR Workshop is to migrate this activity from the data centers and analyst centers to the field stations to the largest extent possible. AlliedSignal Technical Services Corporation (ATSC) has demonstrated [*Husson et al.*, 1994] that problem identification at the system is not only feasible, but it can be successfully done if the system has been methodically characterized [*Pearlman*, 1984] and tested.

The current level of performance in the global SLR community is as diverse as the countries that have SLR ranging capability. The diversity in performance is caused primarily by the differences in configuration (i.e. hardware, software, operational procedures, and tracking philosophy); differences in funding levels; and differences in technical understanding. In the rest of this white paper, we will address the major groups that do performance assessment; address the three major areas of performance evaluation and define system performance goals that each system can and should strive to achieve.

1.1.2 Performance Assessment Centers

Currently, there are three main types of SLR performance assessment centers (data centers, analyst centers and the SLR systems). The SLR global data operational centers are the NASA Crustal Dynamics Data Information System (CDDIS), the European Data Center (EDC), and NASA/ATSC. Historically, the primary analyst centers have been Center for Space Research (CSR) at University of Texas NASA/STX, NASA/STX, Delft

Institute for Earth-Oriented Space Research of the Delft University of Technology and NASA/ATSC. There are also at least another 15-20 analyst centers that are becoming very active in the global community on performance evaluation reporting.

The assessment activities of the data centers include verifying format adherence; monitoring timeliness of normal point data delivery; and generating and distributing regular data quantity reports. The analyst centers also verify format adherence and generate regular data quality and data quantity reports. Currently, some but not all field systems have some capability of evaluating their own data quality.

1.1.3 Data Products

In the early and mid 1990's four SLR data products (full-rate data, full-rate normal points, quicklook sampled data and quicklook normal points) in a variety of formats (MERIT II, SAO, NASA and CSTG) were supported and managed by the global SLR data centers.

1.1.3.1 History

The Subcommission on Satellite Laser Ranging (SLR) and Lunar Laser Ranging (LLR), a subcommission of the International Coordination of Space Techniques for Geodesy and Geodynamics (CSTG), has played an active role in streamlining global data operations, which were necessitated by global budget constraints. At the Berne, Switzerland SLR/LLR CSTG subcommission meeting in December 1995, it was agreed that only a single primary data product would continue to be supported by the global community. This data product would be CSTG normal points. In April 1996, MERIT II full-rate data was discontinued and most stations have stopped providing it to the appropriate data center(s).

1.1.3.2 Field Generated Normal Points

When the CSTG normal point format was originally proposed in 1988, a resolution was passed to keep the new format as close to MERIT II format as possible, but the new format had to satisfy telex line constraints. Both formats did contain the necessary information (i.e. calibration correction, meteorological conditions, time-tags, and time-of-flights) to use the data. In addition in 1988, there was no intention to cease the collection and archiving of full-rate data, and so there was no need for critical information about the structure of SLR full-rate data (i.e. skew and kurtosis) be in the CSTG normal point format.

Note: Skew and kurtosis cannot be reconstructed from the normal points.

Changing the CSTG format were proposed by NASA/ATSC at the Canberra SLR Workshop in 1994 to address these issues. The SLR CSTG decided then, that changing the normal point format at that time would be too costly and time consuming and thus would be addressed at a future date. Now 2+ years have expired and this item is still open.

The global transition to CSTG normal points has been slow. As of January 1996, all SLR systems are providing CSTG normal points. This marks the first time in history that this has occurred. There are still a number of minor CSTG normal points violations, but these are not significant and usually do not impact the use of the data. The definitions of some

of the fields in the CSTG normal point format are being updated by the SLR/LLR CSTG Format Working Group to help remove any ambiguities in the interpretation of these fields.

1.1.3.3 Data Flow

The SLR/LLR CSTG recommends that stations forward their normal point data to the appropriate data center within 24 hours. This is difficult for some stations with limited internet accessibility. The preferred standardized method of transmitting SLR data is via File Transfer Protocol (FTP).

Currently, most stations either have a direct or dial-up internet connectivity. A few stations do not have normal point generation capability. These systems transmit their full-rate to their central facility where the full-rate data is analyzed and normal points are produced. However, this is not the recommended approach because this can cause unacceptable delays of several days or more in the delivery of the normal points.

Currently, ATSC and EDC are the only two data centers that receive normal points directly from the international SLR network. The NASA network and some stations in the Western Pacific Laser Tracking Network (WPLTN) send their data to ATSC. The EUROpean LASer (EUROLAS) network and the other stations in the WPLTN network send their normal point data to the EDC. Currently, the NASA CDDIS stills archives any MERIT II full-rate data that it receives.

1.1.4 SLR Data Quality

SLR data quality performance can be subdivided into precision and accuracy. Precision is usually measured in the terms of a single pass or pass segment, whereas, accuracy is measured over a much longer time interval (i.e. weeks, months, years).

1.1.4.1 Precision

The precision of a system is dependent upon the system's hardware, the tracking philosophy (i.e. single-photoelectron vs. multi-photoelectron), and the satellite array. The precision is usually computed as the single shot RMS of a pass or as the normal point pass RMS. For passes that have only a few normal points, computing the normal point RMS is not meaningful. Typically normal point RMS are 4-5 times lower than their respective single shot RMS. For example, if a system has a 1 or 3 centimeter LAGEOS single shot RMS, then its normal point RMS is typically 2-3 millimeters or 6-8 millimeters, respectively.

Historically, system precisions have been based on LAGEOS, because of it's long history and most systems have LAGEOS ranging capability. Most systems get better precision on satellites with just several corner cubes (i.e. ERS-2, Stella, ADEOS, etc.), because the satellite signature is less pronounced.

The single shot RMS is computed as part of the process of the formation of normal point and therefore is one performance parameter than is best done in the field. A system with a very good precision can have accuracy problems (i.e. a system with 1 centimeter precision may have a 20 centimeter range bias) . Data precision is excellent overall from

the international network (see Figure 1), but data accuracy and data stability are still an issue and a significant problem and one of the primary motivations for writing this paper.

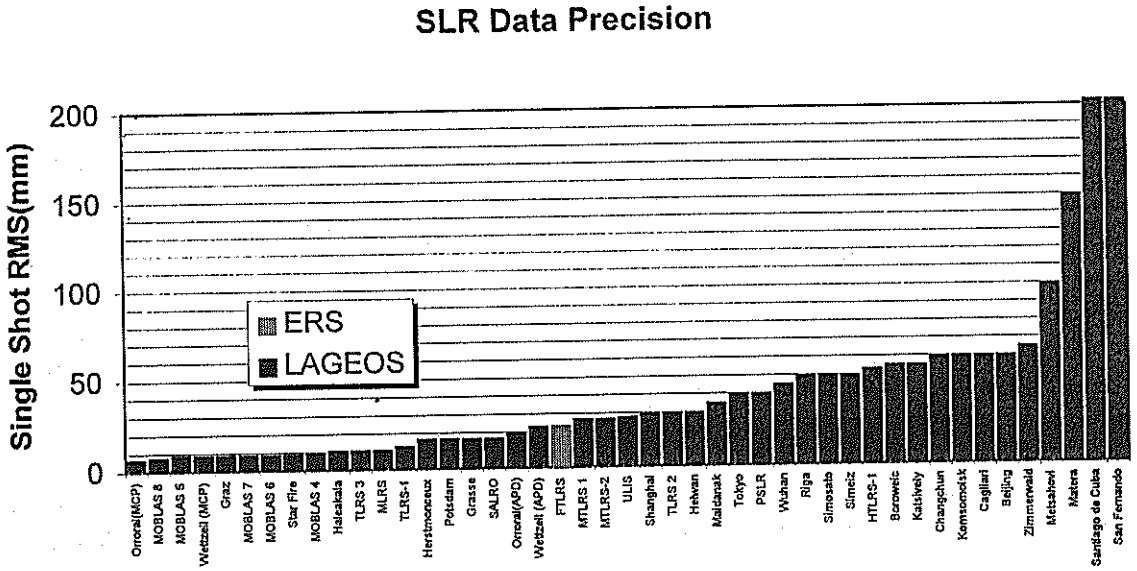

Figure 1. Global Single Shot RMS's

Note: ERS precision values are used for stations that do not have LAGEOS ranging capability.

1.1.4.2 Accuracy

Data accuracy can be measured by several different analysis techniques (long arc, short arc and geometric). Each technique has it's own strengths and limitations. Currently, absolute system accuracy is virtually impossible to measure below the 1-2 cm level. Absolute system accuracy is not only limited by the system's hardware, but is also limited by the accuracy of the geophysical models, atmospheric models, station position determination and satellite signature effects.

The most important factor in data accuracy is not the fact that a system has a near zero range bias, but is that the system range bias is constant both in the short and long term. It is very easy to model a constant bias, but virtually impossible to model a dynamic bias.

1.1.4.3 Long Arc Techniques

Currently, LAGEOS and TOPEX long arc RMS fits of several days are typically 1-2 centimeters and 3-4 centimeters, respectively. As part of the long arc technique, range bias and time bias can be computed. Richard Eanes's weekly LAGEOS report, available via email or the World Wide Web (WWW) contains range and time bias results on a pass-by-pass basis. The Uniform Resource Locator (URL) for CSR analyst results is http://ftp.csr.utexas.edu/slr.html.

For stations that have had stable performance for an extended period of time (i.e. greater than one year) and produce an adequate amount of data (i.e. >200 LAGEOS passes a year), the limitation on LAGEOS range bias and time bias determination are 1-2 cm and

10-20 microseconds, respectively. These levels of problem identification can not be determined on a pass-to-pass basis, but can be determined by aggregating bias results from several passes over short periods of time. The accuracy of range bias determination is maybe no better than 5 centimeters for stations that have never had stable performance for an extended period of time.

1.1.4.4 Short Arc Techniques

Another technique that is used in measuring system performance is a short arc fit to simultaneous data. Graham Appleby from Royal Greenwich Observatory, in September 1996, has semi-automated this technique for LAGEOS and publishes the results via the WWW. The URL is http://www.ast.cam.ac.uk/~gma/bias.html. This technique can identify biases between stations at the 1 centimeter level; however, there a far fewer simultaneous LAGEOS passes than total LAGEOS passes. The largest problem in the SLR analysis community is the lack of a standardized output (i.e. station coordinates, station performance analysis information, etc.). The SLR/LLR CSTG Analyst Centers Working Group was formed at the Shanghai SLR workshop to address this problem.

LAGEOS is still the best satellite for determining system performance using long and short arc techniques and the WWW is currently the preferred medium for publishing SLR analysis results.

1.1.4.5 Geometric

Geometric techniques depend upon quasi-simultaneous data like the short arc technique described above and therefore the technique is limited due to the reduction of available data to work with. Quasi-simultaneous means that two or more stations tracking the same satellite with the tracking time periods overlapping, and tracking does not have to be synchronized. One advantage of the geometric technique is any satellite can be used without loss in accuracy of the results. They are two types of geometric analysis techniques, one for stations that are very close in proximity (i.e. <100 meters), called collocation, and one for stations that are very far apart (i.e. >1000 kilometers). Both geometric techniques require MERIT II full-rate data. Normal point data does not currently support this analysis application.

1.1.4.5.1 Collocation

From a strictly system hardware perspective, the best demonstration and best technique for determining potential system accuracy is collocation. Collocations at NASA/ATSC since the mid 1980's (see Figure 2) have demonstrated that systems are capable of mm level repeatibilities both in the short term (i.e. within a pass and from day to day) and long term (i.e. up to several months). The primary collocation analysis technique that has been accepted by the SLR community is Polyquick, which was developed by ATSC in the early 1980's.

Polyquick is a truly geometric technique that does not have any modeling problems that long and short arc techniques have. Polyquick has been successful in identifying not only centimeter level systematic errors in the NASA network, but also millimeter level systematics. The largest weakness of the Polyquick analysis system is that if a fixed bias exists between two stations, the station with the bias problem may not be able to be determined. However, long arc analysis of collocation data can reveal the station with the

bias problem, if the bias is larger than 2 centimeters. For this reason, Polyquick and long arc analysis are complimentary collocation analysis techniques. Also in the early 1990's, ATSC used Polyquick in verification of the normal points algorithms used by the global community by comparing normal point data to their corresponding full-rate data.

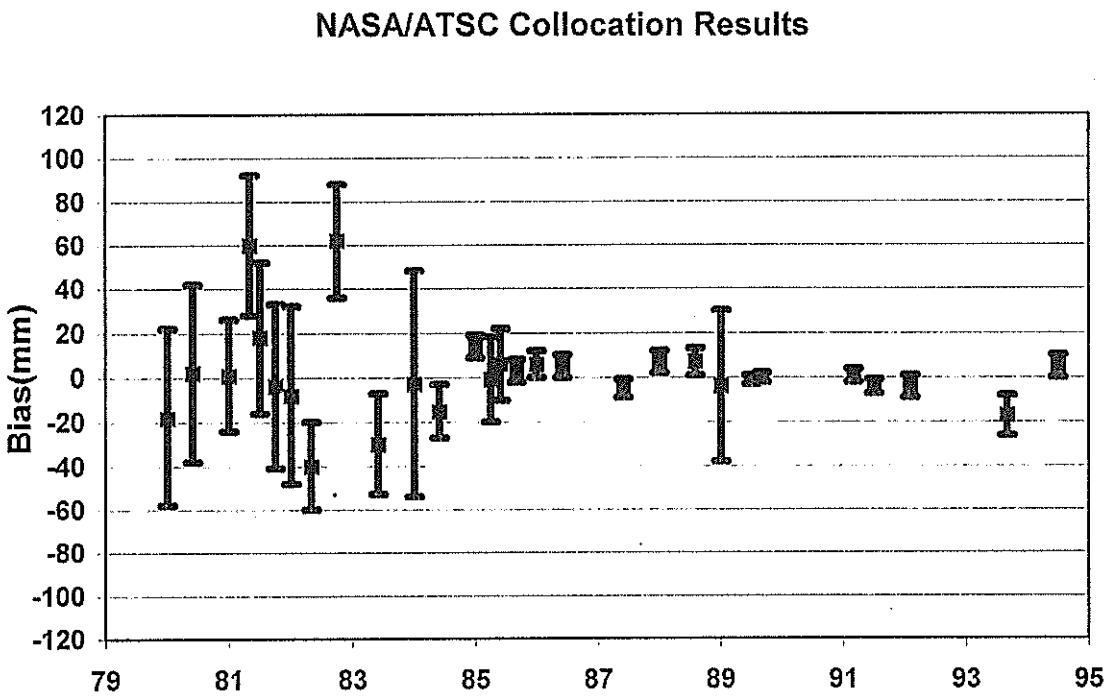

Figure 2. Collocation Results

1.1.4.5.2 Tetrahedrons

The other geometric technique, where stations are not in close proximity, we will call tetrahedrons to distinguish it from collocation analysis. Tetrahedrons requires at least quasi-simultaneous data from at least four stations and does not require synchronous ranging. Quasi-simultaneous means returns only need to be within seconds of each other, not nanoseconds. .This technique also requires an initial estimate of station positions to the several cm level. NASA/ATSC proved this concept can work and be used as a quality control tool in 1991 using historical simultaneous LAGEOS, Etalon, and low satellite data from the NASA and EUROLAS networks [*Degnan et al.*, 1991]. LAGEOS and Etalon are visible over 12% and 25% of the globe, respectively, at any given time. NASA/ATSC found it best to use up to six stations versus four and then intercompare all the possible combinations of four of the six systems.

The reason synchronous ranging is not required is because the interpolation techniques are very accurate (i.e. sub-millimeter) and the added advantage of interpolation is truly simultaneous data can be generated at any frequency without the stations having synchronous ranging capability. Another advantage of interpolation is the RMS scatter of individual measurements is essentially eliminated or dramatically reduced in the interpolation process. Reducing the RMS scatter of individual truly synchronized ranges is still required in synchronous ranging analysis.

The disadvantages of tetrahedrons that collocations do not have are:

1. The stations can not be surveyed by traditional surveying techniques and therefore station coordinates is an error source.
2. The geometry of the stations and the station absolute accuracies is critical to the convergence of four ranges to a single point.
3. The seeing conditions are not the same for the stations and the chances for simultaneous data is greatly reduced.
4. Solid earth tides need to be applied and is a source of error.
5. There will not be much simultaneous data on low earth orbiting satellites.

1.1.5 SLR Data Quantity

Another important parameter in system performance is the amount of data that a system produces (see Figure 3). Many diverse factors determine the data gathering capability of a system. The three primary factors that determine data quantity are the funding support, the weather, and the inherent ranging capability of the system.

Comparing tracking statistics is not fair because of the first two factors, funding support and weather. Some stations only have funding support for an 8 hour tracking period (i.e. single shift) and for maybe only part of the year, while other stations have funding support for 24 hour operations (i.e. 3 shifts), 365 days a year. The weather is the largest weakness of SLR and can vary significantly from location to location. Also, system with different ranging capabilities can and are affected by weather conditions differently (i.e. all systems are not equal).

System ranging capabilities (see Figure 4) can be analyzed as a function of ranging to a satellite as certain altitudes (i.e. Low Earth Orbiting LEO, LAGEOS, or high) and as a function of daytime ranging capability.

1.1.6 Definition of a High Performance System

During the Shanghai SLR Workshop, Mike Pearlman from SAO defined a high performance system. A high performance system is a system that has a stable bias at the 1-2 cm level; has day and night ranging capability on Low Earth Orbiting (LEO) satellites, LAGEOS, and high satellites; and produces 400 LAGEOS passes/year and 1000 LEO passes/year.

1.1.7 References

Degnan J, Conklin B, Bucey S, Husson V, Decker W, "Baselines from Orbit-Free Geometric SLR Solutions", 1991.

Husson V, Horvath J, and Su G, "NASA Automated Quality Control", Proceedings of the Ninth International Workshop on Laser Ranging Implementation, Canberra, Australia, Nov 1994.

Pearlman M, "Laser System Characterization", Smithsonian Astrophysical Observatory, Proceedings of the Fifth International Workshop on Laser Ranging Implementation, Sep 84.

Global SLR Data Volume (October 1, 1995 through September 30, 1996)

System	Tips (Ralph)	Tips (Norton)	GFZ-1	ERS-1	ERS-2	Star-lette	Stel-la	Re-surs	Fi-zeau	Topex	Ajisai	Lag1	Lag2	Eta1	Eta2	Glo63	Glo65	Glo66	Glo67	GPS 35	GPS 36	Pass Total
Yarragadee (M5)	24		196	291	349	382	315	43	172	523	505	467	439	100	42	187			203	74	22	4334
Monument Peak	13		152	220	213	423	191	59	207	447	495	403	366	77	51	153	1		204	122	86	3883
Haleakala	18		77	195	253	308	240	57	131	333	398	326	365	185	107	173			192	171	142	3669
Herstmonceux	50	42	255	233	330	320	318			490	357	445	294	44	46	37			52	26	15	3354
Orroral	5		56	198	240	406	225	18	113	337	459	377	298	15	12	45	7	20	38	4	1	2874
Quincy	38	3	77	145	218	383	203	63	126	463	362	309	247	11	11	36			83	3		2781
Graz	11		177	244	326	269	237	33	60	384	280	303	181	46	35	24			38	12	16	2676
Wettzell (WLRS)	1	3		105	143	243	137	5	42	395	352	408	294	129	96	76			113	79	45	2666
Arequipa	7		31	221	272	266	248	29	153	378	403	170	218									2396
Potsdam	32	21	323	192	267	183	178			369	205	239	146						2	3	1	2161
Grasse	13	10	189	246	343	224	216			363	231	103	88									2026
Greenbelt (M7)	46		47	87	135	241	111	50	91	193	243	213	178	3	2	40	22	52	56	9	5	1824
McDonald	14			125	164	154	125	11	52	360	269	195	170	9	12	15			9	15	12	1711
Greenbelt (M6)	3	1	32	100	120	198	83	7	60	162	180	153	143	3	18	33	1	1	20	15	3	1336
Riga (LS-105)	53	53	135	188	254					49		130	84			2			1	5	4	958
Maidanak			25	103	149					111		140	97	39	70	64			80	19	12	909
Metsahovi	25			97	160	38	87	27	56	222	92	14	10			1						829
Simosato			10	59	55	86	59			92	218	81	81	3	20							764
Changchun	16			58	78	82	77	11	18	108	94	119	71	12	13							757
Matera	1			48	64	89	37	1	5	107	99	95	94									640
San Fernando			1	63	77	73	64	20	24	115	189		1									627
Beijing	5		2	17	26	74	15	5	5	136	236	23	16									560
Boroweic	1		12	47	64	27	33	5	20	103	83	76	31									502
Santiago			6	53	74	55	24	1	7	110	103	14	42									489
Shanghai				13	22	38	15			63	136	61	80	6	14	6			3			467
Santiago de Cuba			24	80	63	41	16			61	54	2	4									346
Komsomolsk			6	15	24					85		64	50	11	21	22			19	1	8	326
**Riyadh					5	50	8			27	34	59	78	1	2				7	4		276
Cagliari	1	1	1	28	35	11	12			43	51	29	35									247
Mendeleevo			2	49	74					97												222
Helwan				15	35	20	34	3	3	39	43	3	1									196
Wettzell (MT1)	3		5	10	15	5	7	3	2	20	7	49	41									167
Yarragadee (PSLR)			2	12	15	21	7		2	18	34	30	13									164
Tokyo				5	1	11	9			18	39	10	22	2	1	7			2			127
Wuhan	1			2	5	6	4		3	11	31	12	25		2	1			1			104
Katsively				13	12					11	4	26	9	4	1	3			11			94
Simeiz				8	9	5	3			16	19	17	6						1			84
**Riga (ULIS)	7	3			3		3			3												19
**Grasse (FTLRS)				1		1	4			2	1											9
Totals	388	137	1843	3686	4692	4733	3346	461	1362	6864	6304	5165	4318	700	676	926	31	73	1136	562	372	47,662

Figure 3. Global SLR Data Volume

Note: ** Indicates a new system or a system that has relocated within this period.

Global System Capabilities (November 1996)

Location and/or System Name	Pad ID	Network	Shifts	LEO Capability	LAGEOS Capability	GPS Capability	Lunar Capability	Internet Connectivity
Maidanak 1, Uzbekistan	1863	WPLTN	inactive	night/day	night	n/a	n/a	n/a
Maidanak 2, Uzbekistan	1864	WPLTN	1.5	night/day	night	night	n/a	dedicated
Evpatoria, Ukraine	1867	EUROLAS	inactive	night/day	night	n/a	n/a	n/a
Komsomolsk-na-Amure, Russia	1868	WPLTN	1.5	night/day	night	night	n/a	dial-up
Balkash, Russia	1869	EUROLAS	inactive	night/day	night	n/a	n/a	n/a
Mendeleevo, Russia	1870	WPLTN	1.5	night/day	n/a	n/a	n/a	dial-up
Sarapul, Russia	1871	WPLTN	inactive	night/day	n/a	n/a	n/a	n/a
Simeiz, Ukraine	1873	EUROLAS	2	night/day	night	n/a	n/a	dial-up
Riga, Latvia	1884	EUROLAS	1	night/day	night/day	night	n/a	dial-up
Riga, Latvia (ULIS)	1885	EUROLAS	1	night/day	night/day	night	n/a	dial-up
Katsively, Ukraine	1893	EUROLAS	1	night/day	night	n/a	n/a	dial-up
Santiago De Cuba	1953	EUROLAS	1	night/day	night	n/a	n/a	dial-up
McDonald Observatory, Texas	7080	NASA	2	night/day	night/day	night/day	night	dedicated
Yarragadee, Australia (MOBLAS 5)	7090	NASA	2	night/day	night/day	night/day	n/a	dial-up
Greenbelt, Maryland (MOBLAS 7)	7105	NASA	3	night/day	night/day	night/day	n/a	dedicated
Greenbelt, Maryland (48 inch)	7106	NASA	1	night/day	night/day	n/a	n/a	dedicated
Quincy, California (MOBLAS 8)	7109	NASA	2	night/day	night/day	night/day	n/a	dedicated
Monument Peak, California (MOBLAS 4)	7110	NASA	3	night/day	night/day	night/day	n/a	dedicated
Haleakala, Hawaii	7210	NASA	2	night/day	night/day	night/day	n/a	dedicated
Wuhan, China	7236	WPLTN	1.5	night/day	night	n/a	n/a	dial-up
Changchun, China	7237	WPTLN	1.5	night/day	night	n/a	n/a	dial-up
Beijing, China	7249	WPLTN	1.5	night/day	night	n/a	n/a	dial-up
Tokyo, Japan	7308	WPLTN	1	night/day	night/day	n/a	n/a	dedicated
Arequipa, Peru (TLRS-3)	7403	NASA	2	night/day	night/day	n/a	n/a	dial-up
Santiago, Chili (TLRS-2)	7404	NASA	2	night/day	night	n/a	n/a	dedicated
Cagliari, Italy	7548	EUROLAS	1	night/day	night	n/a	n/a	dedicated
Wettzell, Germany (MTLRS-1)	7597	EUROLAS	1	night/day	night/day	n/a	n/a	site dependent
Metsahovi, Finland	7805	EUROLAS	2	night/day	night	n/a	n/a	dial-up
Boroweic, Poland	7811	EUROLAS	1	night/day	night	n/a	n/a	dedicated
San Fernando, Spain	7824	EUROLAS	1	night/day	n/a	n/a	n/a	dial-up
Helwan, Egypt	7831	EUROLAS	1	night/day	night	n/a	n/a	dial-up
Riyadh, Saudi Arabia	7832	WPLTN	2	night/day	night/day	night/day	night	dial-up
Grasse, France	7835	EUROLAS	2	night/day	night/day	night	n/a	dedicated
Potsdam, Germany	7836	EUROLAS	3	night/day	night/day	night	n/a	dedicated
Shanghai, China	7837	WPLTN	1.5	night/day	night/day	n/a	n/a	dial-up
Simosato, Japan	7838	WPLTN	2	night/day	night/day	n/a	n/a	dedicated
Graz, Austria	7839	EUROLAS	1.5	night/day	night/day	night/day	n/a	dedicated
Herstmonceux, U. K.	7840	EUROLAS	2.5	night/day	night/day	night/day	n/a	dedicated
Orroral, Australia	7843	WPLTN	2	night/day	night/day	night/day	n/a	dedicated
Yaragadee, Australia (PSLR)	7847	WPLTN	inactive	night/day	night	n/a	n/a	site dependent
Ajaccio, Corsica, France (FTLRS-1)	7848	EUROLAS	1	night/day	n/a	n/a	n/a	site dependent
Albuquerque, New Mexico	7884	US Military	1.5	night/day	night/day	night/day	n/a	dedicated
Greenbelt, Maryland (MOBLAS 6)	7918	NASA	1	night/day	night/day	night/day	n/a	dedicated
Greenbelt, Maryland (TLRS-4)	7920	NASA	inactive	night/day	night/day	n/a	n/a	n/a
Matera, Italy (SAO-1)	7939	EUROLAS	3	night/day	night	n/a	n/a	dedicated
Kootwijk, Netherlands (MTLRS-2)	8833	EUROLAS	inactive	night/day	night/day	n/a	n/a	site dependent
Wettzell, West Germany (WLRS)	8834	EUROLAS	3	night/day	night/day	night/day	night	dedicated
Matera, Italy (TLRS-1)		NASA	inactive	n/a	night/day	n/a	n/a	n/a
Japan (HTLRS-1)		WPLTN	1	night/day	night/day	n/a	n/a	site dependent

Note: n/a means no ranging capability or non applicable

Figure 4. Global System Capabilities as of November 1996

SLR Data Usage, Applications, Performance and Requirements

Michael Pearlman
Smithsonian Astrophysical Observatory
Cambridge, MA, USA

Data Usage and Applications

The SLR analysis centers were recently surveyed to ascertain:

Who is using the SLR data?
What applications are they studying?
What satellites are they using?
Are they satisfied with the data?
What is missing (volume, accuracy, consistency, geographic location, etc)?
What should the network be providing to meet current requirements?

The responses to the surveys showed that more than 25 analysis groups are now using laser ranging data for a wide range of applications including: solid earth sciences, precision orbit determination for altimetry and navigation, lunar science and related relativity, atmospheric and weather sciences, and calibration of other distance measuring techniques such as GPS, GLONASS, Doris, and PRARE (see Table 1). Solid Earth science areas of study include: structure of the static gravity field, modelling of the time-varying gravity field, tides, Earth rotation and polar motion, crustal motions, and Earth mass (Gm) and relativity. Some of the most challenging applications are now centered around measurement of the vertical for hazard assessment and [redacted] lift and the response of the Earth's crust to seasonal changes in

problems of several cm. or more. The major issues as reported in the survey of the analysis groups were (see Table 2):

1. large disparity among stations in data quantity and data quality;.
2. incomplete geographic distribution;
3. large temporal gaps (lapses in data from individual stations); and
4. incomplete and inaccessible system configuration information

Although bias free performance is preferable, a fixed range bias can be accommodated by the analysts for most applications. Difficulty arises from frequent system changes that are not adequately calibrated. The strongest advice to the stations is:

1. leave the systems in a stable configuration, avoiding changes unless absolutely necessary; and

2. when changes must be made, the transition must be accompanied by very careful calibration and documentation of the change.

In addition, we need to:

1. strengthen network quality assurance; and

2. establish on-line, up-to-date engineering/configuration files on each station.

Requirements

Network Configuration

For global reference requirements, the SLR community needs to provide the equivalent of at least a dozen high performance SLR stations, well distributed in latitude and longitude. Some of these "stations" may be provided by "clusters" of SLR sites, as in Europe, China, and Japan where SLR sites are in place for more localized studies, but may also serve to share tracking responsibilities, expand temporal coverage, and overcome the vagaries of weather. This "cluster concept" has been discussed by Prof. Gerhard Beutler later in this report.

The current SLR network has some serious geographic gaps, but station relocations now underway or under serious consideration will help fulfill the global requirement. The MOBLAS-8 system is in the process of being relocated to Tahiti, and serious planning is underway regarding the relocation of MOBLAS-6 to South Africa, TLRS-4 to India, and MTLRS-2 to Indonesia.

Still in need of attention is the improvement in equipment and operations of the Russian and Chinese SLR systems which would play a very important geographic role in the global reference network.

Station Performance Expectation

The SLR global reference network should be comprised of "high performance" stations operations. As a guideline, "high performance" stations should provide:

1. routine day and nighttime ranging;

2. high and low satellites coverage
3. minimum data quantity of:

    a. 1500 passes per year on all satellites
    b. 200 passes per year on LAGEOS

4. stable range bias (<1 cm) over a period of a year
5. punctual data delivery (within 24 hours)
6. strict format compliance
7. up-to-date configuration information
8. up-to-date calibration information

The analysis centers routinely evaluate data and issue reports on data quality by station.
The operations centers have routinely worked with the field stations to diagnose and remedy performance problems. However, the stations must recognize that the evaluation of station performance begins at the station, where the knowledge on the system resides and the source of information is most immediate. Please keep in mind:

1. There is no substitute for careful, on-site engineering and calibration testing of system performance, and

2. Keep the system configuration constant; change things only when necessary.

It is pretty clear that only data from systems that are stable or whose configuration changes are easily traceable and well calibrated will be used in the analysis activities.

SLR Analysis Survey Results

SLR User Organizations

AIUB†
ASI†
AUSLIG
Auston University†
CRL
DGFI
DUT†
GFZ/DLR†
GRGS/CNES and OCA†
IfAG Potsdam†
MIT/Lincoln Labs†
NAL†
NASA GSFC†
NASA JPL
NRL
NSWC
RAS†
RGO†
Shanghai Observatory†
Univ. of Bologna
Univ. of MD
Univ. of Padova†
Univ. of Southampton†
Univ. of TX/CSR†
USAF
+Others

†responded to survey

Satellites Used

AJISAI

ERS-1/2

ETALON-1/2

GFZ-1

GPS-35/36

GLONASS

LAGEOS-1/2

STARLETTE

STELLA

TOPEX

Areas of Investigation

Altimetry and Calibration
Atmospheric Density
Earth Rotation/Polar Motion
Earth Tides
Fundamental Physics
Gravity Field and Long Period Variations
Long Period Aerodynamics/Gas Surface Interactions
Non-Gravitational Acceleration and Perturbations
Ocean Tides
Orbital Analysis
Performance Assessment
Precise Orbits for Altimetry and SAR
Precise Orbits for Calibration of Satellite Surveillance Radars
Position/Motion/Velocity
Technique Comparison/ Combination

SLR Analysis Survey on the WWW: http://cddis.gsfc.nasa.gov/cstg/slr_analysis.html

Table 1

General Comments

- **Data quality:**
  - Large disparity in data quality among stations
  - Often, data of poor quality are worse than no data at all
  - Too many systems with poor data quality
- **Data Volume:**
  - Tracking coverage from some stations is very sporadic and sparse
  - Some stations do not provide a minimum level of contribution
  - Tracking gaps of more than ten days are a problem
  - Weeks with less than 100 LAGEOS passes are sparse
  - Much more data required on ETALON-1 and -2, GPS-35/36, and GLONASS
  - Significant amount of bad ETALON data
  - GFZ-1 data is insufficient
  - STELLA and STARLETTE often marginal (but still useful)
- **Geographic Coverage:**
  - Better geographic coverage needed in the Southern hemisphere, Russia, and China
- **Temporal Coverage:**
  - Tracking gaps over weekends are a problem
  - LAGEOS-1 and -2 data is adequate for three-day resolution, but inadequate for one-day resolution
  - More data on STELLA, STARLETTE, and AJISAI required for one-day resolution of higher order perturbations
- **Local Surveys:**
  - More reliable local surveys and more information about the surveys and local eccentricities required
- **Operational Follow-up:**
  - Lack of communications with some stations regarding problems
- **Satellites:**
  - More satellite targets of high quality needed

Table 2

Station Performance Evaluation
BOROWIEC SLR (7811)

S.SCHILLAK

SPACE RESEARCH CENTRE
OF POLISH ACADEMY OF SCIENCES
BOROWIEC ASTROGEODYNAMICAL OBSERVATORY
62-035 KÓRNIK, POLAND
tel: +48-61-170-187
fax: +48-61-170-219
e-mail: sch@cbk.poznan.pl

New since last Workshop:
- new control computer PC-486 with new real-time software
- new satellite tracking system > better pointing accuracy
- automation of predictions calculations
- automation of post pass data handling
- camera CCD

New in the near future:
- transmitting telescope
- photomultiplier HAMAMATSU H5023
- Time Interval Counter STANFORD SR-620
- shorter laser pulse (35 ps)

Data quality control:

a) on-site; single shot RMS
residuals distribution control
normal points RMS
calibration residuals distribution and means
calibration pre-post

b) off site; LAGEOS Range Bias and Time Bias (CSR Reports) (Fig.)
LAGEOS Raw RMS (CSR Reports)
LAGEOS Raw RMS (DUT Reports)
ERS Raw RMS (GFZ Reports)

Improvements of data quality control:

a) on site; graund target calibration improvement (second target)
control of return signal strength

b) off site; TOPEX and AJISAI Range Bias
Residuals for every normal point

BOROWIEC SLR RANGE BIAS - CSR 1995

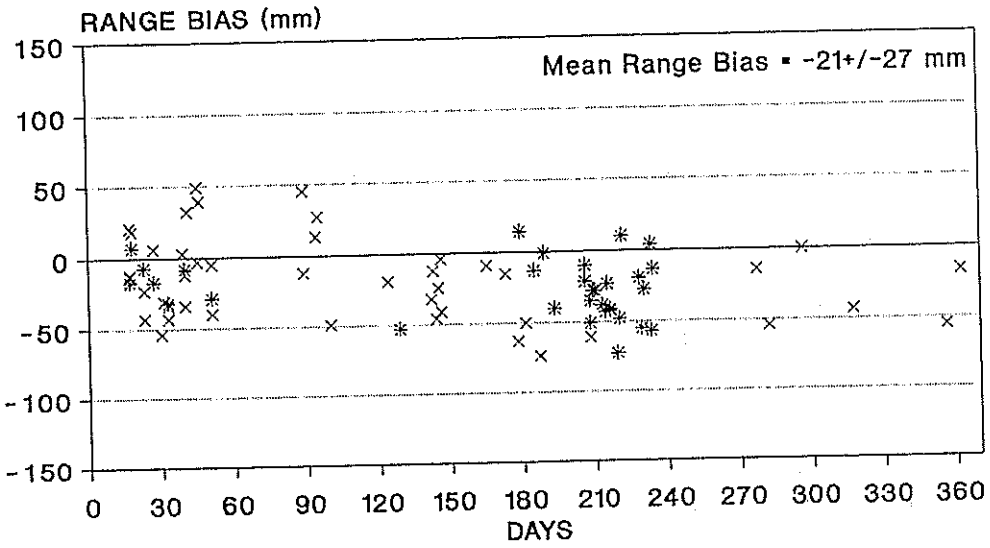

× LAGEOS-1 * LAGEOS-2

Range Bias from weekly Reports of Center for Space Research
University of Texas at Austin

BOROWIEC SLR RANGE BIAS - CSR 1996

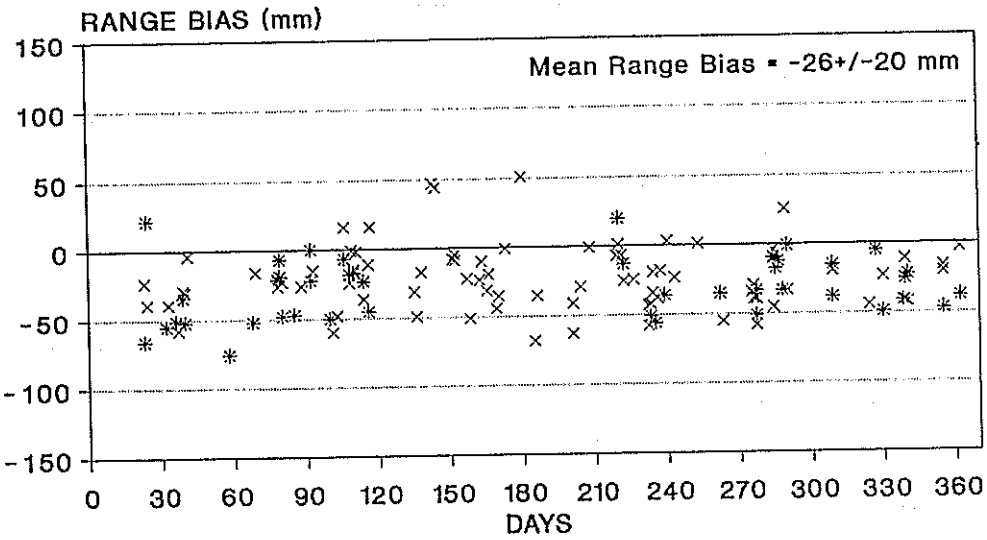

× LAGEOS-1 * LAGEOS-2

Range Bias from weekly Reports of Center for Space Research
University of Texas at Austin

Global SLR: Recognition, Identification, and Resolution of Data Problems.

Tom Varghese, AlliedSignal, 7515 Mission Drive, Lanham, Maryland 20706, USA.
e-mail: varghet@thorin.atsc.allied.com.

The processes within the global SLR community can be significantly improved to realize the full potential of the technique and the resources expended. At the present time, the global SLR systems belong to several classes with varying attributes. The differences in the system behavior are clearly demonstrated in the ranging performance as well as the data problems they exhibit. The data often shows significant instability and inconsistency. We have achieved quite a bit of improvement in the last few years. However, we must accomplish more and is well within the reach of the current technology and processes that we can implement.

The quality of the data is strongly coupled to the station hardware/software performance as well as operational procedures. It is observed that, there is insufficient quality control of data in many stations before the data leaves for the use of the scientific community. Even when problems are identified by the user community, the problem resolution is not always expedient or even attempted. It is extremely important that quality control become a critical part of the station operational and maintenance procedures.

It is common knowledge that there is increasing fiscal pressures on the SLR budget within the global community. This leaves insufficient resources for major hardware or software changes in many stations. Under these conditions, we must explore ways of getting the best scientific value for our data through minimal changes of the systems engineering. A number of improvements can be incorporated by adapting new processes or modifying existing ones.

The instability of station performance is a noticeable characteristic within the SLR data. It must be recognized that the stability of station performance is much more important than sporadic good performance as we are looking for long term answers. Since no science question is solved in one satellite pass or passes within a few days, the long term stability and accuracy must be the top priority of all data producers. Last but not least, there is sparse data coming from several stations. It goes without saying that such data does not impact the global solution and such stations become poor contributors within the framework of the global SLR analysis and solution. Thus minimum standards for data quality and quantity must be met by each station.

How can we improve and where do we go from here? We must define an approach that is simple and can be embraced by the entire community without intruding into the autonomy of the stations. The stations must have access to the "knowledge" required towards doing a great job with their systems. Once this is available, the following

practices may be adopted towards improving the data quality while ensuring adequate data quantity.

- Perform frequent validation of the engineering performance of the system to verify data quality as well as to detect problems.
- improve the on-station QC capability to screen data problems before it becomes a problem for the analysis community.
- Adopt well defined and successful processes from the best practices within the SLR community to facilitate on-station QC efforts.
- expedite data problem resolution when identified by the analyst and take measures to prevent them or obtain early warning prior to becoming a problem.

As indicated earlier, an approach to implement this is to "capture and exploit" the current knowledge and experience in the global SLR community. Having an on-line access to "current SLR systems configuration and the performance characteristics of the data relevant modules " is fundamental to expedient data problem resolution. This will provide the baseline knowledge required for closer interaction between the data users and data producers and timely resolution of problems.

The accompanying slides capture the key points of the proposed approach and outlines a mechanism to accomplish the above goal. The formation of an international engineering data panel is proposed that will frequently examine unresolved engineering problems. This group will also foster close ties between the data users and data producers.

A well coordinated approach is critical to achieve the maximum potential of SLR towards producing the highest quality data. The existing SLR "knowledge" infrastructure needs to be enhanced to handle the additional information that the station needs to facilitate expedient data resolution. The stations must also enhance its knowledge base about the system performance and document it properly for current and future reference. The station must understand the cause of its problem when it occurs and identify it either explicitly or by examination or in consultation within the community. It must also find ways to solve the problem and hopefully prevent them in the future.

In summary, the stations have the ultimate responsibility for their data. It must exploit all available knowledge within the Global SLR community to produce the highest quality data possible for the scientific community. The proposed Global SLR Engineering Data Panel and the improved process steps and information defined in the slides in this document are means to facilitate and accomplish the above goal.

Global SLR: Recognition, Identification, and Resolution of Data Problems

Objectives:

- **Improve the global SLR data quality (accuracy and stability) and data quantity.**
- **Expedite data problem resolution**
- establish a **standardized approach** from best practices.
- improve the **on-station QC capability** to screen data problems.

Approach:

- **"Capture and exploit"** the current knowledge and experience in the global SLR community.

Global SLR: Current Information flow

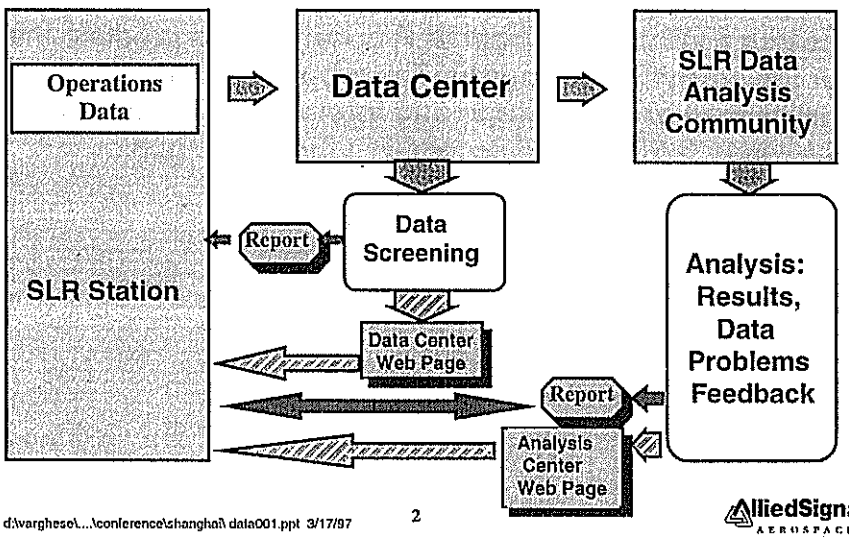

Global SLR: On-station Data Processing, Testing and QC

Operational Data:

- Normal Point Data
- Station Local Survey Data
- Data problems "reported by the station" to the data centers.

Engineering Data /Results

- No engineering test data or results relevant to operational performance is currently maintained in the Data Center.

WHAT ARE WE MISSING?

– on-line access to "current SLR systems configuration"; fundamental to expedient data problem resolution.

– station HW/SW performance data.

– framework for closer interaction between data users and data producers.

Global SLR : FeedBack provided by Data Centers (CDDIS, EDC,...) to the Stations

Data Centers provides the following feedback to the stations.

FORMAT COMPLIANCE:

–Verify compliance with data formats; "minimal problem" within the global SLR Data.

DATA ACKNOWLEDGEMENT:

–provides feedback to the stations on the amount of data received by the Data Center from the respective stations

–DATA ANALYSIS FEEDBACK:

–some "engineering" feedback provided by data centers to the stations

Global SLR : Feedback provided by the analysis community.

CSR:<weekly Report on each **L1, L2 pass based on 3-day arc.**

- **Satellite Data:** Good Obs, single shot RMS*, RMS to an orbit, Precision Estimate of NP, Range Bias, Time Bias, Modeled Bias, Pass Duration, Edited Obs
- **Calibration Data:** Mean*, Std. Dev*., Cal. shift*.

Delft: <weekly Report on **L1, L2 based on 10 day arc.**

- **satellite data:** RMS to an orbit, Range, Time Bias (problem passes), good/bad passes, statistics on day/ night passes, geometric distribution for transportable (TLRS, PSLR, MTLRS) systems, adjustment to station co-ordinates.

Herstmonceux: < monthly graphics dispaly based on daily solutions>

- **satellite Data:** Range Bias and Std. Dev. , intercomparison of stations using short arc analysis of simulatneous passes.

Global SLR

What information do we need in the future?

Global SLR: What information do we need to maintain in the future ?

- SLR system **"current baseline configuration and performance" data.**
- **Data center feedback.**
- **Analyst feedback** on station performance.
- **Lessons learned**: History of Past problems and their solutions.
- **Information on** New Technologies, methods, solutions, results,..

Global SLR : SLR System "Baseline Performance Data"

SLR System Modular Verification

- **Timing and Frequency Devices;** < Epoch and Event time>
  [Stability (Drift), Accuracy, Precision]
- **Detectors** *[Stability (Drift), Accuracy, Precision]*
- **Signal Processing Devices;** *[Stability (Drift), Accuracy, Precision]*

SLR Subsystem Verification:

- **Timing Subsystem** *[Stability, Accuracy, Precision]*
- **Meteorological Sensors** *[Stability, Accuracy, Precision]*
- **Local Survey:** ***Cal Targets, Internal Cal, Telescope eccentricity*** *[Stability, Accuracy]*

System Verification:

Global SLR: Information needed from the Analysis Community

Data Center:

- Format compliance, Data Acknowledgement
- Out-of-bound parameters

Analysts: < multiple satellite solutions for each station>

- **Precision:** RMS fit to a global arc, NP precision, single shot RMS
- **Observations:** Total, Edited, Day/Night
- **Bias:** Modeled Range, Time Bias, Observed Range, Time Bias
- **Stability:** Short term(3 month) and long term(=>6 months) Stability.
- **Systematic signatures:** short term, long term.
- **Station co-ordinates**
- **data assessment:** quantity, quality, adequacy, geometry, significance
- **Others:** barometric pressure, calibration delays, cal. shift, precision.

Global SLR: Examples of Lessons learned

NASA Collocations:

- **Rigorous characterization** of modules and subsystems critical to data.
- **Accurate survey** to eliminate range bias, height dependence, and azimuth dependence errors.
- **Meteorological Closure** especially barometer with national and international standards.
- **Epoch Timing Closure** with UTC.
- **Robust Calibration Procedures** for signal strength, system non-linearities, etc.
- Capability to **verify system behavior** at all satellite ranges.
- Short **stable calibration** targets.
- **Stable clock** frequency.
- **monitoring** of station parameters for out-of-bound values.

Global SLR: Proposed Framework to Solve Data Problems

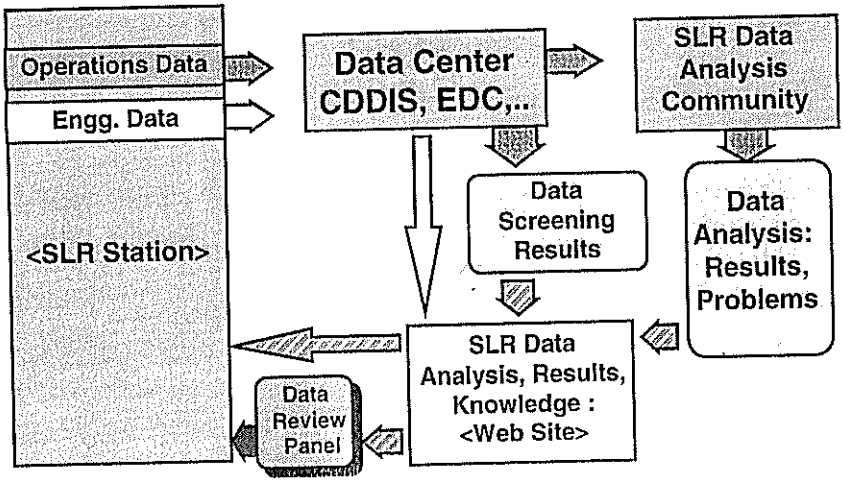

AlliedSignal AEROSPACE

Global SLR : Proposed Approach for Expedient "Recognition, Identification, and Resolution" of Data Problems

- **SLR stations** take full responsibility for the Generation and maintenance of high quality SLR data; stations will maintain its engineering and configuration data file up-to-date and maintain the integrity of the system.
- The **SLR analysis community** in concert with the **data centers** provide appropriate and timely feedback to the stations on the quality and quantity of the data as well as the data problems.
- The operational **SLR stations** expedite the solution of data problems and make "changes" to the stations with proper rationale and close coordination with the user community.
- **The SLR community** share information collectively to solve common data related problems.

AlliedSignal AEROSPACE

New Fixed Station

THE NEW LASER AND ASTROMETRIC TELESCOPE IN ZIMMERWALD

W. Gurtner, E. Pop, T. Schildknecht, J. Utzinger
Astronomical Institute
University of Berne
CH-3012 Berne
Switzerland

U. Wild
Federal Office of Topography
CH-3084 Wabern
Switzerland

J. Barbe
G.I.E. Télas
F-06322 Cannes
France

1. THE OLD SLR SYSTEM

From 1984 till April 1995 a Satellite Laser Ranging Telescope was routinely operated in Zimmerwald by the Astronomical Institute of the University of Berne, during the last few years substantially supported by the Federal Office of Topography.

The telescope was designed and mostly built in-house. It consisted of a Cassegrain receiving telescope of 50 cm aperture and a separate transmitting Galilei telescope which collimated the laser beam with a factor of about five.

The telescope also comprised a ISIT TV camera that used the 50 cm primary mirror of the receiving telescope to allow optical guiding of all sunlit targets during the night.

To test developments in the area of CCD image processing, object recognition, position, and orbit computation of optically tracked targets the TV camera was occasionally replaced by a CCD camera.

The laser used was a Quantel Nd:YAG laser allowing 10 observations per second.

The system, especially the telescope, had some serious limitations:

- Due to difficult and unstable axis alignments between the transmitting and receiving telescope and the limited tracking accuracy it was not possible to narrow the field of view enough for daylight tracking

- The energy budget of the whole system did not allow ranging to high-orbit targets such as GPS, Glonass, and Etalon satellites

- Rapid switching from one satellite to another (pass interleaving) was not possible
- The single-shot accuracy was not adequate anymore. An upgrade to a SPAD detector was not possible because of the bad definition of the optical axes and the limited optical imaging quality
- The Nd:YAG laser has been in operation for more than 10 years, it has practically reached its service life

2. REQUIREMENTS OF THE NEW SYSTEM

In 1991 the SLR group of the Astronomical Institute compiled a detailed list of requirements of a new system that was submitted to six possible telescope manufacturers.

The most important question to answer was: Is it possible and feasible to design and manufacture a telescope for both SLR and astrometric (CCD) observations?

The following requirements were formulated:

2.1 Satellite Laser Ranging

- ranging from low orbiting satellites up to geostationary satellites
- a few millimeters single shot accuracy
- both night- and daytime operation
- pass interleaving, i.e. rapid switching from one satellite to another (requirement affecting the system **and** the dome)
- fully automated operation, on-site operator is necessary only to handle exception conditions
- prepared for two colors
- 10 to 20 deg minimum elevation (requirements for the dome)
- visual tracking support possible
  - large field of view (> 0.5 deg)
  - small object tracking

2.2 Astronomical Observations

- high-precision tracking for
  - zero velocity objects (geostationary satellites)
  - slow objects (minor planets)
  - fast moving objects (low orbiting satellites)

→ two tracking ranges
1) 0 - 1 arcmin/sec; exposure time: several minutes
2) 0 - 1 degree/sec; exposure time: a few 1/10 sec

- high image resolution: ca. 1" per CCD pixel
- small object tracking (a few cm diameter)
- derotation of the field of view
- fast switching from one experiment to another (i.e. several ready to use camera ports with individual focal reductors)

2.3 General Requirements

- Simultaneous SLR and astrographic operation must be possible. A certain reduction in performance (e.g. imaging qualities, laser cadence) however is acceptable
- Switching from SLR mode to pure astrographic mode and vice versa can be done within a few seconds
- The telescope has to fit into the existing building

In parallel we also evaluated

- a laser system
- a station computer
- electronic equipment for the signal processing

Four out of the six manufacturers came up with a coarse concept study and cost estimate. We decided to continue negotiations with G.I.E. Télas, France (a joint venture between the two French companies Aerospatiale and Framatome) and ordered a detailed design study to be realized during 1992.

The results of the first evaluation phase showed that it seemed to be possible to combine the two major tasks (SLR and CCD observations) on the same telescope.

However, the requirements for pass interleaving and low minimum elevation lead to the conclusion that the old dome had to be replaced with a new design, fortunately still fitting onto the existing building.

The following institutions are financing the the new system:

- The Federal Office of Topography
- The University of Berne (Canton of Berne)
- The Department for Civil Engineering of the Canton of Berne
- The Swiss National Science Foundation

The telescope was ordered at Télas in March 1994 and the final Design Review took place end of October 1994.

3. THE NEW ZIMLAT TELESCOPE

The telescope has a 1 m primary mirror and a 30 cm secondary mirror in a Richey-Chretien configuration.

The optical part of the telescope has a Nasmith path to 4 different positions for cameras, each one with its own focal reductor:

Port	Camera	Reductor	Field of view	Focal length
1	CCD Camera	CO1	13 '	4 m
2	CCD Camera	CO2	40 '	4 m
3	CCD Camera	CO3	13 '	8 m
4	TV Camera	FR	45 '	1.2 m

The cameras are radially mounted on motorized slides on a vertical instrument platform fixed at one end of the horizontal axis. A computer-controlled deflection mirror (DM) at the center of the platform selects the camera port to be used. The platform can be rotated around this axis for field of view derotation according to different strategies (elevation-coupled, declination-coupled, along-track-coupled).

The requirement of fast switching between various satellites asked for rather high slew rates and accelerations. Technical reasons didn't allow a 180° range for the elevation axis (which would have allowed an even faster switching and an easier tracking at near zenith). This restriction could be compensated by a relatively high maximum velocity in azimuth:

- Azimuth $< 30°/s$; $10°/s^2$; $\pm 270°$
- Elevation $< 15°/s$; $5°/s^2$; -2° to +90°

The confirmed tracking accuracies are:

- 2 arcsec absolute
- few 1/10 arcsec relative

The laser beam is guided into the telescope through a coudé path and a beam splitter (DBS) mounted in the horizontal axis of the telescope. The laser beam is expanded into a ring shape by means of an axicon (two conical lenses), and it leaves the telescope concentrically around the secondary mirror. The ring diameter is about 35 cm (inner) and 50 cm (outer), respectively.

The receiving path uses the area around the laser ring and it is separated from the transmitted beam through a 45°-mirror with a center hole for the beam. This design does not need a rotating mirror as transmit/receive switch, and the transmitted laser beam does not change its position within the telescope during the tracking. The latter fact facilitates in-pass calibration and beam direction control through retroreflectors.

All the optical components are prepared for two-color ranging (beamsplitter, coudé mirrors, mirrors and lenses on the detector table).

The tracking of sun-lit laser satellites can be checked during night time with the ISIT TV camera mounted on the instrument platform in port number 4. The transmitted laser beam can be seen on the TV screen as a spot (a small part of the beam is reflected into the camera by a very small corner cube reflector mounted on the spider of the secondary mirror).

Although an additional optical component (P1-P2) between the dichroic beam splitter (DBS) and the deflection mirror (DM) has been inserted to decrease the negative effect of the beam splitter, it can be lifted pneumatically to allow completely undisturbed optical observations with each one of the CCD cameras on the instrument platform.

First tests showed that the switching from one satellite to another can be done within 10 to 20 seconds (depending on the relative positions), the time for (re-)acquisition, i.e. until returns are confirmed by the realtime filter, not included.

The following table shows a possible scenario for pass-interleaving automatically generated by the station computer:

```
-------------------------------------------------------------------------------
 # Satellite 07:46:47                    08:03:17                    08:19:17
-------------------------------------------------------------------------------
01 STARLETTE ###++###++##++++-------------------------------------------------
02 LAGEOS-2  --------++++##++++###++++##++++++++++++##++++##++++###++++####++
03 LAGEOS    ----++++++++++##++++###++++++##++++##++++++++++##++++###++++##
04 TOPEX     ------------------------+###++###++##++------------------------
05 ERS-1     ----------------------------++###++##++##--------------------
06 STELLA    ---###++###++##---------------------------------------------------
07 GPS-35    --++++++++++++++##++++++++++++++++++++++++##++++##++++++##++++
-------------------------------- 1 char = 30 seconds ----------------------
```

Figure 1: Tracking Scenario (# = actually tracked)

4. THE LASER

The evaluation of a new laser system finally concentrated on two systems: Either a "classic" Nd:YAG system of a Titanium Sapphire system that has never been used for satellite ranging till now.

We decided to take the risk and order more or less a prototype Titanium Sapphire system One of the major reasons for this choice is the fact that its primary wavelength (846 nm) gives best performances with avalanche diodes. The second harmonic (423 nm) still offers good performance for both photomultipliers and diodes.

The laser was manufactured by BM Industries, France. Shortly after our command the Institute for Applied Geodesy, Wettzell, Germany also ordered a similar laser at BMI for their TIGO system.

The system consists of a diode pumped Cr:LiSAF oscillator and three Ti:Al_2O_3 amplifiers (pumped by a Nd:YAG laser).

The laser experienced some delay in production, it could only be delivered end of January 1996.

The laser basically performs very well. However, we find the power-up procedures very

problems with the beam direction, the reasons of which are not yet clear.

5. CALIBRATION

The old telescope used an internal path for calibration. By setting the range gate accordingly we could easily switch between satellite ranging and calibration. Usually after each 6th satellite observation a calibration measurement was inserted. We are trying to incorporate a similar design into the new system, as well. However, due to the nearly identical transmit and receive path we

7. CONTROL SYSTEM

7.1 General System Control (VAXstation)

The overall computer control of the new system is executed by a VAXstation 4000 running under VMS.

Many of the programs, especially those for prediction generation, general data handling, data screening and data exchange, previously running on a MicroVAX for the old system, could be moved to the VAXstation without much modification.

The following major tasks are run on the VAXstation:

- Administration of incoming orbital element and time bias mails
- Computation of weekly pass lists
- Computation of pass predictions (lists of satellite positions)
- SLR observations (tracking and data acquisition)
- Data preprocessing (calibration corrections, data screening, normal point generation)
- Data reformating (Quick-Look format generation)
- Mailing of quick look data files (through the university's Alpha cluster)

The SLR Observation Program automatically generates the observation scenario for a certain time period (e.g. the next two hours), connects to and controls the telescope PC and the PC controlling the CAMAC Interface System and other equipment, controls the aircraft detection radar, various installations and equipment (like the dome opening, met sensors), checks the Air Traffic Control data (see below), and interacts with the observer.

7.2 Telescope PC

The telescope is controlled by a 486 PC programmed mostly in Fortran with a few assembler and C library routines for special input/output.

The control program runs in two modes:

- a manual (interactive) mode, where the operator can directly control the telescope for "offline-" positioning, star tracking and star calibration, and telescope device control (focusing, movement of optical components, sun cover, power on/off of cameras etc, filter wheel control)

- a remotely controlled mode where the VAXstation sends specific commands to be executed. All functions defined for interactive mode can also be executed through remote control.

The PC contains a special microprocessor card (PMAC) for the drive control of the three telescope axes (azimuth, elevation, instrument platform).

The PC communicates with the telescope devices through several microprocessors (MicroDACs) using a serial line bus system.

7.3 CAMAC PC

The old MicroVAX could directly control the CAMAC interface system by bypassing the standard VMS QIO system. This "trick" is not possible on the new VAXstation, leading to unacceptably long communication cycle times with the individual CAMAC modules. Now the CAMAC control is done by a PC, avoiding the necessity of fast (microsecond) response times for the VAX and simultaneously reducing the command and data transfer to and from the VAX to a reasonable amount.

The PC uses two special interfaces, one for the CAMAC control, one for a realtime clock for system synchronization. The latter is synchronized to GPS time by an IRIG-B time signal generated by a Truetime GPS receiver.

Communication with a MicroDAC microprocessor is done through a standard serial interface.

7.4 CCD Computers

Each CCD camera for astronomical applications is controlled by a special computer. Realtime communications with the station computer will be performed through the local area network in the same way as the communication between the PCs and the VAX (see below).

7.5 Realtime Communication

The realtime transfer of commands and data between the VAXstation and the PCs, (and the CCD camera computers), formally also between programs running simultaneously on the VAXstation, is performed through the local area network (Ethernet) using the TCP/IP basic routines (to open sockets, to connect to a foreign host or to accept incoming calls, to send and receive data packages, and to close connections). These subroutines ("socket library") are available on all major platforms and can easily be called by our Fortran programs.

Current implementations of the TCP/IP libraries are: PC/TCP by FTP Software Inc for the PCs and TCPWare by Process Software Corporation for the VAXstation.

All this communication is organized in client/server relations. One end of a communication link (usually the PCs) acts as a server, i.e. the program opens a "listening" socket and accepts incoming calls from the other end (usually the VAXstation). When the communication link has been established, the data and command transfer is controlled by the client and is done in records of ASCII strings following a message format specially designed for this purpose.

The communications are usually performed ten times per second, i.e. in the same frequency as the basic observation rates.

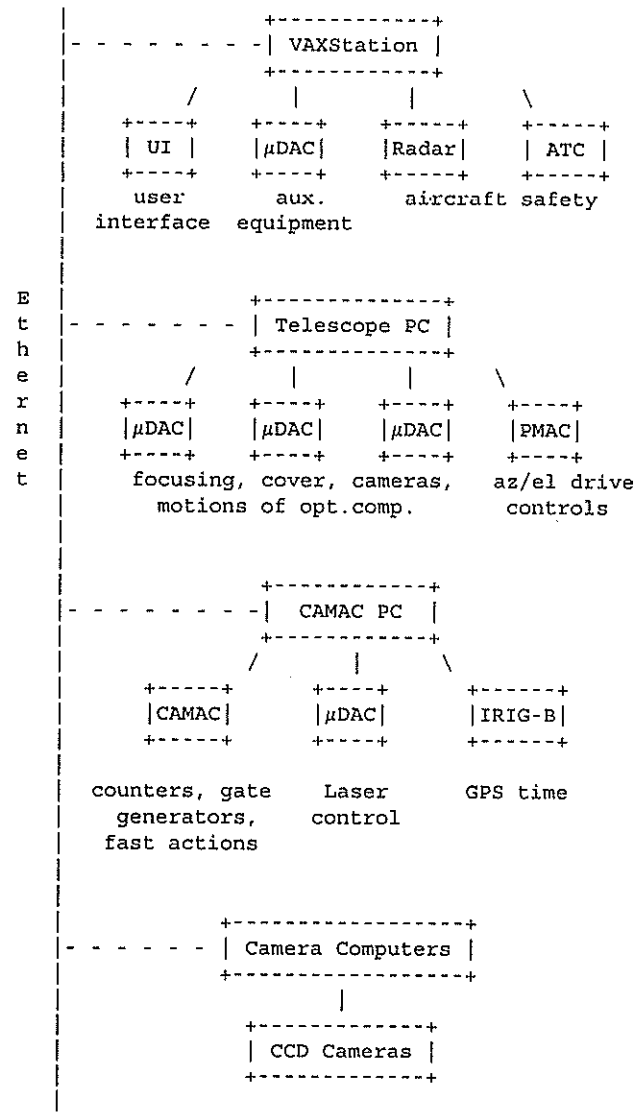

Figure 2: Zimmerwald Control System

7.6 Aircraft Safety

As the system does not operate in an eye-safe mode we have to avoid any interferences of the laser beam with aircraft. Until now we had to get the permission for each pass to observe by the Air Traffic Control a few minutes before the pass. Permission was granted when no aircraft were within a certain radius around the observatory. As the old system could only be used during the night when air traffic was not too heavy, these restrictions were not too serious.

With the new system which will allow daylight operation and with air traffic steadily increasing this solution is not adequate anymore.

The new system contains two components to avoid interference:

- A commercially available boat radar. We replaced the single antenna axis by a microprocessor-driven az/el mount to point the radar parallel to the laser beam. The radar beam width is about

20 deg in azimuth and 2 deg in elevation. Whenever an aircraft is detected, the control electronics disables the laser within a few milliseconds. The radar is capable of aircraft detection up to a range of 10-15 km, which is enough for low-altitude aircraft flying under visual flight rules (helicopters, small planes, etc).

- Positional data of aircraft within a certain radius around our observatory are made available to us in realtime through a dedicated telephone link by the Swiss Air Traffic Control. The data contain positions of transponder-equipped aircraft down to a certain minimum altitude level only. The VAXstation continuously compares the positions of the aircraft with the laser beam and disables the laser whenever an interference could happen.

8. CURRENT STATUS

The telescope without optics arrived, exactly following the original schedule, early July 1995. Due to the very late arrival of substantial parts of the system (laser in January 1996, primary, secondary, and tertiary mirrors end of April 1996) full system tests could only start mid 1996. The first ranges to a terrestrial target were collected in July, the first returns from a satellite (Starlette) succeeded on August 29.

The axicon turned out to be a serious problem: The first one was not of sufficient precision, the ring increased in diameter with the distance. Another axicon, produced by a different manufacturer, also turned out to be of minor quality, it didn't produce a clean ring. A replacement of the first one has a center hole of too large a diameter, so that the laser beam divergence can not be varied within the specified limits. Now the second manufacturer is trying a new approach.

Currently we are ranging as a test without the axicon, using the laser beam shifted off-axis to exit the telescope next to the secondary mirror. Unfortunately the beam position now rotates around the secondary mirror depending on the telescope pointing direction so that no in-pass calibration can be done.

First ranges up to the Lageos satellites sent to the data centers were collected on December 19, 1996. Until February 4, 1997 all major satellites up to Glonass (still without the two GPS satellites) were observed at least once, but during night time only.

9. CONCLUSION

The new Zimmerwald Laser and Astrometric Telescope (ZIMLAT), together with the new Titanium Sapphire laser, the new control system, ranging electronics, and CCD cameras, will be the up-to-date and state-of-the-art basis for the observational activities of the Astronomical Institute in the area of satellite laser ranging (with substantial support by the Federal Office of Topography) and astrometric observations (optical tracking of satellites and other objects, space debris search) for the next twenty years. First tests, both with the SLR and the CCD systems, were performed in 1996. The routine observations will be started early 1997, first during night time only, afterwards in daylight, too.

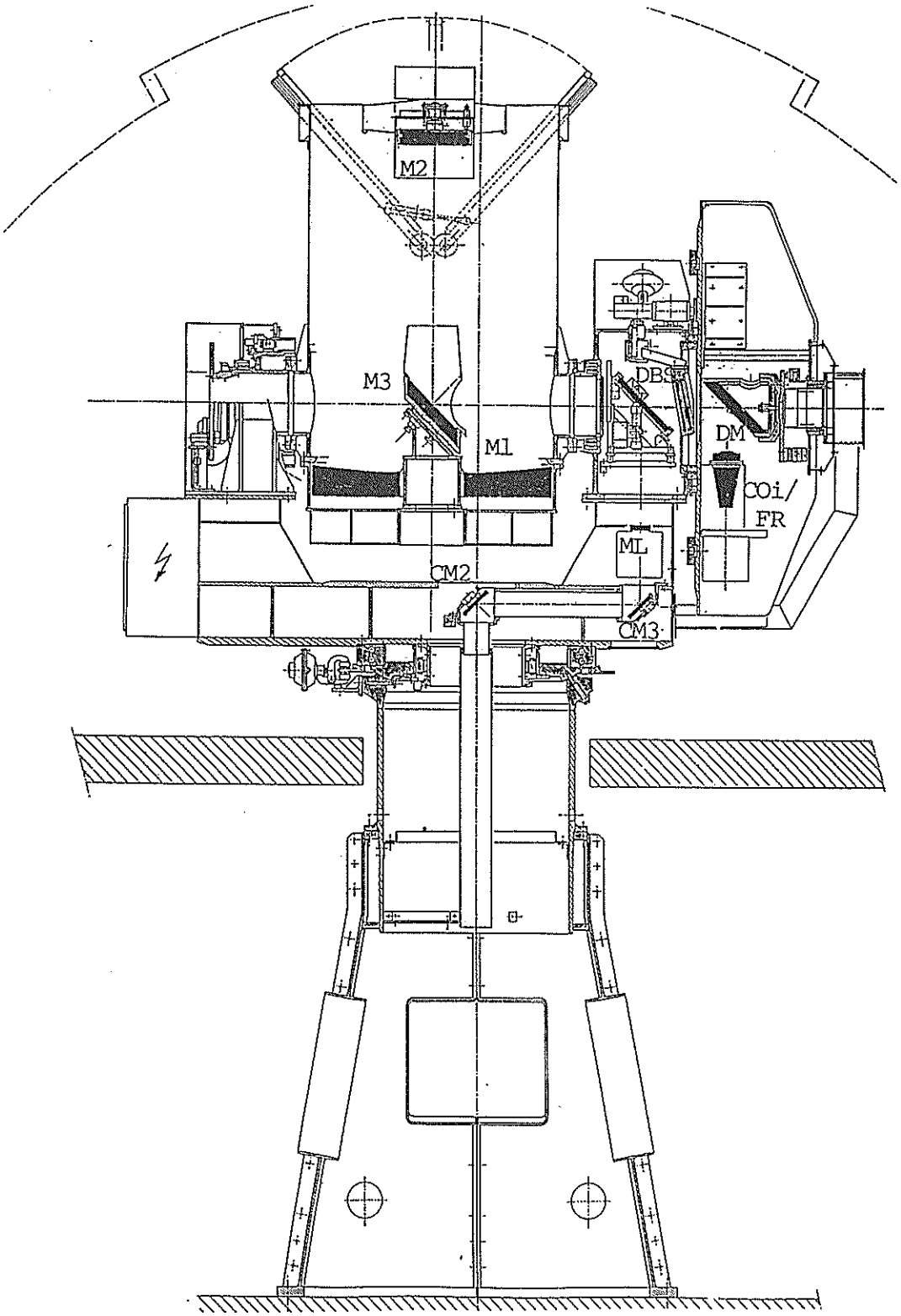

Figure 3: The ZIMLAT Telescope Optics

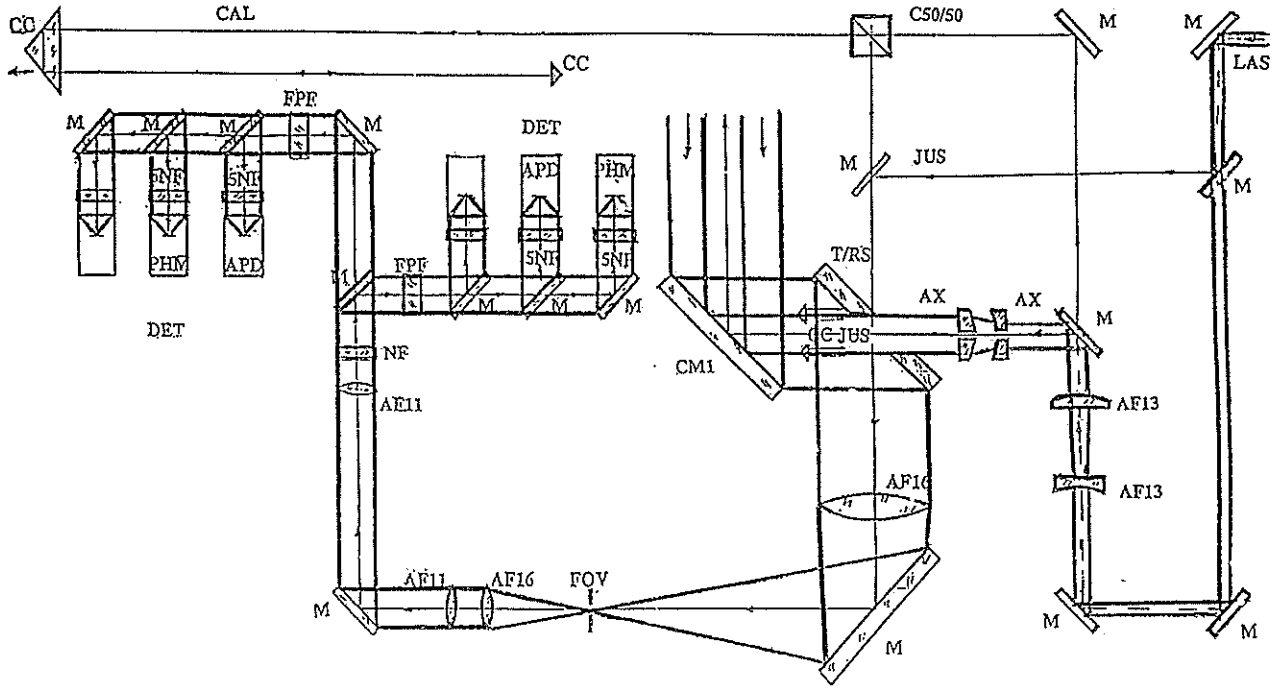

Figure 4: ZIMLAT Transmit/Receive Path

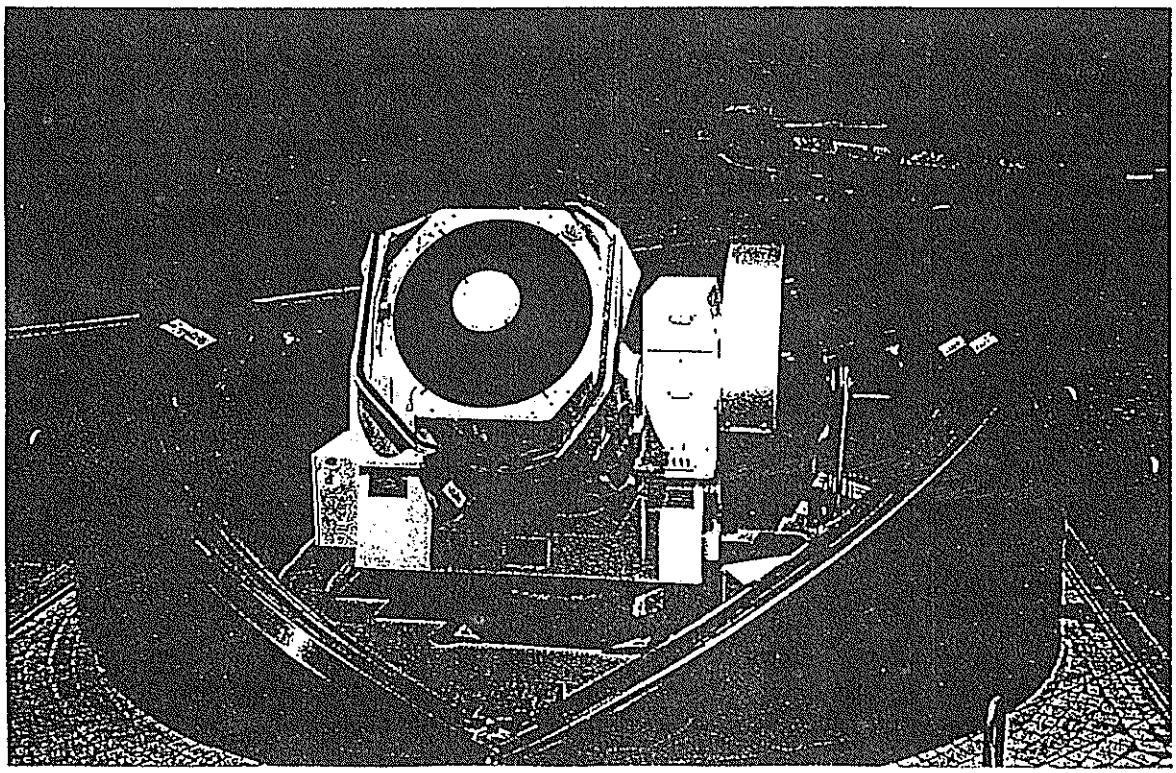

Figure 5: ZIMLAT Dome and Telescope

The Current Status and Development of Changchun SLR System

Liu Zhi, Fan Cunbo, Chen Haiyan, Zhang Xinghua, Liu Chengzhi, Shi Jianyong, Li Yinzhu, Gong Yan, Jin Honglin, Zhao You

Changchun Artificial Satellite Observatory
Chinese Academy of Sciences

ABSTRACT

This paper introduces the current status of Changchun SLR system and its development. It includes the characteristics of the system, the new developments and the developments in the near future. It also shows some problems which need to be solved.

1. Introduction

The third generation of Satellite Laser Ranging (SLR) systems in Changchun observatory has been completed with single shot accuracy of 5-7 centimeter since 1988. But it was not in operation routinely because the components of the original system were unstable. In 1991, we changed the computer control system and adopted a HP 5370B counter routinely. The obtained SLR data have been drastically increasing and 1000 passes data have been obtained this year.

2. Description of the SLR system

The main components of the SLR system are described as follows.

2.1 Laser

An active-passive model-locked Nd:YAG laser made by the North China Research Institute of Optic-electronics is used to generate a 532 nm/second harmonic with 200 ps width optical pulses. The laser has output energy of 100 mj per pulse. The laser firing is controlled by the real-time tracking system, typically 5 pps repetition rate adopted.

2.2 Transmitting path

The laser pulse is guided to the Coude optical path via several 45^0 bending HR mirrors. Before entering the Coude optical path, a small portion of energy of the pulse is separated to a high speed photodiode to generate a signal to start the time interval unit. The rest is guided to a 15 cm diameter transmitting telescope via Coude optical path and transmitted to satellites.

2.3 Receiving path

The laser pulse reflected from the satellite returns into the main telescope with a 60 cm diameter, and then reflected by a dichoic mirror and go into photomultiplier tube. The received light other than 532 nm pass through the dichoic mirror and guided to an ICCD camera for observing satellites.

2.4 Telescope

The telescope at Changchun station is the same as Shanghai station also made by Changchun Institute of Optics and Fine Mechanics. The aperture of the main telescope is 60 centimeters. the main telescope has an azimuth-elevation mount. The maximum speed of azimuth is 12 deg/sec and that of elevation is 5 deg/sec. The maximum accelerations are 10 deg/sec/sec and 5 deg/sec/sec respectively. The azimuth-elevation encoders have a resolution of 1.2 arcsecond.

2.5 Receiving system

The receiving system is composed of photomultiplier tube (PMT GDB49A, China-made), discriminator(TC454) and time interval unit (HP5370B).

The photomultiplier converts photons into photoelectrons and multiplies them. The discriminator accepts an input pulse from PMT and generates a regulated output pulse. The purpose of time interval unit is to measure the flight time of the optical pulse.

2.6 Controlling system

All of the operations in Changchun SLR system are completely controlled by a AST286 computer. There is a controlling card in it. Its main functions include laser firing, range gate controlling, telescope real-time tracking, data collection.

The computer is also used to predict the satellite positions and ranges and pre-process the obtained SLR data.

2.7 Timing system

The timing system consists of a rubidium frequency standard and a GPS receiver. The rubidium frequency standard generates a 5MHz signal which is for time interval unit. The frequency is also doubled to 10MHz for station clock. The GPS receiver gives a second pulse which is used to synchronize the station clock to UTC.

2.8 Terrestrial ranging

The terrestrial ranging is adopted to calibrate the system delay. A corner cube reflector is installed on a mountain building. One way distance is 1268.6215m. The laser energy is controlled and very small receiving aperture is adopted during terrestrial ranging in order to simulate the actual satellite ranging.

3. The current development

The SLR data of Changchun observatory had some problems before April 11, 1996. It was suspected that the rubidium frequency standard did not work well. So air-conditioners were installed at the beginning of this year and a new power-supply with higher stability has been adopted to supply the power to the rubidium frequency standard since April. After doing these, the SLR system became more stable and the data became much better.

In order to improve ranging accuracy, a microchannel plate (MCP)PMT is planned to substitute the photomultiplier tube (PMT) for ranging. Several experiments of ranging to the satellites have been done and the data of satellites LAGEOS-1,2 with an accuracy of less than 2cm have been obtained. For low orbit satellites, the accuracy of obtained data sometimes is about 3cm. The MCP has not been routinely used until now, because some technical problems have not been solved.

In order to improve the tracking accuracy and stability, a new encoder electronics with higher precision has been used since mid-April, 1996. It has a resolution of 0.15 arcsecond.

4. Future plan

In order to obtain more data and utilize the whole capability of current SLR system, the SLR system in Changchun observatory is planned to be operated in day time. So some new developments must be done in the near future.

In order to reduce background noise in day-time ranging, the returned pulse should be guided to the receiver via spectral and spatial filters.

Modeling the telescope's mount and optical alignment should be done to improve pointing accuracy within a reasonable range for day-time ranging. This will also be necessary to observe the unseen satellites which are passing through the earth shadow.

A new serving system is also planned to be installed to substitute the old one in order to avoid the tracking problems.

References

(1) J.J.Degnan, "Satellite laser ranging: Current status and future prospects", IEEE Trans Geosci. Remote Sensing, Ge-23, 4, pp.398-413, Jul. 1985.

(2) H.Kunimori et al., "New development of satellite laser ranging system for highly precision space and time measurements", Journal of Communications Research Laboratory, 38, 2, pp.303-317, July 1991.

Matera Laser Ranging Observatory Software System

Tenth International Workshop on Laser Ranging
Shanghai Observatory, Chinese Academy of Sciences
November 11-15, 1996

Matthew Bieneman, C. Bart Clarke, J. Michael Heinick, David McClure, Bhashyam Nallappa, Michael Selden

AlliedSignal Technical Services Corporation
Greenbelt, Maryland

Dr. Giuseppe Bianco
ASI
Matera, Italy

Abstract

The MLRO software has been developed as an object-oriented multi-processor distributed system. A team of software engineers have been working to develop this advanced environment. The software will be described and an update on the progress of its development will be provided. This paper will describe both the methodology used for the software development as well as some of the new features of the MLRO software system.

MLRO Software System

The MLRO software system was designed with several important goals. Some of these are specific to the MLRO, but many are focused on improving the ATSC software engineering capabilities. Some of these goals include:

- Meeting the functional requirements of the MLRO software system.
- Providing the foundation to the MLRO system to allow for future system improvements such as:
  - ⇒ high-speed (kHz) ranging operations,
  - ⇒ automation,
  - ⇒ two-color ranging,
  - ⇒ astronomy,
  - ⇒ and other special applications.

- Providing for easy software maintenance and for customer additions to the system functions.
- Developing a set of generic modules (class libraries) which can be used by AlliedSignal to produce real-time control systems on any computer with a C++ compiler and for any application (SLR, manufacturing and quality control, traffic-management, or any other type of work we might do). This will allow us to develop software systems for future customers **very rapidly** and at a reduced price and risk to the customers.
- Operator control through an X-Windows interface with widgets and tools that comply with Motif standards where possible. These applications should also be portable to the maximum extent possible.
- Development of the Non-Real-Time (Data Processing and Analysis) software to allow for easy maintenance and functional flexibility.
- Developing software to support ATSC's custom-built instruments.

Software Description

The MLRO software is divided into five subsystems. These are: 1) real-time control and data acquisition, 2) non-real-time data processing and analysis, 3) electronic on-line hypertext documentation, 4) Man-Machine Interface (MMI) software (which uses the X-Windows graphical interface), and 5) the communications software which acts as the software backbone. A diagram depicting this software system is illustrated in Figure 1.

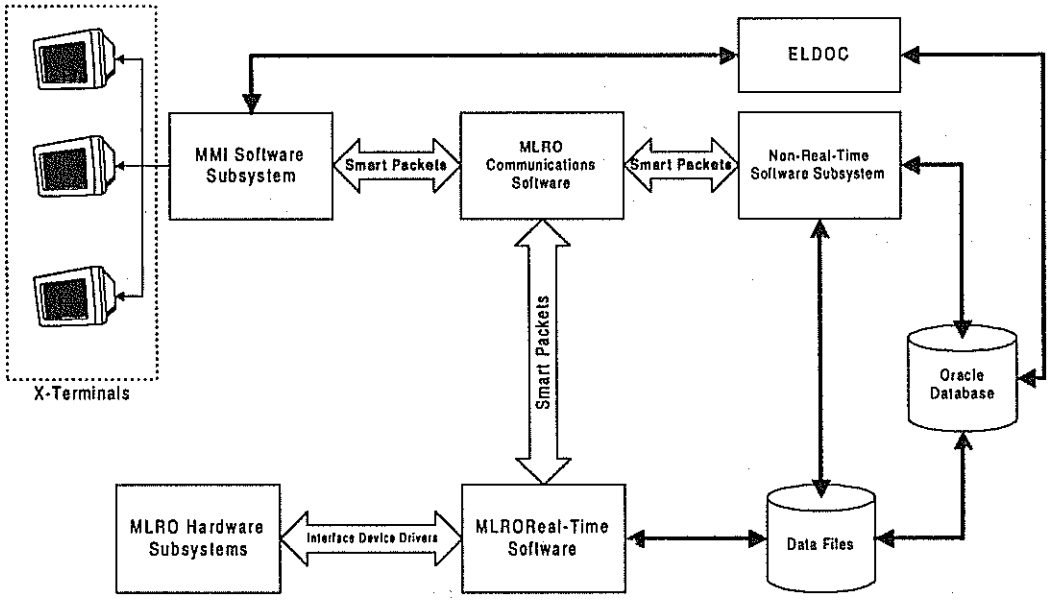

Figure 1: MLRO Software Block Diagram

Real-Time Software

The real-time object-oriented software performs the data acquisition, control and real-time modeling of systematic non-linearity for the various hardware units. Real-time feedback is provided to the MMI software subsystem to allow personnel to monitor the data or to adjust system parameters. Data acquired during laser ranging operations is stored to disk and can be accessed by the data processing (Non-Real-Time) subsystem.

The real-time software allows for laser ranging applications, calibration and modeling of laser ranging instrumentation, and automated diagnostics and simulations for the MLRO system and various subsystems. The real-time applications are linked to a series of X-Windows applications to allow for real-time user interaction with the instrumentation and real-time feedback about the data acquired and the system status.

The real-time software is built on a layered approach with hardware and device-drivers at the lowest level, device server processes (or daemons) and control processes at the intermediate level and main processes at the highest level. A diagram depicting this relationship is illustrated in Figure 2. The real-time daemons (device server processes) are composed of elements (class library objects) produced during the initial development phase of the MLRO project (called the MLRO "real-time utilities") and process-specific data structures like command and response sets and configuration data. Control processes use the daemons and are themselves combined to perform various applications (like laser ranging, calibrations, etc). These relationships are illustrated in Figure 3.

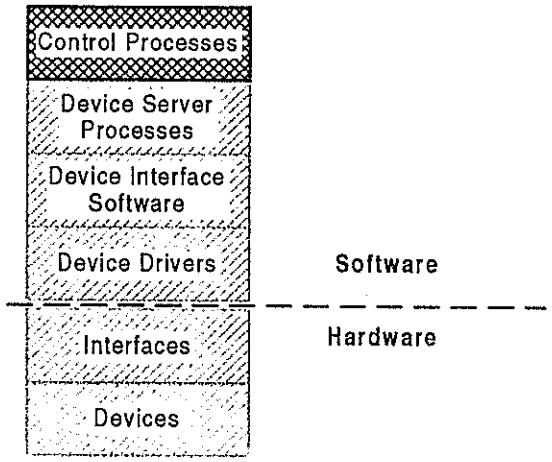

Figure 2: Real-Time Architecture

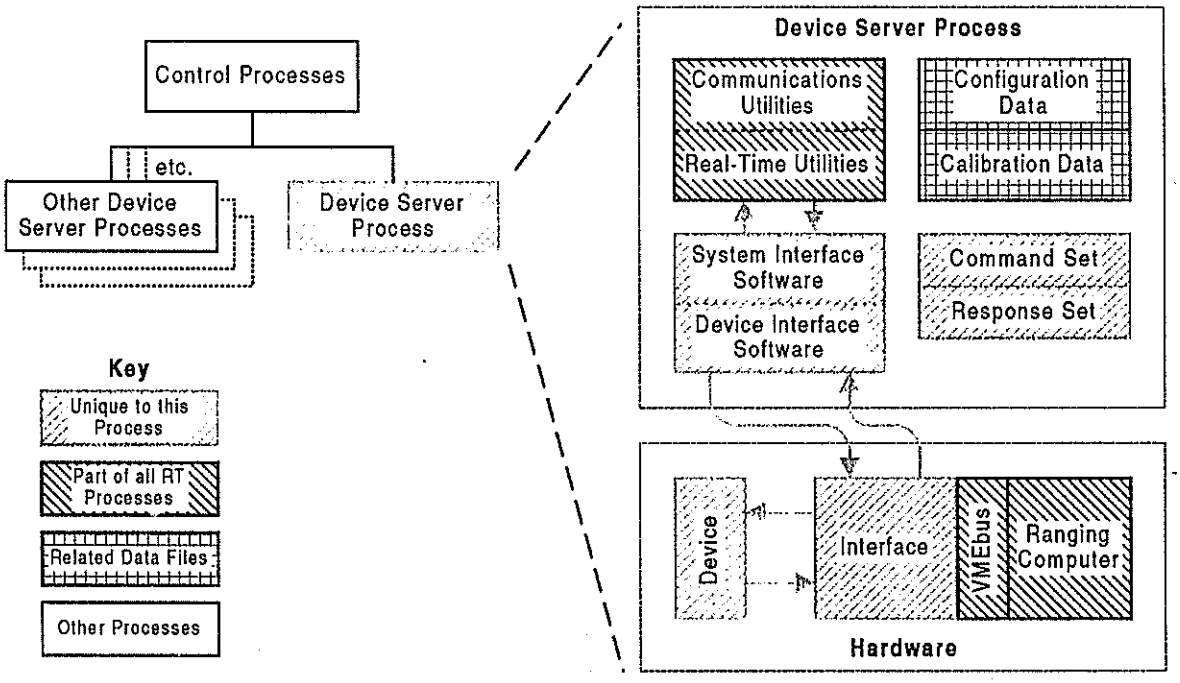

Figure 3: Interrelationship among Real-Time Processes

Non-Real-Time Software

The Non-Real-Time software performs the data processing, system scheduling, predictions, and analysis functions. The software takes maximum advantage of the Oracle database as a central data repository to store important information like scheduling input parameters, system parameters, satellite characteristics, ground target information, special applications information (like instrument calibrations, scientific data, etc.), satellite pass summary data, and long-term trend analysis data. This information is used by virtually all NRT applications and provides unparalleled configuration management, precluding errors caused by multiple copies of important data and allows the capability to generate reports about the information and its evolution. The Non-Real-Time software includes the following components:

Scheduler

The system scheduler, which allows for scheduling of events including satellites, interlaced satellite segments, lunar ranging, calibrations, and other special events. The software will determine the schedule by assessing the relative priority and other associated parameters of each available event. Among these parameters are minimum and maximum tracking time restrictions, elevation restrictions, and any special optimization parameters selected by the user. These optimization parameters include fine-interleaving optimization, geodetic (sky coverage) optimization, altimetric (high elevation) optimization, and ascending/descending optimization. The scheduler is interfaced to an oracle database

which it shares with the prediction software and the data analysis software. It is also interfaced to a set of X-Windows applications which allow the user to interface with the software parameters and to view the various schedules and satellite coverage plots.

Single-Pass Analysis Software (SPAS)

SPAS is derived from the analysis software that has been used by ATSC to process SLR data for years. This software was significantly improved for modularity and to allow for the enhanced system capabilities and accuracy that the MLRO provides. SPAS uses an Oracle database to store important processing parameters and to store summary information about satellite pass events for long-term reports and analysis. SPAS is linked with a number of X-Windows applications to allow for user interaction with the data processing parameters and to view the data graphically. SPAS can be run manually, or scheduled to run automatically as data is acquired.

Lunar Ranging Analysis

ATSC is adapting lunar software provided by Dr. Christian Veillet of Centre d'Etudes et de Recherches Geodynamiques et Astronomiques (CERGA) to enhance the MLRO lunar ranging capability. The software is being incorporated within the framework of the scheduling, prediction and data processing strategy and a number of X-Windows applications are being developed to support data processing.

Prediction Software

The MLRO prediction software produces satellite or lunar predictions for both scheduling and tracking purposes. The software may be run automatically at given time intervals or manually for one-time predictions. The software can produce satellite predictions using NORAD elements, Tuned IRVs, or GEODYN ephemerides. When GEODYN ephemerides are used, the software produces a new ephemeris (using GEODYN) by either propagating an existing ephemeris forward in time or by producing updated orbit information using new satellite ranging data. Lunar predictions are produced using JPL ephemerides files. The prediction software uses X-Windows applications to modify the various prediction parameters and to activate the prediction process.

Collocation Analysis Software

The MLRO collocation analysis software is derived from the software used for NASA collocations. The software has been improved for modularity and a set of X-Windows applications are being developed to provide interaction with the summary results. The collocation results are stored in an Oracle database for trend analysis and graphical summary.

Long-Term Trend Analysis

The MLRO long-term trend analysis (LTTA) software is being developed to allow for monitoring of the MLRO system performance over an extended period of time. This software will allow for monitoring of system-level, as well as instrument-level

performance. A set of X-Windows applications are being developed to allow for interaction with the data stored in the LTTA Oracle database.

ELDOC

The Electronic (On-Line) documentation system is a stand-alone UNIX-based set of applications developed for ATSC by Dataspazio Company in Rome, Italy. The subsystem uses Prologue, Oracle, and Knowledge Management System (KMS) to provide the context-sensitive on-line documentation and the MLRO configuration control management tools.

Internal Communications Software

The communications subsystem allows the various MLRO applications to communicate with each other, regardless of the relative physical locations of the applications.

All of the real-time processes, and the MMI software, communicate with each other using a standardized, object-oriented mechanism. Each process using this mechanism has assigned to it a service name, which allows the communications subsystem to find it. Each computer also has a unique cpu identifier. Each process has (automatically) assigned to it a shared memory block and a semaphore. The shared memory block contains a queue of commands and data directed to that process, and the semaphore is used to control access to that queue.

As an example, the Meteorological Daemon has a service name 'METD'. For a process to send a command it calls SendTo ('METD'). The communications software will attempt to find the process with the identifier 'METD'. If it is on the same computer, the command is delivered to that process immediately to that process's queue. If 'METD' is not found on the same computer, the command is immediately delivered to the process 'DATQ'. This is a special process (called gateway) which transmits data to other computers. In either case, the commanding process can resume its real-time duties without slowing for communications transmission time.

This mechanism maximizes performance and is easy to use in application programs, because it automatically decides whether to use the interprocess communications subsystem or the interprocessor communications program (gateway). Client applications only need to know the service name of the process that they want to communicate with. Server applications only need to call the Reply( ) method to have data automatically sent back to the client.

Man-Machine Interface (MMI) Software

Man Machine Interface are used on the MLRO project to allow the operator to interface with the system for virtually all of the MLRO applications including:

Operation

- Laser Ranging
- Calibration
- Simulations
- Diagnostics
- Verification
- System Alarms and Errors
- Scheduling

Data Analysis

- Single Pass Analysis Software (Satellite and Lunar)
- Prediction
- Collocation Analysis
- Long Term Trend Analysis
- ELDOC support

The MMI is primarily designed using Motif. Commercial Vendors like DataViews were used to implement non-Motif parts of the project.

The MMI is divided into two domains, Real Time MMI and Non Real Time MMI. The MMI applications run on the HP-UX machine. During real time computing, the MMI acts as a client to the data sent by the real time machine. The data transfer and updating of the screen is dependent on the real time event being processed. The MMI sends commands and data to the real time system and in turn receives data and status messages. Non Real Time MMI involves display of graphs and plots along will interaction with the ORACLE database. The operator can, through standard Motif forms, send SQL queries to the ORACLE database and in turn receive data and error messages which are displayed by the form. These screens are used by the operator to create, update and delete various parameters. The analysis software also allows the operator to view graphs and plots. Most of the MMI applications are written in C++. Classes are used so that the applications are reusable.

Software Environment

The MLRO software system is hosted on five computers these include two Hewlett Packard UNIX workstations (an HP J200 workstation and an HP 715/100 workstation) and three Hewlett Packard real-time VME computers (HP 743 RT). Each of the HP743 workstations is roughly equivalent to a 715 / 66 MHz UNIX workstation. The two UNIX workstations host the HP-UNIX operating system and the three real-time machines host the Hewlett-Packard HP-RT real-time operating system which is a POSIX-compliant UNIX-like operating system originally based on the *LYNX* kernel, but modified and improved by HP. A diagram of the MLRO computing subsystem is illustrated in Figure 4. The system has been configured to allow for expanded capability. Each real-time computer

has ample excess capacity to support added functionality, but our plan is to add new functions in a modular fashion to provide a certain level of orthoganality between machines and functions. It should be noted that the software is designed to be portable to other platforms and could all be run on a single computer.

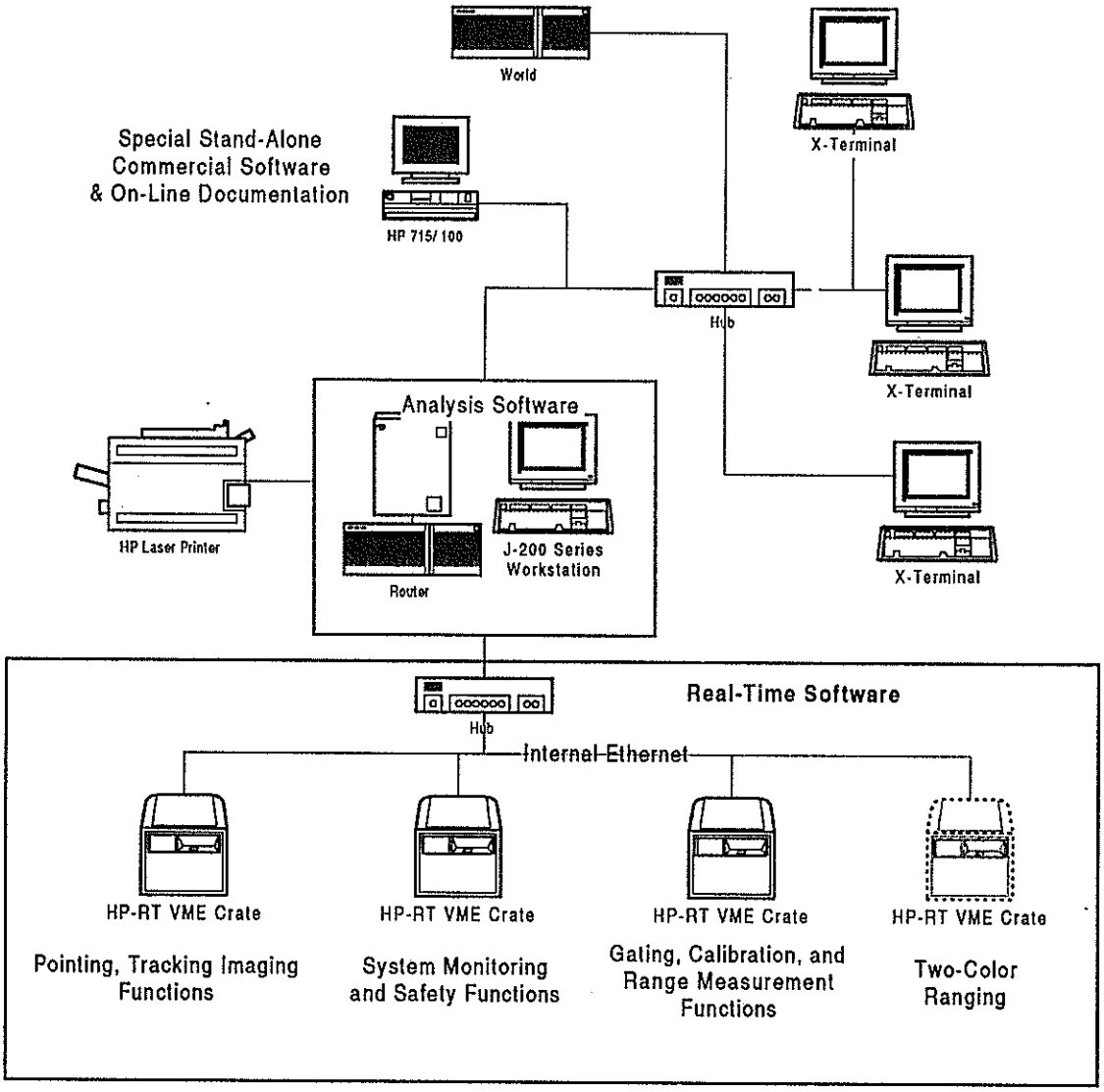

Figure 4: MLRO Computing Environment